This dissertation has been 65-9752
microfilmed exactly as received

MCLEOD, Jr., Harry O'Neal, 1932-
A STUDY OF THE MECHANISMS BY WHICH PENTANE AND HEXANE ARE ADSORBED ON SILICA GEL.

The University of Oklahoma, Ph.D., 1965
Engineering, chemical

University Microfilms, Inc., Ann Arbor, Michigan

Downloaded from SHAREOK. Persistent Handle URL: https://hdl.handle.net/11244/1883

THE UNIVERSITY OF OKLAHOMA

GRADUATE COLLEGE

A STUDY OF THE MECHANISMS BY WHICH PENTANE AND HEXANE ARE ADSORBED ON SILICA GEL

A DISSERTATION

SUBMITTED TO THE GRADUATE FACULTY

in partial fulfillment of the requirements for the

degree of

DOCTOR OF PHILOSOPHY

BY

HARRY O. MCLEOD, JR.

1965

A STUDY OF THE MECHANISMS BY WHICH PENTANE AND HEXANE ARE ADSORBED ON SILICA GEL

APPROVED BY

DISSERTATION COMMITTEE

DEDICATED TO MY WIFE

ACKNOWLEDGMENT

Sincere gratitude is extended to Dr. John M. Campbell, School of Petroleum Engineering, who directed this work. His understanding and guidance were responsible for the completion of this work. Appreciation is also expressed to Riley B. Needham, who shared the problems and challenges of this project, for his help and enthusiasm.

The assistance received from the Davison Chemical Company is gratefully acknowledged.

Appreciation is also due the many others who have given their time, encouragement, and suggestions.

TABLE OF CONTENTS

Page

LIST OF TABLES viii

LIST OF ILLUSTRATIONS. x

Chapter

I. INTRODUCTION. 1

II. ADSORPTION EQUILIBRIA 6

A. Theories of Adsorption Equilibria

B. The Langmuir Monolayer Theory

C. The Multilayer Theory

D. Importance of Adsorption Equilibria for Dynamic Adsorption

III. RATE MECHANISMS OF ADSORPTION 14

A. Transfer Rate Equations
1. Fluid-Phase External Diffusion
2. Fluid-Phase Pore Diffusion
3. Reaction of Phase Change
4. Solid-Phase Internal Diffusion

B. Mass Transfer Rate Studies
1. External Fluid-Phase Mass Transfer
2. Internal Diffusion Rates

IV. DYNAMIC ADSORPTION PROCESSES. 23

A. Nomenclature
1. Concentration Nomenclature
2. Column and Flow Parameters
3. Dimensionless Time and Distance Parameters

B. Material Balance - The Continuity Equation

Page

C. Fixed-Bed Behavior
1. Proportionate Pattern Case (Unfavorable Equilibrium)
2. Constant-Pattern Case (Favorable Equilibrium)
a. Fluid Phase Diffusion Controlling
b. Solid Phase Diffusion Controlling
3. Reaction-Rate Solution
4. Column Dynamics Under Linear Equilibrium
5. Column Dynamics with an Equilibrium Parameter, r

V. EXPERIMENTAL MATERIALS AND PROCEDURE 35

VI. ANALYSIS OF EXPERIMENTAL DATA. 42

A. Evaluation of the Equilibrium Parameter, r

B. Analysis Assuming Stabilized Zones

C. Correction of Effluent Curve Midpoints to Obtain Overall Transfer Coefficient

D. Gas Phase Mass Transfer Coefficient

E. Evaluation of "b" Parameter

F. Calculation of the Particle Mass Transfer Coefficient

G. Pore Diffusion

VII. PREDICTION OF EFFLUENT CURVES. 63

VIII. SIGNIFICANCE OF RESULTS. 71

A. Isotherm Shape

B. Adsorbate Concentration

C. Transfer Zone Stability

D. Equilibrium Adsorption

E. Particle Transfer Mechanism

F. Restatement of Concepts

Page

IX. CONCLUSIONS 86

BIBLIOGRAPHY 91

APPENDICES

A. EXPERIMENTAL DATA. 102

B. EXAMPLE CALCULATIONS - RUN 210 128

C. HYDROCARBON DIFFUSION COEFFICIENTS 131

D. METHOD OF OBTAINING EFFLUENT CURVE CONCENTRATION-TIME SLOPE FROM PLOT ON PROBABILITY - COORDINATE PAPER 141

E. CORRECTION OF TRANSIENT MIDPOINT SLOPES TO LIMITING VALUES 144

F. DIFFUSIVITY CORRELATIONS 151

G. COMBINED TRANSFER COEFFICIENT. 158

H. SOLUTION FOR x WHEN Z = ONE. 162

I. INFLUENCE OF r ON EFFLUENT CURVE SHAPE . . . 165

J. MASTER CURVES FOR THE LIMITING CASE. 169

K. CORRELATION OF PARTICLE MASS TRANSFER COEFFICIENTS BASED ON THE ASYMPTOTIC SOLUTION 174

L. PORE DIFFUSION 179

M. EXAMPLE CALCULATIONS FOR FLUID PHASE MASS TRANSFER COEFFICIENTS 180

N. EFFECT OF USING DIFFERENT GAS DIFFUSIVITY ON $k_p a_p$ CORRELATION. 185

LIST OF TABLES

Table		Page
I.	Physical and Chemical Characteristics of Silica Gel	40
II.	Properties of Silica Gel, Grade 03	41
III.	Calculated Transfer Coefficients - Pentane	53
IV.	Calculated Transfer Coefficients - Hexane	55
APPENDICES		
A-I.	Pentane Effluent Data	104
A-II.	Hexane Effluent Data	112
A-III.	Experimental Conditions - Pentane Runs	120
A-IV.	Effluent Curve Parameters - Pentane Runs	121
A-V.	Calculated Adsorption Values - Pentane Runs	122
A-VI.	Experimental Conditions - Hexane Runs	123
A-VII.	Effluent Curve Parameters - Hexane Runs	124
A-VIII.	Calculated Adsorption Values - Hexane Runs	125
C-I.	Physical Properties of Hydrocarbons	135
C-II.	Calculated Diffusivity of Hexane in Methane	136
C-III.	Experimental Diffusivities	137
E-I.	Calculated Values of x and Z - Pentane	146
E-II.	Calculated Values of x and Z - Hexane	148
E-III.	Midpoint Slope Computation	150

Table Page

K-I. Asymptotic Particle Transfer Coefficients - Pentane 177

K-II. Asymptotic Particle Transfer Coefficients - Hexane. 178

LIST OF ILLUSTRATIONS

Figure		Page
1.	Five Basic Isotherm Shapes	8
2.	Particle Diffusion Coefficient	20
3.	Effect of Porosity on Adsorbent Permeability	22
4.	Dynamic Adsorption Flow System	36
5.	Typical Effluent Curve	42
6.	Evaluation of r Parameter - Pentane	45
7.	Evaluation of r Parameter - Hexane	46
8.	Particle Mass Transfer Coefficient - Master Curve Analysis - Pentane	48
9.	Particle Mass Transfer Coefficient - Master Curve Analysis - Hexane	49
10.	Transient Midpoint Slope Correction	51
11.	Particle Transfer Coefficient Versus C_o/X_T - Pentane	58
12.	Particle Transfer Coefficient Versus C_o Pentane	59
13.	Particle Transfer Coefficient Versus C_o/X_T - Hexane	60
14.	Particle Transfer Coefficient Versus C_o - Hexane	61
15.	Effluent Curve Prediction - Run No. 56	64
16.	Effluent Curve Prediction - Run No. 63	65
17.	Effluent Curve Prediction - Run No. 70	66

Figure Page

18. Effluent Curve Prediction - Run No. 208. 67

19. Effluent Curve Prediction - Run No. 208. 70

20. Stabilized Zone Run - Hexane 73

APPENDICES

A-1. Equilibrium Adsorption Values - Pentane. 126

A-2. Equilibrium Adsorption Values - Hexane 127

C-1. Temperature Dependence of Diffusivity. 138

C-2. Hydrocarbon Diffusion Coefficients at 21°C 139

C-3. Estimation of Critical Volume of Dry Gas (S.G. - 0.64). 140

I-1. Effect of r Parameter on Effluent Curve Shape - Particle Diffusion 166

I-2. Effect of Diffusion Mechanisms on Effluent Curve Shape - Pentane. 167

I-3. Effect of Diffusion Mechanisms on Effluent Curve Shape - Hexane 168

J-1. Asymptotic Effluent Curves - Pentane - Particle Diffusion. 170

J-2. Asymptotic Effluent Curves - Pentane - Fluid Phase Diffusion. 171

J-3. Asymptotic Effluent Curves - Hexane - Particle Diffusion. 172

J-4. Asymptotic Effluent Curves - Hexane - Fluid Phase Diffusion. 173

A STUDY OF THE MECHANISMS BY WHICH PENTANE AND HEXANE ARE ADSORBED ON SILICA GEL

CHAPTER I

INTRODUCTION

The purpose of this study is to determine the controlling mechanisms involved in the dynamic adsorption of hydrocarbons on silica gel. Two principal investigations of this system have been published (M2, D1). The conclusions in each case are inconsistent with the experimental results. This study will show how these inconsistencies arise from improper use of mathematical solutions for mass transfer.

The ultimate objective in a program of dynamic adsorption research is a design method for the separation of multi-component hydrocarbons from a natural gas. However, the mechanisms of transfer for a single hydrocarbon component from a weakly adsorbable carrier gas stream must first be defined before we can deal effectively with the more complicated case.

Mathematical solutions for the adsorption of a trace component are derived from three relationships: the mass balance or continuity equation, an equilibrium relationship

between the gas and solid phases, and a mass transfer rate equation which depends on the adsorbate concentration gradient within a phase. These derived solutions usually give the adsorbate gas concentration as a function of time and distance from the adsorbing bed inlet. The adsorbate concentration is expressed as a dimensionless ratio relative to the inlet concentration. Some solutions give the adsorbate concentration as a function of throughput ratio. Throughput ratio is the amount of adsorbate which has entered the bed divided by the bed capacity. The bed capacity is the amount of adsorbate contained in the bed in equilibrium with the inlet concentration.

The general form of these solutions - usually called effluent curves - is determined by the continuity equation and gives an "S" shaped curve. These forms occur in many processes of diffusional transfer.

The main difference in mathematical models of adsorption arise from what equilibrium isotherm is assumed. The isotherm is a plot of the amount of adsorbate in the adsorbed phase versus the amount of adsorbate in the gas phase at a constant temperature. There are two primary models for separation of a trace component in a fixed bed. Model A assumes a linear isotherm; Model B assumes a curved isotherm. Both models use the same differential transfer rate equation. The differential adsorption rate is directly proportional to the difference between adsorbate concentration across a hypothetical

film either in the gas phase or in the solid phase. Fluid phase diffusion controls the transfer rate through this film or boundary layer around the dessicant particle. Diffusion along the surface of the pores or through the pores of the dessicant particle controls the transfer rate inside the particle. When one resistance dominates, the transfer is controlled by either fluid phase diffusion or particle diffusion.

The effluent curves predicted by these mathematical models differ in two important ways. First, the transfer zone of Model A increases in length proportional to the square root of the distance from the bed inlet. The transfer zone of Model B reaches a constant length at a rate depending upon the curvature of the isotherm. Second, the effluent curve of Model A has the same "S" shape regardless of which diffusion resistance controls the transfer rate. However, the effluent curve of Model B is more asymmetric around its midpoint. The first half of the curve is steeper than the last half when particle diffusion resistance is greater. The reverse is true when the fluid phase diffusion resistance is greater. As the curvature of the isotherm increases, the effluent curve becomes more asymmetric.

When either Model A or B is used to obtain mass transfer rate coefficients from fixed bed experiments, the following relationships must apply. The fluid phase coefficient varies approximately with the square root of velocity. It is not a function of adsorbate concentration for trace

components. The particle coefficient is not a function of velocity, but is a strong function of adsorbate concentration.

The functional relationship calculated from experimental data must agree with the diffusion mechanism shown by the effluent curve shape. Marks, et al. (M2) and Dale, et al. (D2) neglected this important point. Marks et al. used Model A with fluid phase diffusion as the main resistance to mass transfer. They reported constant length adsorption zones which contradicts the increasing zone length of Model A. Instead of using another model for their correlation, they used the square root of bed depth as a correction factor in their correlation for the mass transfer coefficient.

Dale, et al. used Model B in their hydrocarbon adsorption study. They recognized the curvature of the isotherm, but did not account for the transient change of an adsorption zone before it reaches a constant length. The bed distance required to reach constant-length-zone transfer depends on velocity. If Model B is used to evaluate transient effluent curves, the transfer coefficient will also depend on velocity as the authors showed. They also reported that the adsorption capacity of the bed varied with particle size. This suggests particle diffusion to be the controlling mechanism and contradicts the authors assumption of transfer control by a gas film around the particle.

In this study, single component adsorption runs were made by adding either pentane or hexane into a dry natural

gas which flowed through a silica gel bed. An equation for ion exchange was used to describe the transient change of a transfer zone which reaches a constant length. Midpoint slopes of the experimental data in this study were corrected for transient conditions with this equation and were used to calculate mass transfer coefficients. Model B for particle diffusion controlling matches the experimental effluent curves obtained when these transfer coefficients are used.

The results of this investigation show that particle diffusion controls the mass transfer rate of pentane and hexane onto silica gel. Use of a favorably curved isotherm relationship and corrections for transient zone growth clarify earlier hydrocarbon adsorption studies.

CHAPTER II

ADSORPTION EQUILIBRIA

The adsorption process may be described as the concentration of molecules of a fluid at the interface of a solid. This distribution is usually expressed as the mass of gas adsorbed per unit mass of solid. The gas constituents adsorbed are referred to as the adsorbate, and the solid is the adsorbent.

Adsorption is divided into two classes: physical and chemical. Physical adsorption is rapid, reversible (except for hystersis from capillary condensation in porous adsorbents), and occurs as a result of weak forces of attraction between gas and solid with energies of adsorption about one-third greater than those of liquefaction; chemical bonds as such are not involved. Chemical adsorption may be either rapid or slow and may occur above or below the critical temperature of the adsorbate. Some degree of chemical interaction produces quite large energies of adsorption, and desorption may be accompanied by chemical changes.

The relationship of the surface concentration of the adsorbate on the solid to the vapor pressure or concentration

of the adsorbate in the fluid phase is usually expressed graphically as an isotherm or constant temperature curve.

Brunauer, Deeming, Deeming, and Teller (B12) identified the five types of isotherms shown in Figure 1. The first type is considered the Langmuir (L2) or monolayer isotherm. Type II is perhaps the most common isotherm and corresponds to multilayer formation. Type III is rare and is characterized by a heat of adsorption less than the heat of liquefaction of the pure adsorbate. Types IV and V are similar to Types II and III escept that they reflect pore-size-limited adsorption and may show hysteresis as a result of capillary condensation.

A. Theories of Adsorption Equilibria

Most of the adsorption theories were developed for predicting the form of the isotherm from suggested mechanisms of the adsorption process and the state of the adsorbed molecule.

The important attractive forces are those between the adsorbed molecules themselves and those between the adsorbed molecules and the surface of the adsorbent. The important theories which have resulted follow. The idea of a monomolecular layer was described by Langmuir (L2) and another view of the monolayer as a two dimensional condensed film is that of Harkins and Jura (A1). Brunauer et al. (B11) extended the description of adsorption into the multilayer region. The

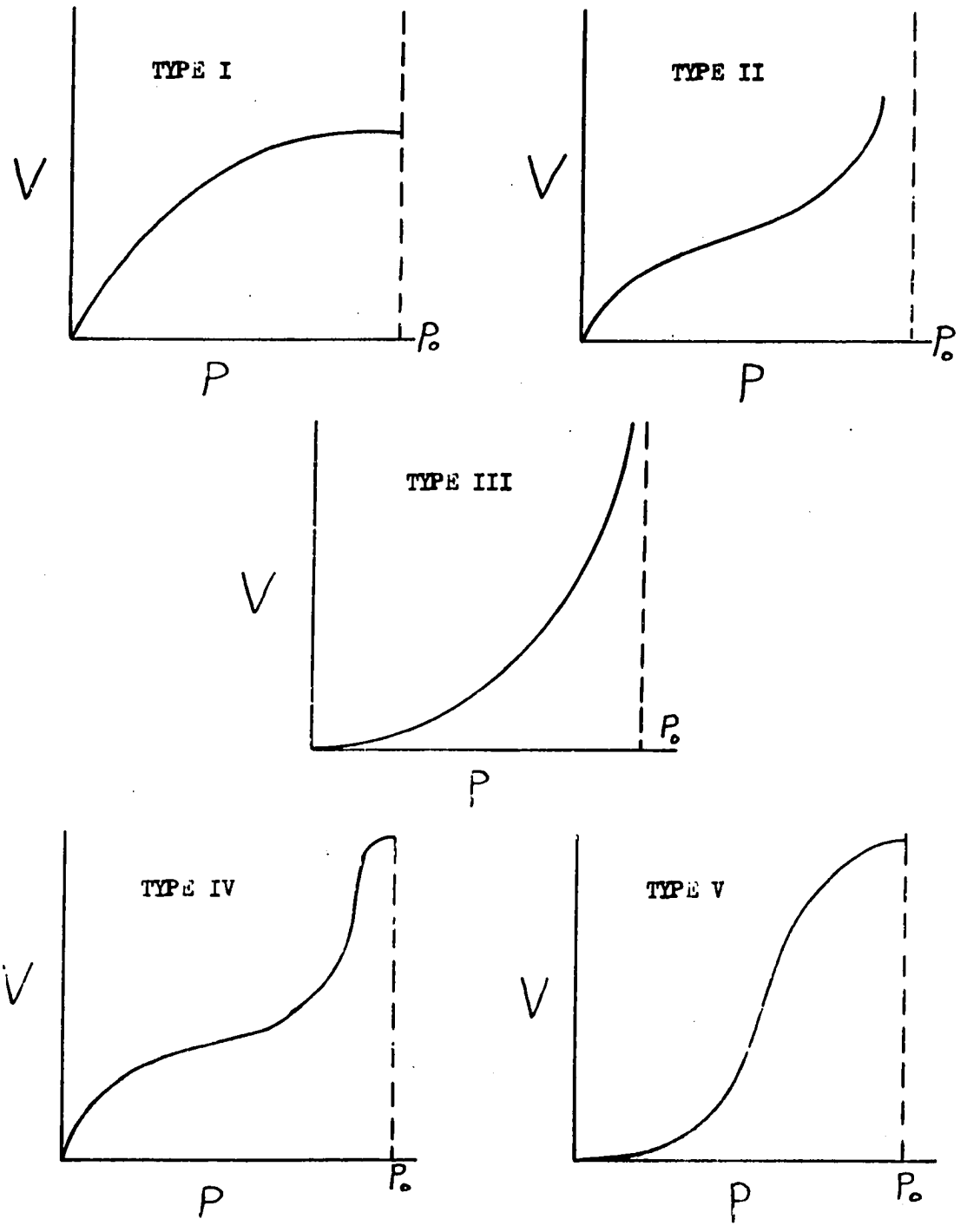


FIGURE 1. FIVE BASIC ISOTHERM SHAPES

importance of capillary condensation in cylindrical pores was proposed by Zsigmondy [see Adamson (A1)]. Polanyi (A1) considered the work involved in moving the adsorbate from the gas phase to the surface and consequently derived an adsorption potential for the adsorbate layer compressed by the surface attractive forces. This equation is quite useful to predict the effect of temperature on equilibrium capacities.

B. The Langmuir Monolayer Theory

In the theory of Langmuir (L2), the adsorbate molecules are believed attracted to active points on the surface of the adsorbent. By considering the dynamic equilibrium of this otherwise immobile layer with the molecules in the gas phase, Langmuir obtained the following relationship.

$$q^* = \frac{q_m K_L P}{1 + K_L P} \qquad (2\text{-}1)$$

where:

q^* = moles of gas adsorbed per unit weight of solid

q_m = adsorbate concentration of gas necessary to give a monolayer

P = vapor pressure of the gas in equilibrium

K_L = a constant.

This relation corresponds to the Type I isotherm. This relation has been redefined in terms of the maximum concentration for a particular gas composition in an adsorption column separation. If q_o^* is the solid phase concentration

that is in equilibrium with the maximum inlet gas concentration, P_o, represented as a partial pressure, then

$$\frac{q^*}{q_o^*} = \frac{(1 + K_L P_o)P}{(1 + K_L P)P_o} . \qquad (2\text{-}2)$$

Use is made of a dimensionless equilibrium parameter, r, defined in this case as

$$r = \frac{1}{1 + K_L P_o} . \qquad (2\text{-}3)$$

In terms of r the isotherm becomes

$$\frac{q^*}{q_o^*} = \frac{P/P_o}{r + (1-r)P/P_o} . \qquad (2\text{-}4)$$

This is also applied in terms of gas concentration in moles of component per unit volume of gas phase.

$$\frac{q^*}{q_o^*} = \frac{C/C_o}{r + (1-r)C/C_o} . \qquad (2\text{-}5)$$

The only available general treatment for dynamic adsorption in fixed beds is based upon this equation or a similar form as an equilibrium expression (V2).

When $r>1$, the Langmuir or Type I isotherm results. When $r<1$, the Type III isotherm form is obtained. These two isotherm shapes are very important in the behavior of dynamic adsorption in fixed beds.

C. The Multilayer Theory

A more general theory for adsorption isotherms is that developed by Brunauer, Emmett, and Teller (B11). The B.E.T. theory is the basis for the following equation. They considered molecular layers subsequent to the first to have vaporization and condensation properties of a liquid.

$$\frac{q^*}{q_m^*} = \frac{K_B P}{[P_o + (K_B-1)P][1-P/P_o]} \quad . \qquad (2\text{-}6)$$

This equation describes the Type 2 isotherm when $K_B>1$ and Type 3 when $K_B<1$.

In order to allow for a maximum of n molecular layers on an adsorbent surface because of pore size restrictions, Brunauer, Deeming, Deeming, and Teller (B12) proposed the following relationship.

$$\frac{q^*}{q_m^*} = \frac{K_B\ P/P_o}{1\ -\ P/P_o} \cdot \frac{1-(n+1)(P/P_o)^n + n(P/P_o)^{n+1}}{1+(K_B-1)(P/P_o)-K_B(P/P_o)^{n+1}} \quad . \qquad (2\text{-}7)$$

No one value of n is specific for any one material because of the wide variation in pore sizes, but calculated curves have the same limiting characteristics as experimental runs. This equation describes the Type 4 isotherm ($K_B>1$) and the Type 5 isotherm ($K_B<1$). When n equals 1, the above equation reduces to the Langmuir isotherm Type I.

For more detailed information on adsorption of gases for a single monolayer or less, the recent work by Ross and

Olivier (R3) considers the effects of surface heterogeneity on a mobile two-dimensional adsorbed phase and goes into more detail on adsorption potentials.

Young and Crowell (Y1) give a review of adsorption work since 1930 but this book is useful only as a reference for those quite familiar with recent work in statistical thermodynamics and the application of force potentials to describe interactions between adsorbate molecules.

D. Importance of Adsorption Equilibia for Dynamic Adsorption

In dynamic adsorption of gases we are at present only concerned with the description of the gas-solid equilibria as given by adsorption isotherms, empirical or otherwise. We are not concerned with a rigorous thermodynamic justification of the applicable isotherm because the equilibrium isotherm is used only to relate two-phase concentrations of the adsorbate molecule at the gas-solid interface. The isotherm equation chosen is one which can lead to a mathematical description of the dynamic adsorption process in conjunction with the continuity equation and the mass transfer rate equation. Only the linear or Henry's law isotherm and the Type I and III isotherms have been used in obtaining analytical solutions of the mass transfer process of adsorption.

In the adsorption of pentane and hexane from dilute solutions in natural gas, the Langmuir isotherm more nearly fits the equilibrium behavior. Heretofore in the analysis of

dynamic adsorption of hydrocarbons, only the linear relationship has been used. Since most isotherms are far from linear, the curved isotherm will be emphasized in this study (02).

In dynamic adsorption the isotherms control the growth rate of the mass transfer zone and are usually referred to as favorable, linear, or unfavorable. The Type I isotherm is favorable and causes the mass transfer zone to attain a constant length. The linear isotherm results in a mass transfer zone that grows in length proportional to the square root of the distance traveled through a fixed bed. The unfavorable, or Type III, isotherm produces a proportionate zone that is as long as the bed; i.e., the whole fixed bed is the transfer zone regardless of it's length. These basic concepts are very important in the analysis of fixed bed behavior.

CHAPTER III

RATE MECHANISMS OF ADSORPTION

If other parameters are held constant, the transport rates of molecules from the gas, into the solid pores, onto the solid surface, and along the surface, determine the mass transfer zone length. These transfer rates are usually expressed in terms of equations which show the rate as a function of the concentration gradient within the given phase. Only one or two transport phenomena may control the total transfer rate between the bulk gas phase and the dessicant particle interior.

A. Transfer Rate Equations

The two most important resistances are the diffusion through the fluid phase or stagnant gas film around the particle and the diffusion of adsorbate inside the particle. The molecular transfer rate through this gas film depends upon the molecular diffusivity of the component and the film thickness which is a strong function of the gas velocity past the particle.

The particle diffusion may be open pore diffusion, solid surface diffusion, or both concurrently. In dessicants

with small pores and a large surface area, the surface diffusion usually controls the transfer within the particle except at very small surface concentrations of adsorbates.

Reaction or phase change in some exchange processes may contribute to mass transfer rate, but this is not likely in natural gas adsorption. Nevertheless the form of the reaction rate equation yields a solution which empirically is very important as a general adsorption solution.

1. Fluid-phase External Diffusion

This is sometimes called film diffusion in which there is counter diffusion of A from the bulk fluid to the outer surface of the solid particle and of B from the particle to the bulk fluid. The rate of mass transfer of A from the gas stream to the outer surface of the particle may be expressed by:

$$\frac{dq_A}{dt} = k_f a_p \frac{\epsilon}{\rho_B} (C_A - C_A^*) \qquad (3\text{-}1)$$

where:

k_f = fluid phase mass transfer coefficient

a_p = external area of particles per unit bulk volume of the packed tower

ϵ = fraction of external voids

t = time

ρ_B = bulk density of the packing

2. Fluid-phase Pore Diffusion

This occurs in porous bodies whose pores are freely accessible to the bulk fluid outside. There can be counter diffusion of A through the pores of the particle to the point where exchange occurs and of B from the pore surface back to the outer surface of the particle. For a sphere the pore-diffusion rate adapted from Barrer (B1) is

$$D_{pore}\left(\frac{\partial^2 C_i}{\partial r^2} + \frac{2}{r}\frac{\partial C_i}{\partial r}\right) = \chi\frac{\partial C_i}{\partial t} + \rho_P\frac{\partial q_i'}{\partial t} \qquad (3\text{-}2)$$

where:

D_{pore} = diffusivity

ρ_P = density of adsorbent particle

C_i = fluid phase concentration of component within the particle at radius

χ = void fraction of pores within particle

q_i' = $q_i - \chi C_i$ which will generally be in equilibrium with C_i.

The mean concentration of the particle, of total radius r_P, is

$$q = 3/r_P^3 \int_o^{r_P} q_i\, r^2\, dr \; . \qquad (3\text{-}3)$$

These equations are normally written for the component being adsorbed.

3. Reaction or Phase Change

Desorption of B from the solid phase at a pore surface or at the outer surface occurs with the adsorption of A in its place.

This is represented by a reaction rate equation (V2)

$$\frac{d(qA)_i}{dt} = k_i \left\{ C_A\left[(q_A)_o - (q_A)_i\right] - r(q_A)_i\ (C_o - C_A) \right\} \quad . (3\text{-}4)$$

Here $(q_A)_i$ is the solid-phase concentration at the surface, and k_i is the rate of surface reaction which is usually very fast compared to mass transfer rates, so that experimental values of k_i are not known. When this surface-reaction equation is used empirically for the entire rate behavior, as will be discussed later, k_i is to be replaced by k_{kin}.

4. Solid-phase Internal Diffusion

This is sometimes called particle diffusion. This includes diffusion through a homogeneous, permeable (absorbing) non-porous solid, diffusion in a mobile, adsorbed phase covering the pore surfaces of a porous solid whose crystalline portion is impermeable, or diffusion in an absorbing fluid held in the pore spaces of a solid.

The rate of internal diffusion is expressed by

$$D_p\left(\frac{\partial^2 q_i}{\partial r^2} + \frac{2}{r}\frac{\partial q_i}{\partial r}\right) = \frac{\partial q_i}{\partial t} \quad . \qquad (3\text{-}5)$$

Here D_p is the diffusivity and q_i is the solid-phase concentration at radius r. This equation has been solved only for the irreversible [see Vermuelen (V2)] and linear equilibrium cases (R2) of fixed bed operation. It is usually approximated by the linear-driving-force relation (G6)

$$\frac{dq_A}{dt} = k_p a_p (q_A^* - q_A) \qquad (3\text{-}6)$$

where $k_p a_p (=60\ D_p/d_p^2)$ is the mass transfer coefficient, q_A is the concentration of A averaged over the particle, and q_A^* is the concentration the particle would have if it were in equilibrium with the instantaneous, fluid-phase concentration at the outer surface of the particle.

B. Mass Transfer Rate Studies

Correlations have been made for transfer rate coefficients. Most of these have considered only fluid phase diffusion to be the controlling transfer resistance. More recent studies tend to place a greater emphasis on the adsorbed phase diffusivity (C4,C6).

1. External Fluid-Phase Mass Transfer

External fluid-phase diffusion rates appear to conform to the general mass-transfer correlations as developed by Wilke and Hougen (W5) for gases. Evidence of this general agreement has been provided by Dryden [see Vermuelen (V2)], who found an additional resistance attributable to pore

diffusion, Dodge and Hougen (D5) and Eagleton and Bliss (E2). The correlation of Wilke and Hougen, for example, in the present notation is

$$k_f = \frac{U}{H_f a_p} = 1.82\, U\left(\frac{d_p U \epsilon \rho}{\mu}\right)^{-0.51} \left(\frac{\mu}{\rho D_f}\right)^{-0.67} \qquad (3\text{-}7)$$

where U is mean linear velocity; $U\epsilon$ is the superficial velocity; H_f is the height of a transfer unit (or H.T.U.), μ is the viscosity of the fluid; D_f is the bulk diffusivity of the solute in the fluid; d_p is the effective particle diameter, and ρ is the density of the fluid.

2. Internal Diffusion Rates

Internal diffusion rates include both pore diffusion and adsorbed phase mobility. They are placed together here since the movement takes place inside the particle, and the gas effluent behavior does not distinguish between them.

Wheeler (W3) discussed the theory and relations for pore diffusion. For gases in fine pores and dilute solutions, Knudsen-flow diffusion is encountered if the molecular mean free path is larger than the pore radius.

Carman and others (H5 , C4, C6, F3, G5) have studied the flow of gases and vapors through adsorptive plugs formed from compressed non-porous carbon and silica powders. Figure 2 is a representation of Carman's (C6) results with a curve of surface diffusion coefficients of adsorbed Freon as a function of its concentration on Linde silica plugs. In the

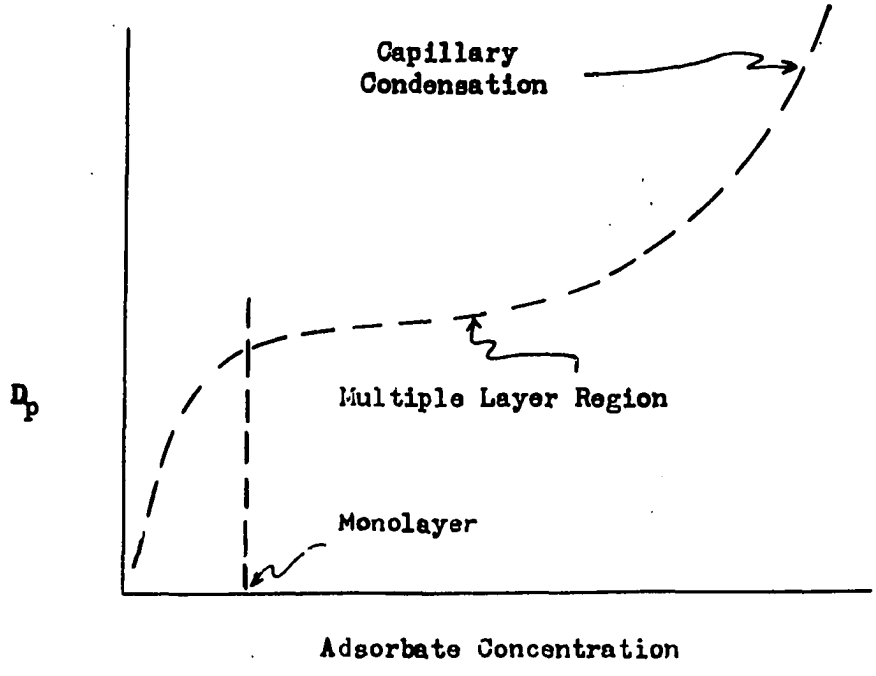


FIGURE 2. PARTICLE DIFFUSION COEFFICIENT

region where the adsorbate concentration is less than a monolayer, the diffusion rate is least but it increases with concentration. In this region the activation energy for surface diffusion is highest. After formation of the monolayer, the diffusion coefficient remained essentially constant during formations of further layers. An increase takes place when capillary condensation began. Studies in activated charcoal by Flood et al. (F3) and by Gilliland et al. (G5) on unsintered Vycor glass show similar characteristics. Carman (C2) claculated pressure differences across plugs in the condensate from the Kelvin equation and therefore the permeability for liquid flow. These values for freon and sulphur dioxide on silica agreed within 20% of the permeabilities calculated from the Kozeny equation used for viscous flow.

When considerable adsorption of vapor occurs, flow rates of the adsorbed phase can be many times that possible from only gaseous flow in the pores. Figure 3 for freon in silica plugs shows the effect of reduced pore size (lower porosities) in reducing gas phase porous diffusion and increasing adsorbed phase flow.

From this view of internal diffusion, a correlation of solid phase transfer coefficients should show a dependence upon concentration of the adsorbate in the gas phase and the adsorbate capacity of the particle.

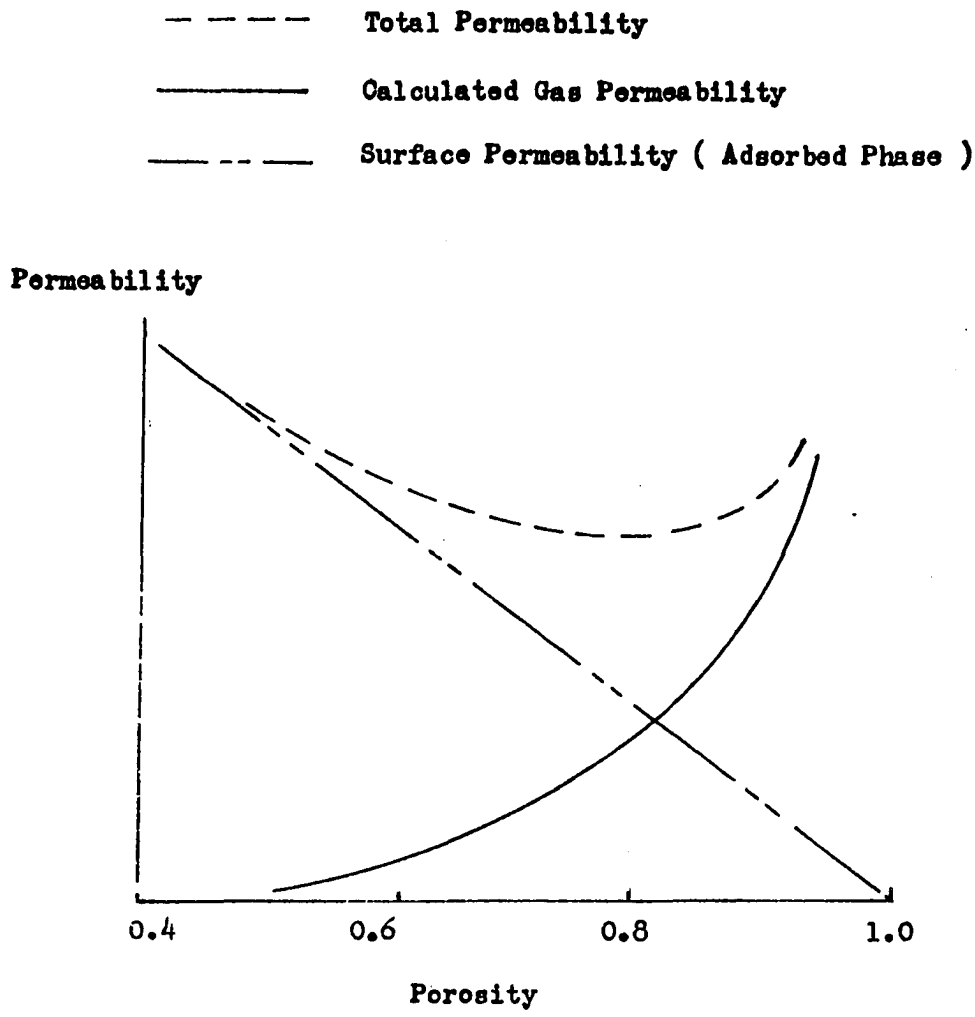


FIGURE 3. EFFECT OF POROSITY ON ADSORBENT PERMEABILITY

CHAPTER IV

DYNAMIC ADSORPTION PROCESSES

The most important concept developed in recent years is the effect of the isotherm shape on the form of the effluent concentration-time curve which reflects the adsorption zone behavior.

During adsorption a fixed bed of dessicant usually consists of three zones A, B, and C. The first zone, A, near the entrance of the bed is completely saturated with the incoming gas. At the end of the bed, zone C is free of the adsorbing constituent. In the remaining zone, B, transfer of the adsorbable constituent is occurring.

As time passes this transfer zone will move toward the end of the bed. When it reaches the end, the adsorbing constituent composition in the effluent gas will rise depending upon the mass balance of material in the gas stream and in the solid phase, the mass transfer rate between phases, and the equilibrium behavior of the component in the gas and solid phases.

A. Nomenclature

The notations of Vermuelen (V4), will be used in the presentation and development of the continuity equation and the important mathematical descriptions of adsorption in a fixed bed.

1. Concentration Nomenclature

q = moles solute per pound of dessicant

q_o = solute capacity of dessicant at C_o

C = moles solute per cubic foot of gas

C_o = inlet concentration to tower of solute in gas

$x=\frac{C}{C_o}$ = dimensionless concentration of solute in gas

$y=\frac{q}{q_o}$ = dimensionless concentration of solute on solid dessicant

r = equilibrium parameter to express relationship between x and y

$$y = \frac{x}{r + (1-r)x} \quad . \tag{4-1}$$

2. Column and Flow Parameters

v = column volume, ft^3 = hS

h = height of tower, ft

S = superficial cross section area, ft^2

ϵ = bulk porosity of packing

$v\epsilon$ = effective fluid volume of tower, ft^3

F = volumetric flowrate of gas, cubic feet/minute

$\frac{v\epsilon}{F}$ = residence time for gas, min.

$U=\frac{F}{S\epsilon}$ = linear flowrate, ft./min.

V = total volume of gas that has entered column at time, t, cu. ft.

$V-v\epsilon$ = total volume of gas that has passed out of column at time, t, cu. ft.

ρ_B = bulk density of dessicant in column, lb./ft.^{3}

$q_o\rho_B v$ = stoichiometric capacity of column, lb. moles solute

D = distribution ratio - a limiting saturation value for tower

$$D = \frac{q_o \rho_B}{C_o \epsilon} . \qquad (4\text{-}2)$$

3. Dimensionless Time and Distance Parameters

N = number of transfer units - dimensionless distance

a. for external diffusion

$$N_f = k_f a_p \, v \epsilon / F . \qquad (4\text{-}3)$$

b. for internal particle diffusion

$$N_p = k_p a_p \, Dv\epsilon / F . \qquad (4\text{-}4)$$

Z = throughput ratio - this value reaches unity when the volume of feed which has passed through the column contained an amount of the component adsorbed numerically equivalent to the adsorption

capacity of the column

$$Z = \frac{V - v\epsilon}{V_{stoic}} = \frac{C_o(V - v\epsilon)}{q_o \rho_B v} = \frac{V - v\epsilon}{Dv\epsilon} \qquad (4\text{-}5)$$

θ = time modulus

$$\theta_f = N_f Z \qquad (4\text{-}6a)$$

$$\theta_p = N_p Z \qquad (4\text{-}6b)$$

B. Material Balance - The Continuity Equation

The continuity equation for an infinitesimal thickness of bed at any given cross section v demands that any loss of component A from the solution flowing through the thin section must equal the gain of component A on the solid and in the solution in that section.

$$-\left(\frac{\partial C_A}{\partial v}\right)_V = \rho_B \left(\frac{\partial q_A}{\partial V}\right)_v + \epsilon \left(\frac{\partial C_A}{\partial V}\right)_v \qquad (4\text{-}7)$$

By replacing the feed volume V with the volume of solution which has passed through the column, $V - v\epsilon$, equation (4-7) simplifies to:

$$-\left(\frac{\partial C_A}{\partial v}\right)_{V - v\epsilon} = \rho_B \left(\frac{\partial q_A}{\partial V}\right)_v \qquad (4\text{-}8)$$

which can also be expressed as

$$-\left(\frac{\partial x}{\partial v}\right)_{Zv} = \left(\frac{\partial y}{\partial Zv}\right)_v \qquad (4\text{-}9)$$

or as

$$-\left(\frac{\partial x}{\partial N}\right)_{ZN} = \left(\frac{\partial y}{\partial ZN}\right)_{N} \qquad (4\text{-}10)$$

The special behavior of the fixed bed adsorption process is reflected by this continuity equation rather than by the rate equations used with it.

C. Fixed Bed Behavior

The behavior of the fixed bed adsorption process will be examined for different types of controlling isotherms. The three main types of behavior are the proportionate pattern case for the unfavorable isotherm, the constant pattern case for the favorable isotherm, and the intermediate case for the linear isotherm. Since the first two cases are generally solved as limiting or asymptotic equations, a section is also added concerning the empirical use of the reaction rate equation for adsorption. This has been solved to give the column dynamics for the time before a constant or proportionate pattern has been reached.

1. Proportionate-Pattern Case (Unfavorable Equilibrium)

This case has been treated by De Vault (D4), Walter (W2), Wilson (W7), and Weiss (V2). It is assumed in this case that equilibrium is maintained everywhere in the column, that is, that N approaches infinity due to high mass transfer rates or to long residence times. For the case of a constant

equilibrium parameter r, first treated by Walter (W2), the solution is

$$x = \frac{(r/Z)^{\frac{1}{2}} - r}{1 - r} \quad . \tag{4-11}$$

The limits of validity are: $x = 0$ at $Z = \frac{1}{r}$ and $x = 1$ at $Z = r$. This solution gives a proportionate pattern curve for concentration because x depends on Z only and not upon N or v. In this case the relative sharpness of the breakthrough curve cannot be increased by lengthening the column. For the weak adsorption of this case where $r<1$, the whole bed behaves as an adsorption zone. This case is unimportant in hydrocarbon adsorption but is important in desorption and may give important information if used with Equation 4-27. For $r \leq 1$, Equation 4-11 does not apply. For $r \geq 10$ the equation will apply at all N values greater than 10. Where $1<r<10$, the general result, Equation 4-27 should be used.

2. Constant-Pattern Case (Favorable Equilibrium)

If a stable length zone is assumed, the continuity equation reduces to:

$$y = x \quad . \tag{4-12}$$

a. <u>Fluid phase diffusion controlling.</u> Equation 3-1 in dimensionless form is:

$$\frac{dy}{d(ZN_f)} = x - x^* \quad . \tag{4-13}$$

In combination with Equation's 4-12 and 4-1, Equation 4-13

integrates for a particular N_f to:

$$\frac{1}{1-r} \ln \frac{x_2(1-x_1)}{x_1(1-x_2)} + \ln \frac{1-x_2}{1-x_1} = N_f(Z_2-Z_1). \qquad (4\text{-}14)$$

This equation was first solved by Michaels (M5) and has been applied by Dale, et al. (D1) to hydrocarbon adsorption.

b. Particle diffusion controlling. Equation 3-6 in dimensionless form is

$$\frac{dy}{d(ZN_p)} = y^* - y \qquad (4\text{-}15)$$

and in conjunction with Equations 4-1 and 4-12 integrate for a particular N_p to

$$\frac{r}{1-r} \ln \frac{x_2(1-x_1)}{x_1(1-x_2)} + \ln \frac{(1-x_1)}{(1-x_2)} = N_p(Z_2-Z_1) . \qquad (4\text{-}16)$$

This was first solved by Glueckauf and Coates (G6), but has not been applied to natural gas adsorption.

3. Reaction-rate Solution

The empirical limiting case for the kinetics of surface reaction as the controlling mechanism has been derived from Equations 3-4 and 4-12 to give

$$\frac{1}{1-r} \ln \frac{x}{1-x} = N_R(Z-1). \qquad (4\text{-}17)$$

This result was also obtained by Walter (W2) and Sillén (S4) and much earlier in the case of r = 0 by Bohart and Adams (B7). This is said to be useful in preliminary

investigation of data when the rate mechanism is not known (V4).

4. Column Dynamics Under Linear Equilibrium

Linear equilibrium involves constant-separation-factor conditions with the value of r equal to unity. When r=1, the same form of equation is obtained from several rate-determining mechanisms. For external diffusion, internal diffusion, pore diffusion, and the surface reaction expression, the same dimensionless equation results. In each case

$$\left(\frac{\partial Y}{\partial ZN}\right)_N = x - y \quad . \tag{4-18}$$

Integration of this equation with Equation 4-10 has been carried out by several people (V2 , H4, M6). The results can be expressed as

$$x = J(N,ZN) \tag{4-19}$$

$$y = 1 - J(ZN,N) \tag{4-20}$$

where the function, J, of two variables s and t is given by

$$J(s,t) = 1 - \int_o^s e^{-t-\xi} I_o(2\sqrt{t\xi})\, d\xi \tag{4-21}$$

where I_o is a modified Bessel function of the first kind. The limits of this function are

$$J(0,t) = 1 \quad ; \quad J(s,0) = e^{-s}$$

$$\lim_{s\to\infty} J(s,t) = 0 \quad ; \quad \lim_{t\to\infty} J(s,t) = 1 \quad .$$

In the region where the variables of the argument are both greater than 10, use has been made of an asymptotic expansion suggested by Onsager (V2) and given by Thomas (T1) which reduces to:

$$J(s,t) = \tfrac{1}{2}\left\{1 + \operatorname{erf}(\sqrt{t} - \sqrt{s}) + \frac{e^{-(\sqrt{s} - \sqrt{t})^2/4}}{(\sqrt{t} + \sqrt{st})}\right\} \quad (4\text{-}22)$$

accurate to within 1% when $\sqrt{st} \geq 6$, where (for any number Z)

$$\operatorname{erf}(Z) = \frac{2}{\sqrt{\pi}} \int_0^Z e^{-n^2}\, dn \quad (4\text{-}23)$$

as given in standard tables. At $\sqrt{st} \geq 60$, the last term of Equation 4-22 can be dropped. Plots of the J function are given by several authors (H3, V2, K5). At r = 1, combinations of the rate equations can be made by adding transfer resistances, for instance

$$\frac{1}{k_{kin} C_o} = \frac{D}{k_f a_p} + \frac{1}{k_p a_p} . \quad (4\text{-}24)$$

The mathematical results are still the same as Equations 4-19 and 4-20.

The exact integration of Equation 3-2 or 3-5 for r = 1, has in conjunction with Equations 4-24 and 4-10, been performed by Rosen (R2) and by Kasten et al. (K2). The results are available in graphical and tabular form (R2). Rosen's variables have the following correspondence

$$x = \frac{N_p}{5} , \quad \frac{Y}{x} = \frac{2}{3} Z , \quad \frac{x}{v} = N_f .$$

Rosen and also Wicke (V2), have given an asymptotic relation for solid-phase diffusion or for pore diffusion, at r = 1, which can be expressed as

$$x = \tfrac{1}{2}\left[1 + \text{erf } \tfrac{1}{2}\sqrt{N}\,(Z-1)\right] \qquad (4\text{-}25)$$

Equation 4-22 gives for the same cases

$$x = \tfrac{1}{2}\left[1 + \text{erf } \sqrt{N}\,(\sqrt{Z} - 1)\right] \qquad (4\text{-}26)$$

If Z is near unity, these two expressions are numerically equivalent.

This case which assumes a linear isotherm has been applied more often to natural gas adsorption than any other. Even though experimental results have contradicted this theory, the equation is still used for analysis. It is therefore not surprising that correlations based on this theory are no better than they are.

5. Column Dynamics with an Equilibrium Parameter, r

The most general relation that has been developed for breakthrough behavior is that of H. C. Thomas (T1) which includes the equilibrium parameter r as an independent variable along with the number of transfer units, N_R, and the throughput ratio , Z. Equations 3-4 and 4-10 have been solved to give

$$x = \frac{J(rN_R, ZN_R)}{J(rN_R, ZN_R) + e^{(r-1)N_R(Z-1)}\left[1-J(N_R, rZN_R)\right]} \qquad (4\text{-}27)$$

and a similar relation for y (V2, eq. 156). An extensive graphical representation of x has been given by Hiester and Vermuelen (H3) and numerical values have been computed and tabulated by Opler and Hiester (O1).

Equation 4-27 contains only the J function as a limiting case at r = 1. This equation also has been shown to reduce to the constant pattern result (Equation 4-17) with $r \ll 1$, and to the proportionate- pattern result (Equation 4-11) with $r \gg 1$, in work by Heister and Vermuelen (H3) and Gilliland and Baddour (G4). Goldstein (G7) has reviewed this result from a mathematical viewpoint; and has presented limiting forms which give accurate approximations in certain regions. His variables u, s, and y correspond respectively to x, N, and ZN in this writing.

By reference to this solution all other solutions are found to be classifiable in terms of their r and N values. This equation can be used to check the validity of the limiting equations for the constant pattern zone. In other words, it can be seen how far the adsorption zone, or front, is from stabilization, or how much error is involved in assuming stabilization for a given system and operation.

For the above kinetic expression, the variable, N_R, is defined by:

$$N_R = k_{kin}\, C_o D v \epsilon / F \ . \qquad (4\text{-}28)$$

The transfer Coefficient, $k_{kin}C_o$, is used empirically as a

combined transfer coefficient which is related to the particle and gas phase coefficients by:

$$\frac{b}{k_{kin}C_o} = \frac{D}{k_f a_p} + \frac{1}{k_p a_p} . \qquad (4\text{-}29)$$

The parameter b is primarily a function of r and is described more thoroughly in Appendix G.

In conjunction with the combined mechanism equation in Appendix G, this solution will be used to analyze the experimental data of this research study. Its very nature, although empirical, makes it the most valuable solution available for unstable adsorption zone behavior with non-linear isotherms.

CHAPTER V

EXPERIMENTAL MATERIALS AND PROCEDURE

Dry city gas was supplied at a pressure of 70 to 100 psig by an Oklahoma Natural Gas Company line laid to the Natural Gas Engineering Laboratory on the North Campus of the University of Oklahoma. A typical gas analysis showed the following composition:

Component	Mole %
C_1	88.37
C_2	9.85
C_3	1.70
I-C_4	.01
n-C_4	.003
I-C_5	.06

The equipment components used were located as shown in the Flow diagram, Figure 4.

The incoming dry gas entered a spherical separator. Gas could also be returned to this separator from the orifice meter run. The dry gas from the supply line was compressed to 800 psig and passed through the horizontal carbon dessicant bed to remove the heavier hydrocarbons, principally butane,

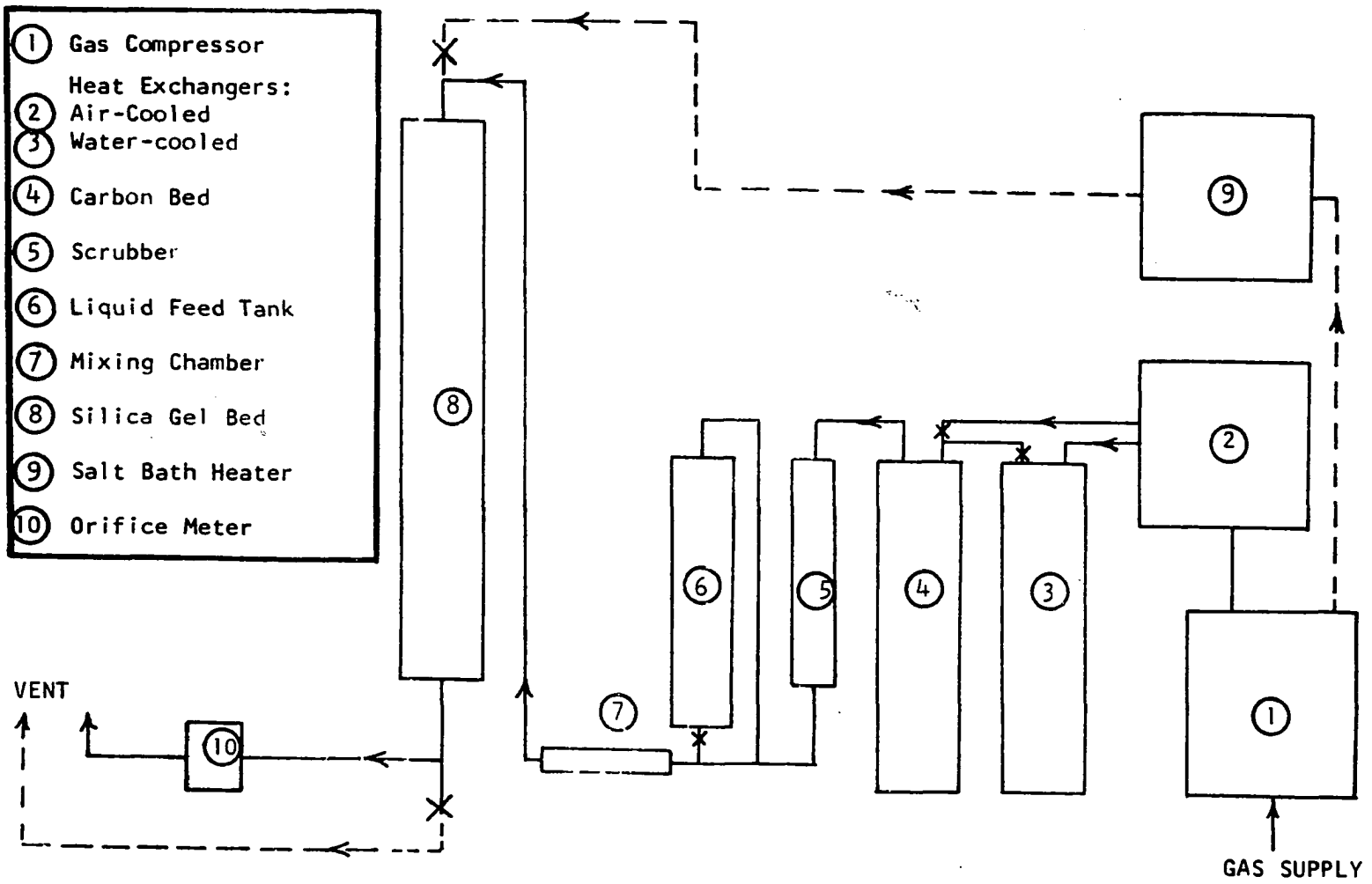


FIGURE 4

DYNAMIC ADSORPTION FLOW SYSTEM

pentane, and hexane.

The gas passed through an air-cooled heat exchanger and a water-cooled heat exchanger to cool the outlet compressor gas to a temperature of 90°F. For the winter season a valve had to be installed to allow a certain amount of bypassing around the air cooler to maintain a temperature as high as 90°F. (See Figure 4.) For summer ambient temperatures, water from an evaporative cooling tower was circulated through the water-cooled heat exchanger in order to maintain the temperature at the level of 90°F.

The gas flow rate was controlled by changing compressor loading and by regulating a bypass valve between the suction and pressure headers near the compressor. When the proper gas flow rate was obtained as indicated by the differential and static pressure on the orifice meter, a liquid hydrocarbon, either normal pentane or normal hexane, was added to the flowing gas downstream of the carbon bed. During this adjustment period in the run, the gas is vented to the atmosphere. The liquid feed rate was adjusted by a needle control valve to give a specific composition for the component. When the pentane or hexane composition reached the correct value and remained constant for a period of ten minutes, the gas stream was turned through the silica gel column. The relative value of the component's composition in the gas was recorded automatically every 2 minutes and forty seconds by the recorder attached to the chromatographic analyser. The

chromatograph analysed the rich inlet gas at first. After the gas was turned through the tower, the tower effluent gas was analysed.

The time at which the gas was turned into the tower was recorded, and the relative value of the pentane or hexane effluent composition was recorded throughout the length of the run. The run was over when the outlet gas composition from the tower reached a constant value in the range of the inlet composition.

During the run pertinent data were recorded. This included chromatograph readings for supply gas and feed gas, outlet pressure and inlet temperature, static pressure and differential pressure for the orifice meter, and liquid feed tank level. From these readings the appropriate data were calculated for analysis.

A gas gravitometer was used to detect any major changes in supply dry gas gravity and feed gas gravity. This sometimes detected liquid at the sample end, and would also indicate important variations in liquid feed rate to the gas.

After a run was completed, the silica gel bed was regenerated by dry gas passed through a salt bath heater to a temperature of 500°F to 575°F. This provided an inlet temperature to the tower about 50°F less because of the heat losses between the heater and silica gel bed. The bed was normally heated by gas flowing at a superficial velocity of 40 to 50 ft./min. The temperature reached in the bed usually

ranged from 400°F to 500°F. The regenerative gas flow direction was the same as that for the adsorption process.

After two runs the carbon bed was also regenerated to an outlet temperature of 400°F. The gas from both regenerations was vented to the atmosphere.

The beds were cooled by circulating dry gas through the beds and the air-cooled heat exchanger before the next run. The carbon bed was normally regenerated at night so that some of the heat could be lost by radiation and conduction to the atmosphere. The carbon bed was located outside the gas lab building as were all the heaters and heat exchanger equipment.

The liquid feed tank was refilled manually each time with either pentane or hexane for the next run.

The silica gel was changed twice in the 14.65 foot towers for the first group of runs listed in the tables (Numbers 90 and below). Additional runs were made a year later to clarify the data analysis.

The liquids used in the runs were commercial grade n-pentane and n-hexane manufactured by the Phillips Petroleum Company which are guaranteed 95% pure hydrocarbon.

The Silica Gel, Grade No. 03, was supplied by the Davison Chemical Company. The general properties of this gel are listed in Table II.

The experimental data from these test procedures are presented in Appendix A. These results are analysed in Chapter VI which follows.

TABLE I

PHYSICAL AND CHEMICAL CHARACTERISTICS

OF SILICA GEL

Typical Analysis - Dry Basis

Component	Weight Percent
Silica as SiO_2	99.71
Iron as Fe_2O_3	.03
Aluminum as Al_2O_3	.10
Titanium as TiO_2	.09
Calcium as CaO	.01
Sodium as Na_2O	.02
Zirconium as Zr_2O	.01
Trace Elements	.03
	100.00
Total Volatile at 1750° F	5.0 to 6.5 %
Specific Heat	0.22 Btu/lb/°F
True Density of Silica (no porosity)	137 lbs/cu. ft.
Thermal Conductivity	1 BTU/sq.ft./hr/°F/in
Reactivation Temperature Range (350° F bed temperature is adequate for most uses)	250 - 600° F

TABLE II

PROPERTIES OF SILICA GEL, GRADE 03

Sieve Analysis

Mesh Size	Weight Fraction
3-4	.189
4-6	.454
6-8	.318
Fines (through 8 mesh)	.037
	.998

Bulk Density - lbs/cu. ft.	45.0
Total Volatile Percent at 1750°F (max.)	6.0
Surface Area (sq.meters/gm) (precision ± 25 m^2/gm at 95% basis)	750-800
Pore Volume - cc/gm (precision ± .02 cc/gm)	0.43
Calculated Average Pore Size	22 Angstrom Units

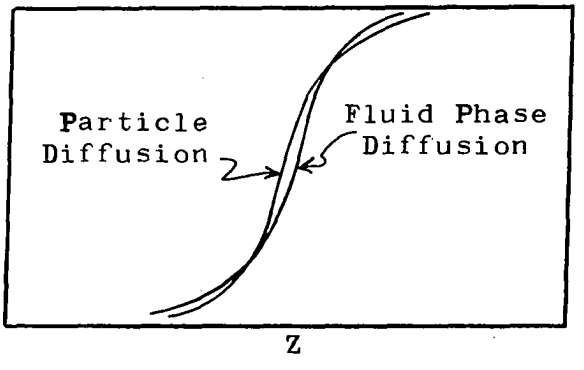
CHAPTER VI

ANALYSIS OF EXPERIMENTAL DATA

A stabilized zone concept has been used in the analysis of dynamic hydrocarbon adsorption in the literature (D1), but the influence of the equilibrium adsorption isotherm upon the effluent curve was neglected. This equilibrium isotherm influences the shape of effluent curves as shown in Figure 5 when $r<1$. This shape is more throughly discussed in Appendix I.

FIGURE 5

TYPICAL EFFLUENT CURVE $\frac{C}{C_o}$



This analysis will show that particle diffusion is the controlling transfer mechanism. The calculated effluent curves for transfer controlled by particle diffusion match the effluent data best. Moreover, the calculated particle transfer coefficient is a function of adsorbate concentrations as theory

demands.

Effluent data curves were first matched with master curves calculated according to the constant zone length model. The effluent curves were assumed stable, but the calculated results did not agree with all of the theory. The disagreement occurred because constant transfer zone lengths were not obtained in all of the experimental runs. The results of this first evaluation are presented below.

In order to evaluate mass transfer coefficients an approach was needed to analyze the transient effluent curve. The Thomas Equation (Equation 4-27) provided this approach. The midpoint slopes of all effluent curves were evaluated. These slopes were corrected to the stabilized or limit value using the Thomas equation. The combined mass transfer coefficient was calculated with the corrected slope. The combined mass transfer coefficient is equivalent to a combination of the fluid phase diffusion and particle diffusion coefficients. The equation for resistances in series is modified because of the non-linear isotherm. The modifying parameter, b, depends mainly upon r and is discussed below. The fluid phase diffusion coefficient was calculated according to the correlation of Wilke and Hougen (W5). The particle diffusion coefficient was then calculated from the combined resistances equation.

The following analysis is presented as (1) an evaluation of the equilibrium parameter, r (2), the results of a first analysis assuming a stabilized zone (3), correction of

the effluent curve midpoint slopes for transient condition (4), calculation of the gas phase mass transfer coefficient (5), calculation of the "b" parameter for combined transfer resistances, and (6) calculation of the particle mass transfer coefficient.

A. Evaluation of the Equilibrium Parameter, r

The equilibrium isotherms for pentane and hexane are not straight lines. A straight line relationship has been assumed in several previous analyses of fixed-bed adsorption data. The adsorption equilibrium isotherms were replotted in order to obtain the parameter, r. This parameter - a measure of the curvature of the isotherm - is described by Equation 4-1. For pentane, the values of 1.69 mole percent and 0.1461 grams pentane per gram dessicant were chosen for C_o and X_{T_o}, respectively. All adsorption values were calculated as ratios (C/C_o, $\frac{X_T}{X_{T_o}} = \frac{q}{q_o}$) to these large numbers, and plotted on a log-log graph as shown in Figures 6 and 7. On this graph were also plotted calculated K curves. (K is equal to the reciprocal of r.) The equilibrium adsorption values were scattered, and values of K for hexane and pentane were chosen by visual interpretation. The K values chosen for hexane and pentane were 2.5 and 1.5 respectively, which gives r values of 0.4 and 0.667. These equilibrium parameters were used in the following analysis of the data.

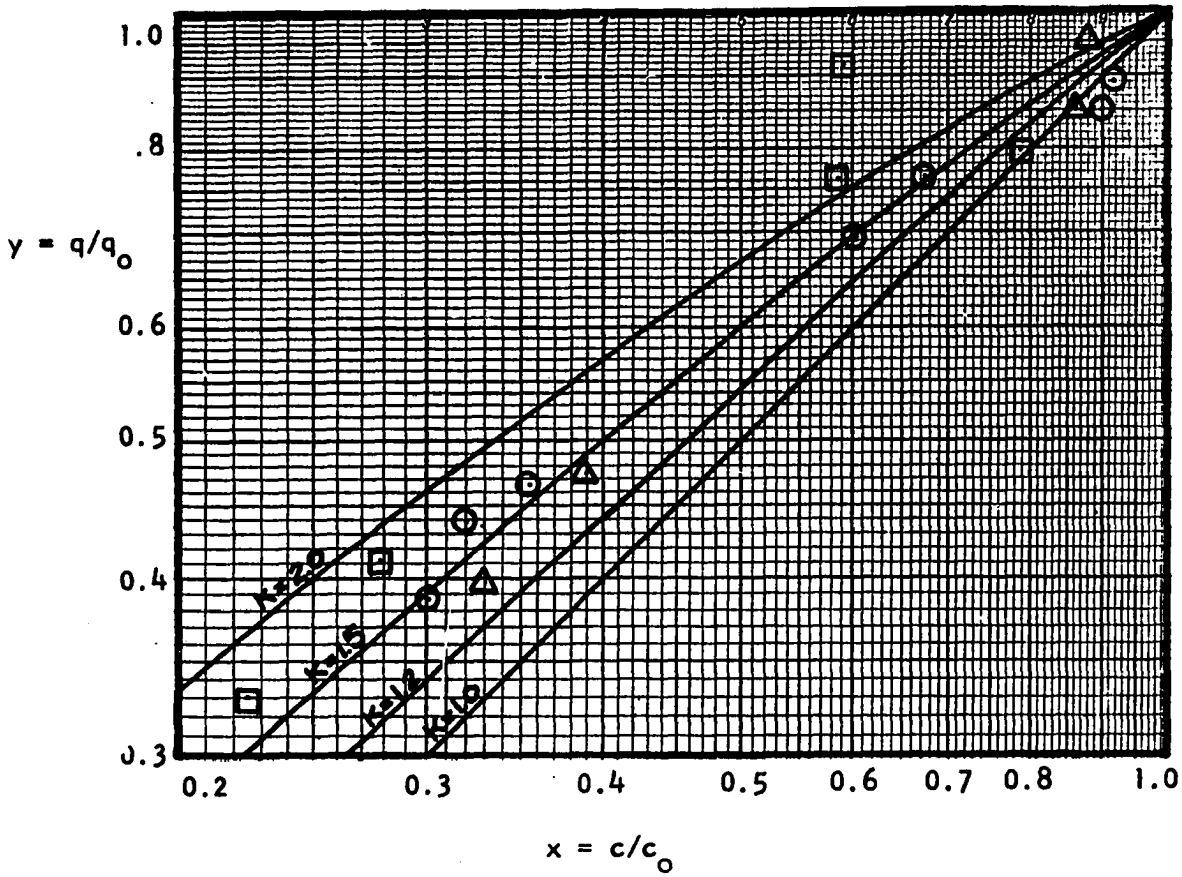


FIGURE 6 - EVALUATION OF r PARAMETER - PENTANE

⊡ HIGH VELOCITY

⊙ MEDIUM VELOCITY

△ LOW VELOCITY

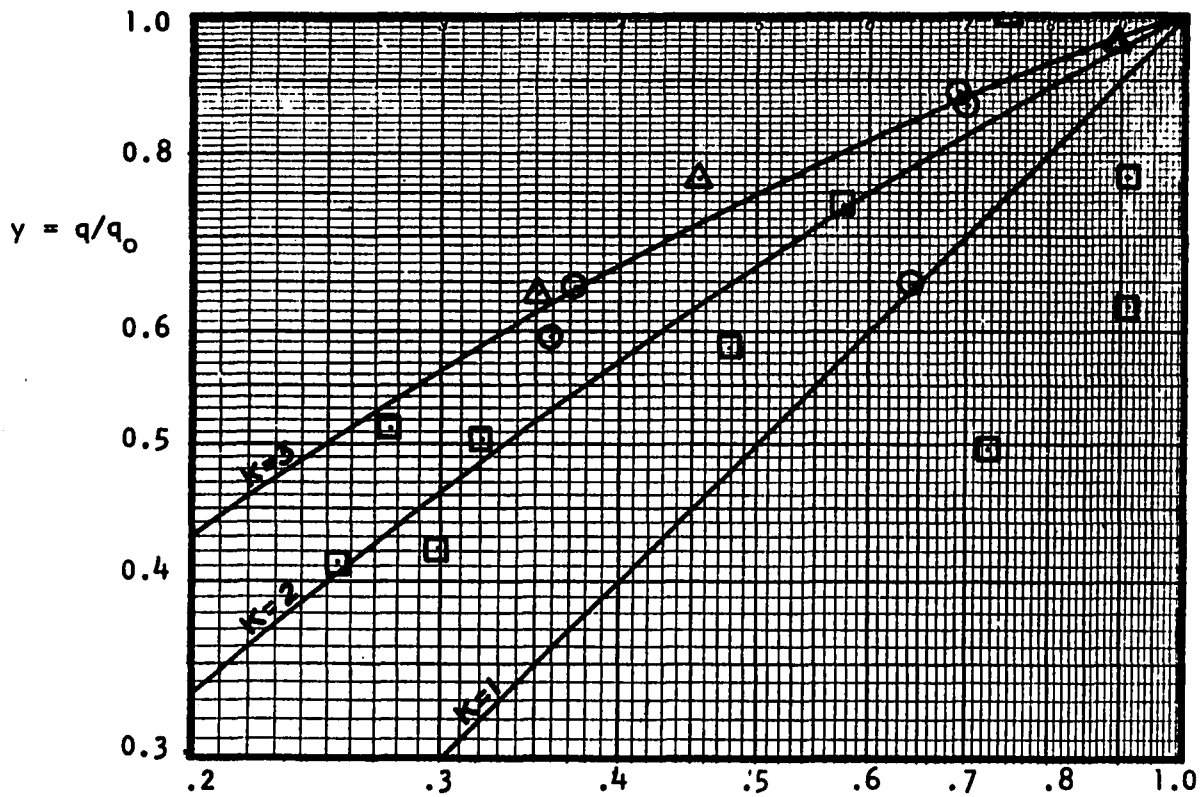


FIGURE 7 - EVALUATION OF r PARAMETER - HEXANE

⊡ HIGH VELOCITY

⊙ MEDIUM VELOCITY

△ LOW VELOCITY

B. Analysis Assuming Stabilized Zones

Generalized master curves were constructed on the basis of stabilized transfer zones to compare with effluent data. These curves calculated from Equations (4-14) and 4-16) are discussed in Appendix J. The shape of the hexane effluent curves showed that particle diffusion controlled the mass transfer. The effective difference in effluent curve shape for the two mechanisms, gas phase diffusion and particle diffusion, is discussed in Appendix I. The master curves based on fluid phase diffusion did not match the actual curves well enough to give a correlation. The evaluated particle transfer coefficients are presented in Figures 8 and 9. The theory of adsorption transfer states that the particle transfer coefficient is a function of adsorbate concentration, but it is not a function of velocity. Consequently, this first analysis was wrong.

The transfer coefficient may depend upon velocity for two reasons: (1) if the zone is not yet stabilized, the transient change of the zone length will be affected by velocity, or, (2) the mass transfer is strongly influenced by gas phase diffusion. Vermuelen (V2) gave some typical dimensionless zone length values which are necessary for stabilized zone conditions for given values of r. These are listed below:

	r	0	0.2	0.5	0.8
minimum	N	4	10	25	75

The N values calculated from the first analysis showed

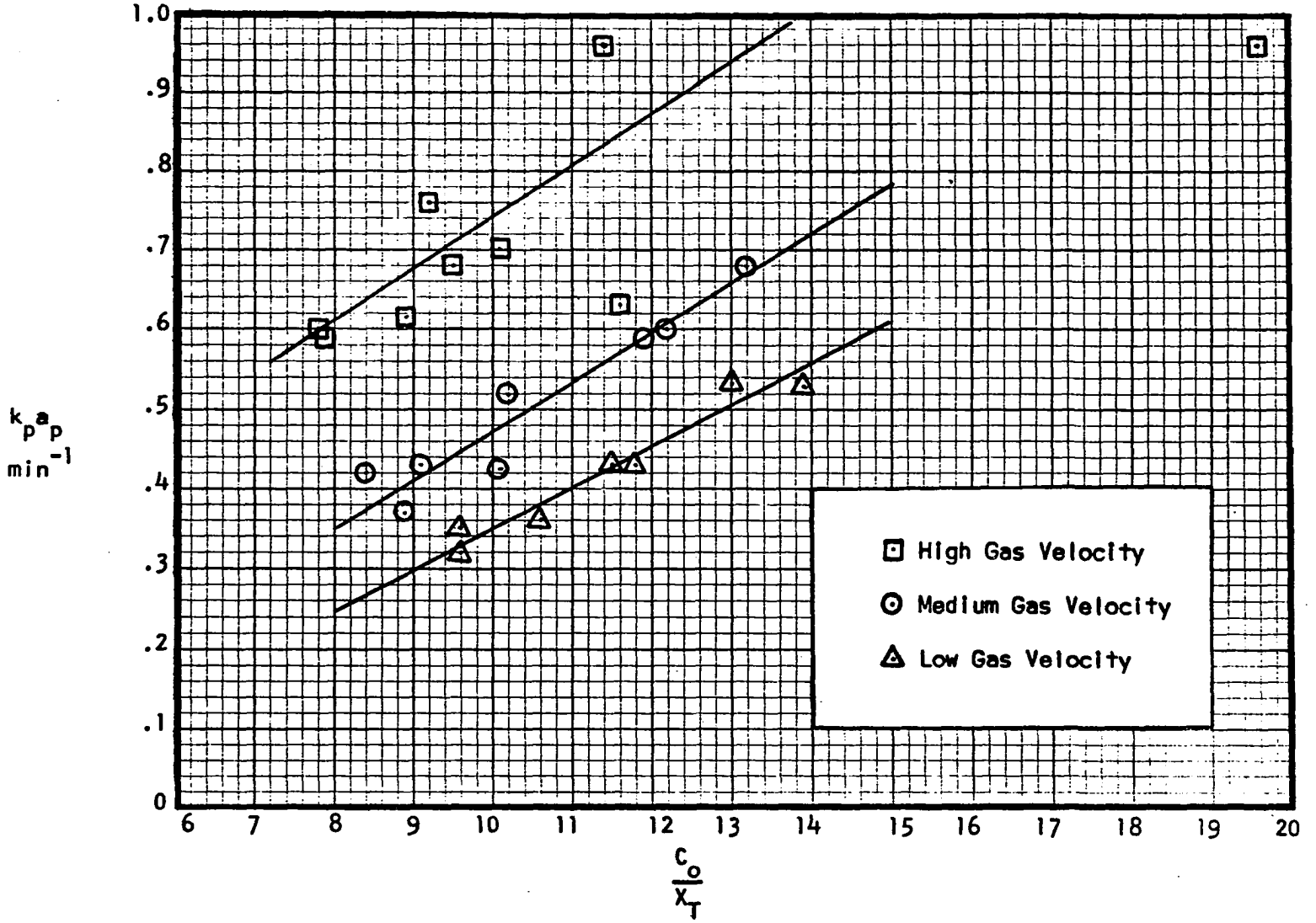


FIGURE 8 - PARTICLE MASS TRANSFER COEFFICIENT
MASTER CURVE ANALYSIS - PENTANE

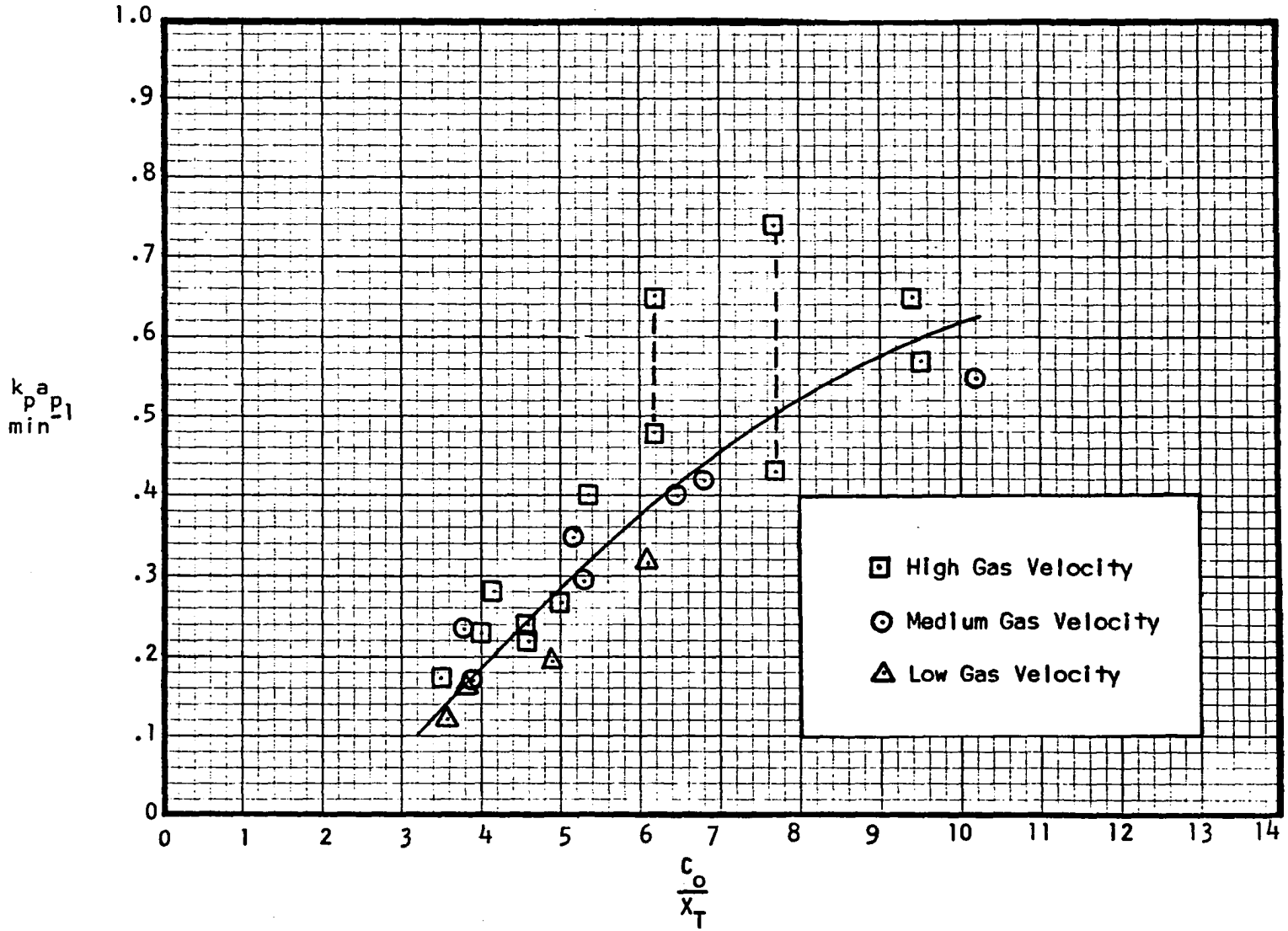


FIGURE 9 - PARTICLE MASS TRANSFER COEFFICIENT
MASTER CURVE ANALYSIS - HEXANE

that most of the hexane runs had developed constant length transfer zones, but the pentane runs had not. The Thomas equation was then used to calculate a stabilized mass transfer coefficient as described below.

C. Correction of Effluent Curve Midpoint Slopes to Obtain Overall Transfer Coefficient

The Thomas equation describes a transient transfer zone which approaches a zone of constant length. Effluent curves for different values of N_R were calculated using the Thomas equation. The dimensionless bed length N_R is based upon the kinetic mass transfer coefficient, $k_{kin}C_o$. The asymptotic solution, Equation (4-17), was calculated for the same values of N_R. Both of these solutions were plotted on probability paper. The transient slopes as given by the Thomas curve were measured graphically since the differentiation of the Thomas equation is quite involved. Two slopes were thus obtained, the transient slope as given by the Thomas solution and the stabilized slope as given by the asymptotic solution. The transient slopes were plotted in Figure 10 versus the asymptotic slopes. With this curve an effluent curve slope may be taken from unstabilized data and corrected to give the stabilized effluent curve slope. This curve showed that all the hexane runs were fairly well stabilized. The bed length in the experimental runs was sufficiently long to provide a stabilized midpoint slope. The asymptotic curve slopes and the transient curve slopes for all the experimental

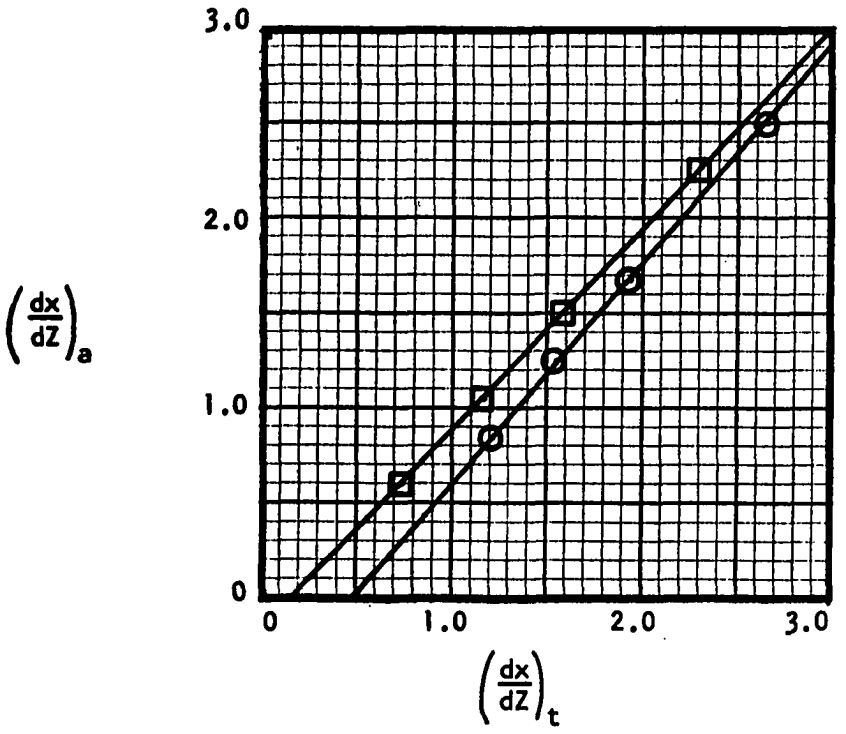


FIGURE 10 TRANSIENT MID-POINT SLOPE CORRECTION

pentane runs differed; so the pentane runs represent transient transfer zones. The combined mass transfer coefficient, $k_{kin} C_o$, was calculated for each run using the differential of Equation (4-17) in Appendix G. The combined mass transfer coefficients are listed in Tables III and IV.

D. Gas Phase Mass Transfer Coefficient

In order to determine the relative importance of fluid phase diffusion, the fluid phase mass transfer coefficient was evaluated according to the correlation of Wilke and Hougen (W5). Before this correlation could be used, a value of diffusivity for both pentane and hexane had to be obtained. This search for valid diffusivity data is discussed in Appendix C.

The diffusivities obtained were used with other physical data in the Wilke and Hougen correlation to give the fluid phase mass transfer coefficients. Those coefficients are tabulated in Tables III and IV.

E. Evaluation of "b" Parameter

The combined mass transfer coefficient, $k_{kin} C_o$, and the fluid phase mass transfer coefficient, $k_f a_p$, are known, and the "b" parameter must be evaluated in order to calculate the remaining particle transfer coefficient. This parameter which primarily depends upon r is discussed and evaluated in Appendix G. Its value for the pentane and hexane data respectively is 1.2 and 1.43.

TABLE III

CALCULATED TRANSFER COEFFICIENTS - PENTANE

Run Number	C_o	X_T	C_o/X_T	$\left(\frac{dx}{dz}\right)_t$	$\left(k_{kin}C_o\right)_t$
58	1.46	.124	11.77	2.25	.466
59	1.69	.146	11.5	2.29	.476
60	.66	.069	9.62	2.28	.384
61	2.04	.157	13.0	2.75	.621
62	1.49	.139	10.65	2.40	.448
63	.56	.058	9.62	2.02	.348
205	1.75	.125	13.9	2.46	.646
56	1.02	.101	10.11	1.48	.539
57-A	.51	.056	9.1	1.54	.496
57-B	.60	.068	8.86	1.33	.467
64	1.52	.124	12.2	1.59	.708
65	1.14	.112	10.21	1.52	.589
66	1.55	.130	11.9	1.62	.717
68	.54	.064	8.4	1.43	.454
209	1.75	.134	13.16	1.77	.756
84	1.23	.134	9.17	1.28	.828
86	.38	.048	7.88	1.22	.671
87	1.62	.160	10.11	1.10	.769
88	.47	.060	7.82	.97	.540
89	.99	.111	8.93	1.28	.788
90	1.60	.168	9.53	1.27	.864
193	.43	.037	11.63	1.42	1.20
194	1.94	.098	19.62	1.21	1.74
210	1.33	.117	11.47	1.105	.911

TABLE III--Continued

Run Number	$\left(\frac{dx}{dz}\right)_a$	$\left(k_{kin} C_o\right)_a$	$k_f a_p$	$k_f a_p / D$	$k_p a_p$
58	2.04	.423	338	3.16	.397
59	2.09	.435	344	3.12	.410
60	2.08	.350	334	2.58	.329
61	2.62	.592	338	3.44	.576
62	2.22	.414	337	2.86	.392
63	1.775	.306	342	2.60	.282
205	2.29	.636	324	4.24	.605
56	1.145	.417	484	3.83	.382
57-A	1.22	.393	476	3.45	.362
57-B	.975	.342	481	3.34	.312
61	1.275	.568	489	4.64	.517
65	1.195	.463	496	3.97	.427
66	1.31	.580	490	4.62	.541
68	1.09	.346	495	3.27	.316
209	1.49	.636	473	4.62	.598
84	.92	.596	686	4.76	.554
86	.85	.467	680	4.06	.431
87	.71	.496	676	5.18	.448
88	.55	.306	680	4.11	.272
89	.92	.566	673	4.60	.526
90	.91	.619	687	5.02	.575
193	1.08	.91	699	6.09	.862
194	.83	1.19	699	10.4	1.096
210	.71	.585	691	6.01	.530

TABLE IV

CALCULATED TRANSFER COEFFICIENTS - HEXANE

Run Number	C_o	X_T	C_o/X_T	$\left(\frac{dx}{dz}\right)_t$	$\left(k_{kin}C_o\right)_t$
71	.61	.158	3.85	5.43	.236
72	1.20	.197	6.1	6.25	.437
73	.47	.131	3.58	4.17	.183
				3.39	.144
74	1.00	.204	4.91	6.17	.355
69	.50	.133	3.78	2.94	.289
70	.93	.182	5.13	3.97	.512
76	1.37	.201	6.80	3.57	.555
77	.94	.178	5.29	3.47	.40
78	.48	.123	3.91	2.46	.211
192	1.37	.140	10.21	4.59	.927
208	.86	.134	6.46	3.78	.553
79	.43	.104	4.15	2.07	.397
80	.37	.106	3.50	1.40	.246
81	.76	.151	5.03	1.50	.331
82	1.22	.159	7.70	2.40	.865
83	1.31	.211	6.21	3.57	1.04
190	0.40	.087	4.61	1.843	.294
				1.312	.413
191	1.22	.129	9.44	2.26	1.04
204	.97	.102	9.53	2.24	.953
206	.34	.085	4.00	1.85	.350
207	.64	.120	5.35	2.09	.534

TABLE IV--Continued

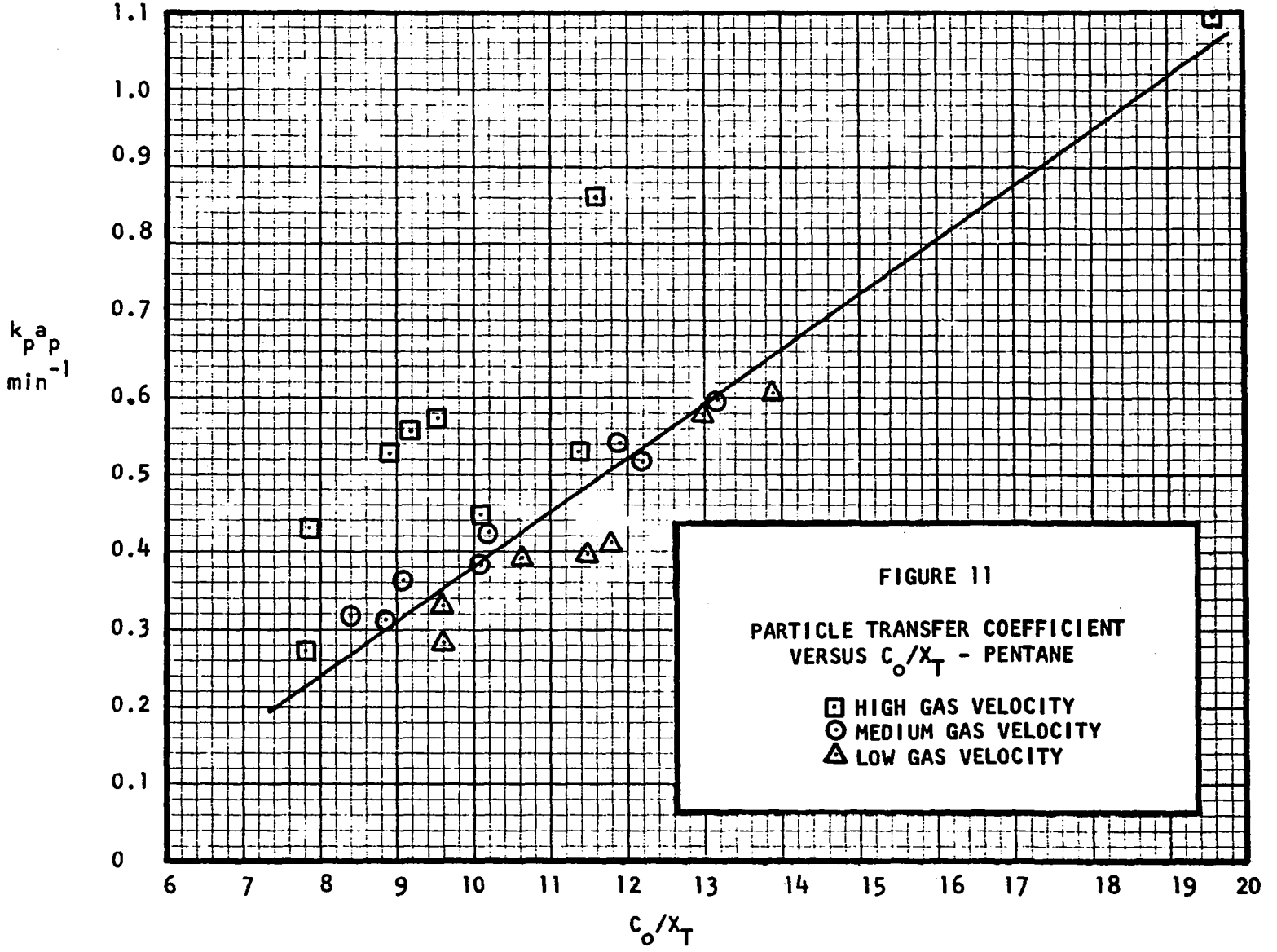
Run Number	$\left(\frac{dx}{dz}\right)_a$	$\left(k_{kin}C_o\right)_a$	$k_f a_p$	$k_f a_p/D$	$k_p a_p$
71	5.43	.236	296	1.08	.195
72	6.25	.437	299	1.72	.372
73	4.17	.183	304	1.02	.146
	3.39	.144			.112
74	6.17	.355	306	1.37	.303
69	2.92	.287	448	1.57	.230
70	3.97	.496	440	2.12	.430
76	3.57	.555	417	2.69	.453
77	3.47	0.40	405	2.07	.324
78	2.46	.214	416	1.52	.166
192	4.59	.927	409	3.57	.792
208	3.78	.553	419	2.44	.459
79	2.07	.386	590	2.26	.223
80	1.40	.231	597	1.97	.176
81	1.50	.312	563	2.64	.244
82	2.40	.851	603	4.18	.694
83	3.57	1.04	608	3.40	.926
190	1.765	.395	621	2.56	.310
	1.205	.270			.204
191	2.20	1.015	620	5.24	.820
204	2.18	.927	596	5.11	.743
206	1.77	.336	619	2.20	.263
207	2.03	.519	619	2.94	.292

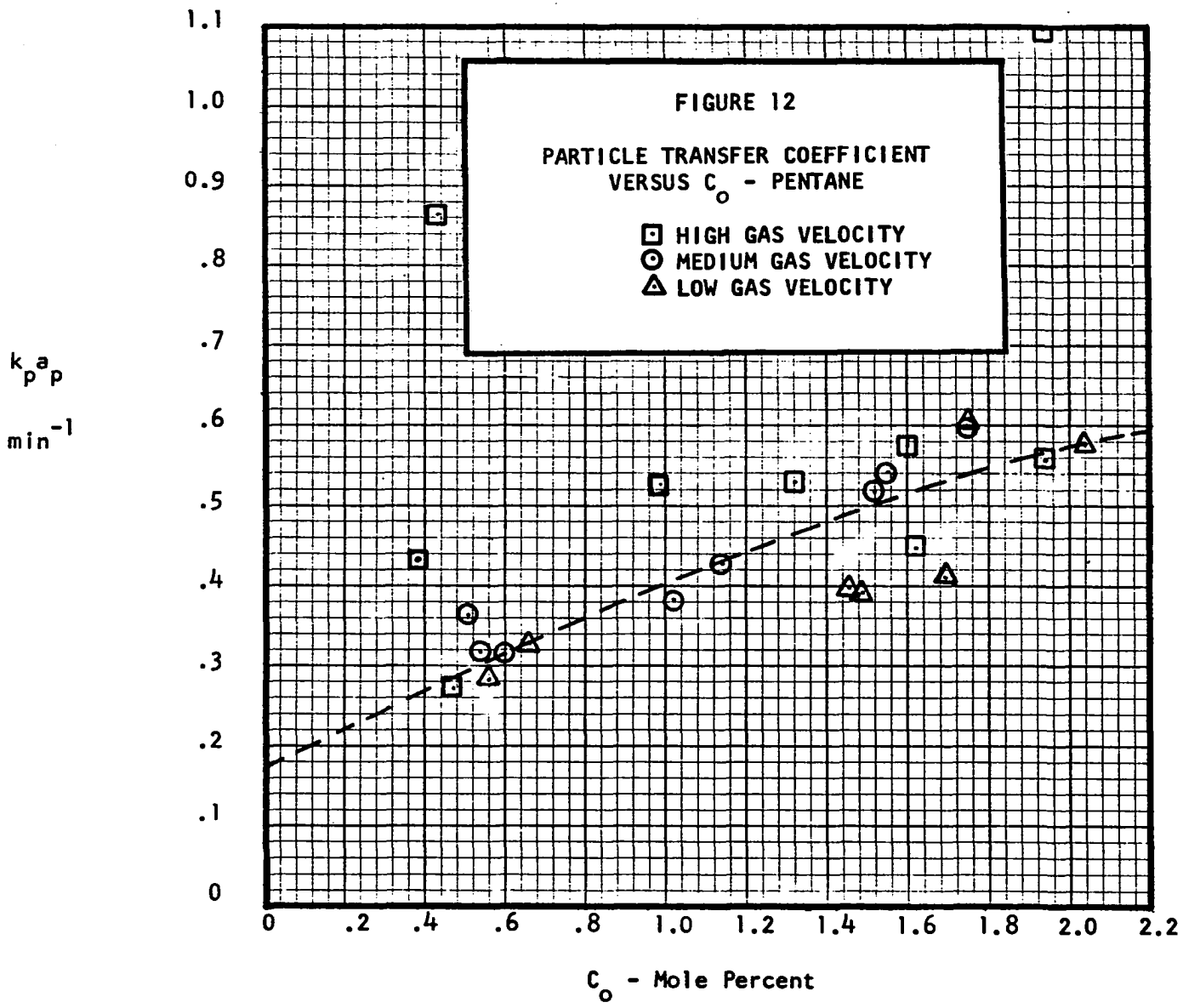
F. Calculation of the Particle Mass Transfer Coefficient

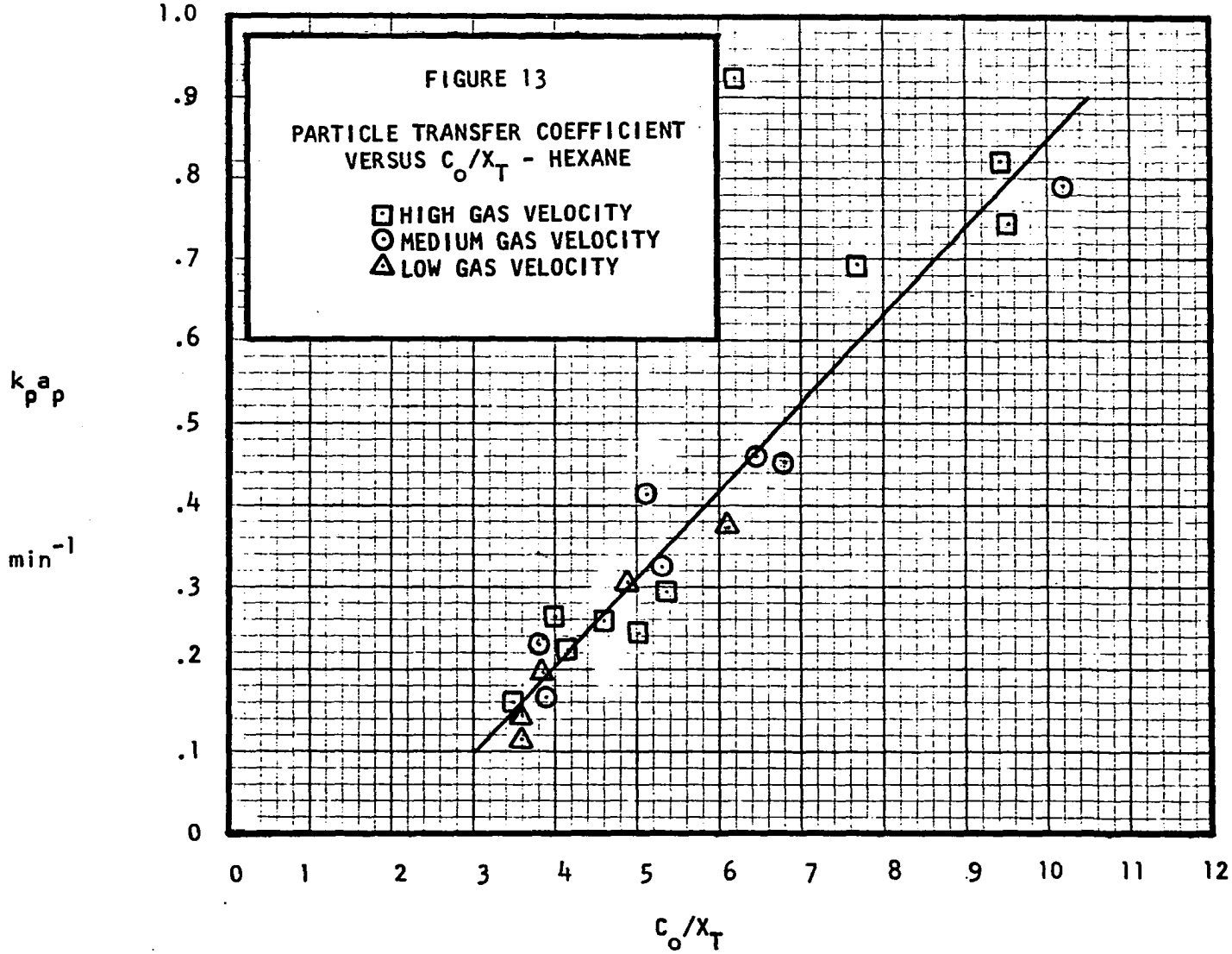
Using Equation (4-29), the particle transfer coefficient, $k_p a_p$, was calculated. According to these calculations, the fluid phase resistance is only 10 to 20 percent of the particle resistance to transfer. These values are tabulated in Tables III and IV.

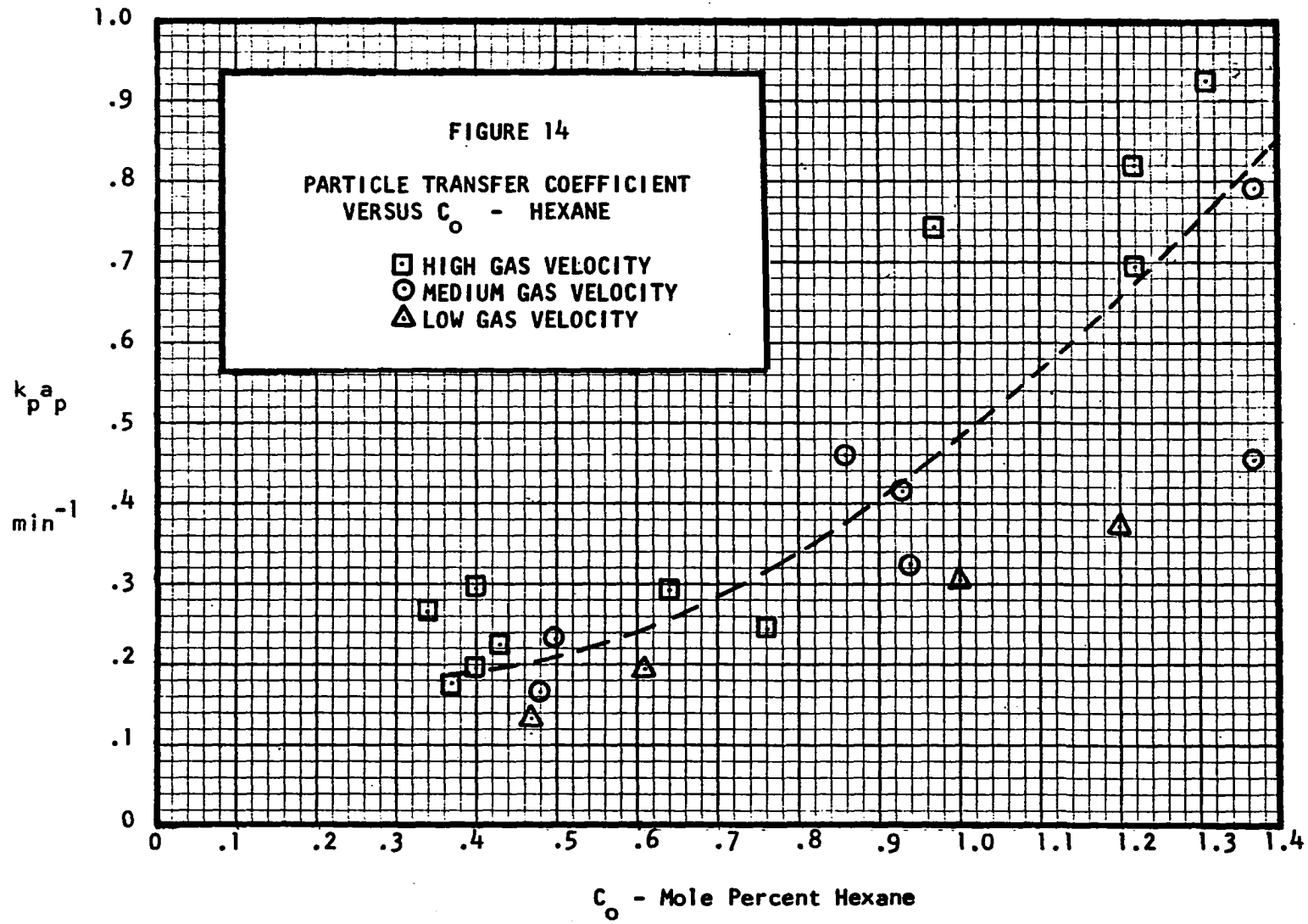
If a lower diffusivity value for pentane and hexane had been used, the gas phase diffusivity would have been more important, but would not have changed the results much. A lower value, which was taken from the data of Carmichael, Sage, and Lacey (C7) was used in Appendix N to show this.

Figures 11, 12, 13 and 14 show the final results of the data analysis. The particle mass transfer coefficients were first plotted versus mole percent of the adsorbate in the gas. These figures show the strong dependence upon adsorbate concentration. The first plots versus gas phase concentration alone showed some scatter. The scatter was almost eliminated by plotting the mass transfer coefficient versus a dimensionless adsorbate concentration, C_o/X_t. This strong dependence of the mass transfer coefficient upon adsorbate concentration supports the fact that particle diffusion controls the mass transfer rate. For low concentrations of hydrocarbon in a natural gas, the ordinary gas diffusivity changes very little with concentration of the hydrocarbon component (C8). However, Carman and others (C4, C6, S7) show


1.1
1.0
0.9
0.8
0.7
0.6
0.5
0.4
0.3
0.2
0.1
0
$k_p a_p$ min^{-1}
6
7
8
9
10
11
12
13
14
15
16
17
18
19
20
C_o/X_T
FIGURE 11
PARTICLE TRANSFER COEFFICIENT VERSUS C_o/X_T - PENTANE
HIGH GAS VELOCITY
MEDIUM GAS VELOCITY
LOW GAS VELOCITY


FIGURE 12
PARTICLE TRANSFER COEFFICIENT VERSUS C_o - PENTANE
HIGH GAS VELOCITY
MEDIUM GAS VELOCITY
LOW GAS VELOCITY
$k_p a_p$
min^{-1}
1.1
1.0
0.9
.8
.7
.6
.5
.4
.3
.2
.1
0
0
.2
.4
.6
.8
1.0
1.2
1.4
1.6
1.8
2.0
2.2
C_o - Mole Percent


FIGURE 13
PARTICLE TRANSFER COEFFICIENT VERSUS C_o/X_T - HEXANE
HIGH GAS VELOCITY
MEDIUM GAS VELOCITY
LOW GAS VELOCITY
$k_p a_p$
min^{-1}
1.0
.9
.8
.7
.6
.5
.4
.3
.2
.1
0
0 1 2 3 4 5 6 7 8 9 10 11 12
C_o/X_T


FIGURE 14
PARTICLE TRANSFER COEFFICIENT VERSUS C_o - HEXANE
HIGH GAS VELOCITY
MEDIUM GAS VELOCITY
LOW GAS VELOCITY
$k_p a_p$
min^{-1}
1.0
.9
.8
.7
.6
.5
.4
.3
.2
.1
0
0 .1 .2 .3 .4 .5 .6 .7 .8 .9 1.0 1.1 1.2 1.3 1.4
C_o - Mole Percent Hexane

that surface diffusion is strongly dependent upon the surface concentration of adsorbate.

The scatter shown on the plots is to be expected since the transfer coefficients are very sensitive to small changes in the slopes of the breakout curve. These slopes are affected by small variations in effluent compositions. Many of the runs showed a scattering of effluent points as given by chromatographic analysis. Because of the rather small number of points measured for some effluent curves, a wide choice in midpoint slopes exists for several of the adsorption runs.

G. Pore Diffusion

A transfer coefficient assuming pore diffusion was calculated for each hydrocarbon, although surface diffusion inside the particle is most important. These calculations are given in Appendix L. Because of the high gas pressure, diffusion through the pores was ordinary gas diffusion and not Knudsen diffusion. The mass transfer coefficient calculated this way was smaller than any of the evaluated particle transfer coefficients.

At low hexane or pentane concentrations, pore diffusivity will contribute to the total transfer within the particle, but at higher concentrations of adsorbate in the particle, pore diffusion transfer is negligible.

The particle mass transfer coefficients calculated for pore diffusion were .085 and .043 per minute for pentane and hexane respectively.

CHAPTER VII

PREDICTION OF EFFLUENT CURVES

In order to check the accuracy of the $k_p a_p$ correlation for pentane and hexane, effluent curves were predicted for Runs Numbers 56, 63, 70, and 208 (Figures 15, 16, 17, and 18). In these predictions the exact value of adsorbed hydrocarbon was used in order to note the effect of $k_p a_p$ variation only. The equilibrium adsorption correlation was used to predict the effluent curve in Figure 18.

The effluent curves were calculated around the point on the curve at which the throughput parameter Z equals 1.0. For hexane, this point is x = .56, and for pentane, it is x = .53. Consequently the deviation of the actual mass transfer coefficient from the straight line correlation (Figures 11 and 13 - Chapter VI) will change the slope of the effluent curve and thereby cause the predicted points to deviate from the actual curve. The method used to calculate the dimensionless effluent curve is as follows:

Step No. 1 - Given C_o and X_T, select $k_p a_p$ from Figure 11 or Figure 13.

Step No. 2 - Calculate $k_f a_p$ using Equation (3-7) and

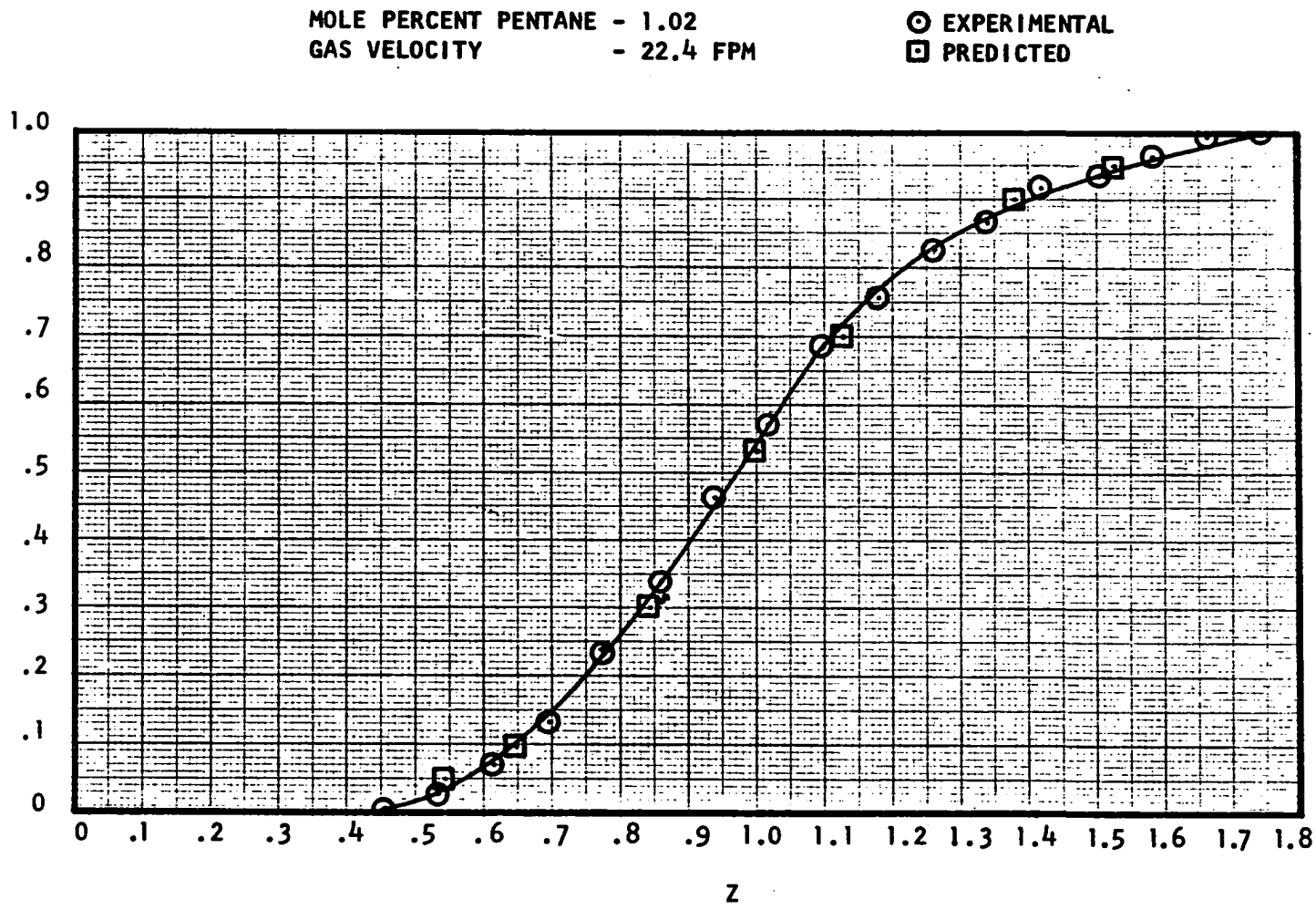


FIGURE 15 EFFLUENT CURVE PREDICTION - RUN NO. 56

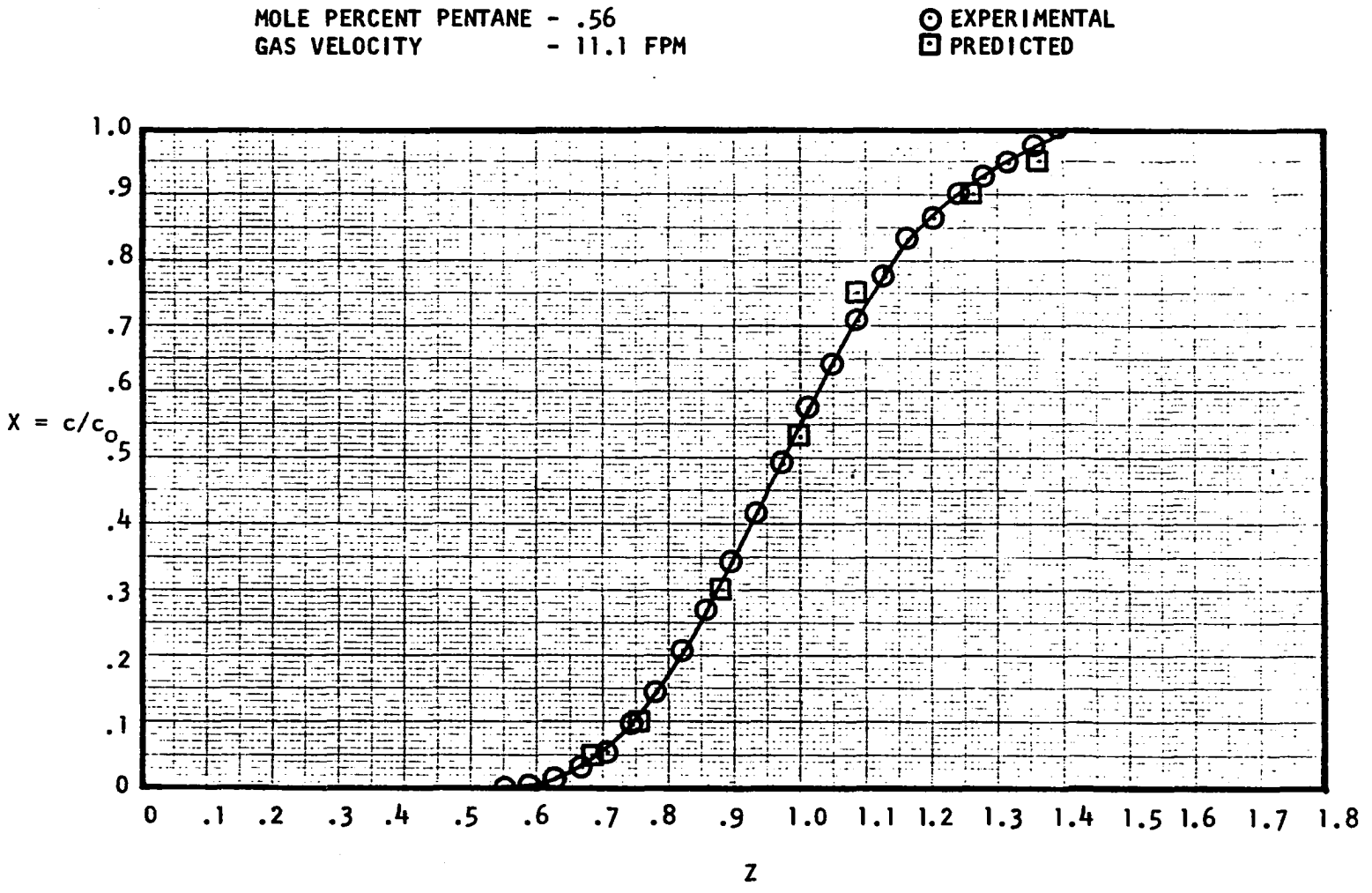


FIGURE 16 EFFLUENT CURVE PREDICTION - RUN NO. 63

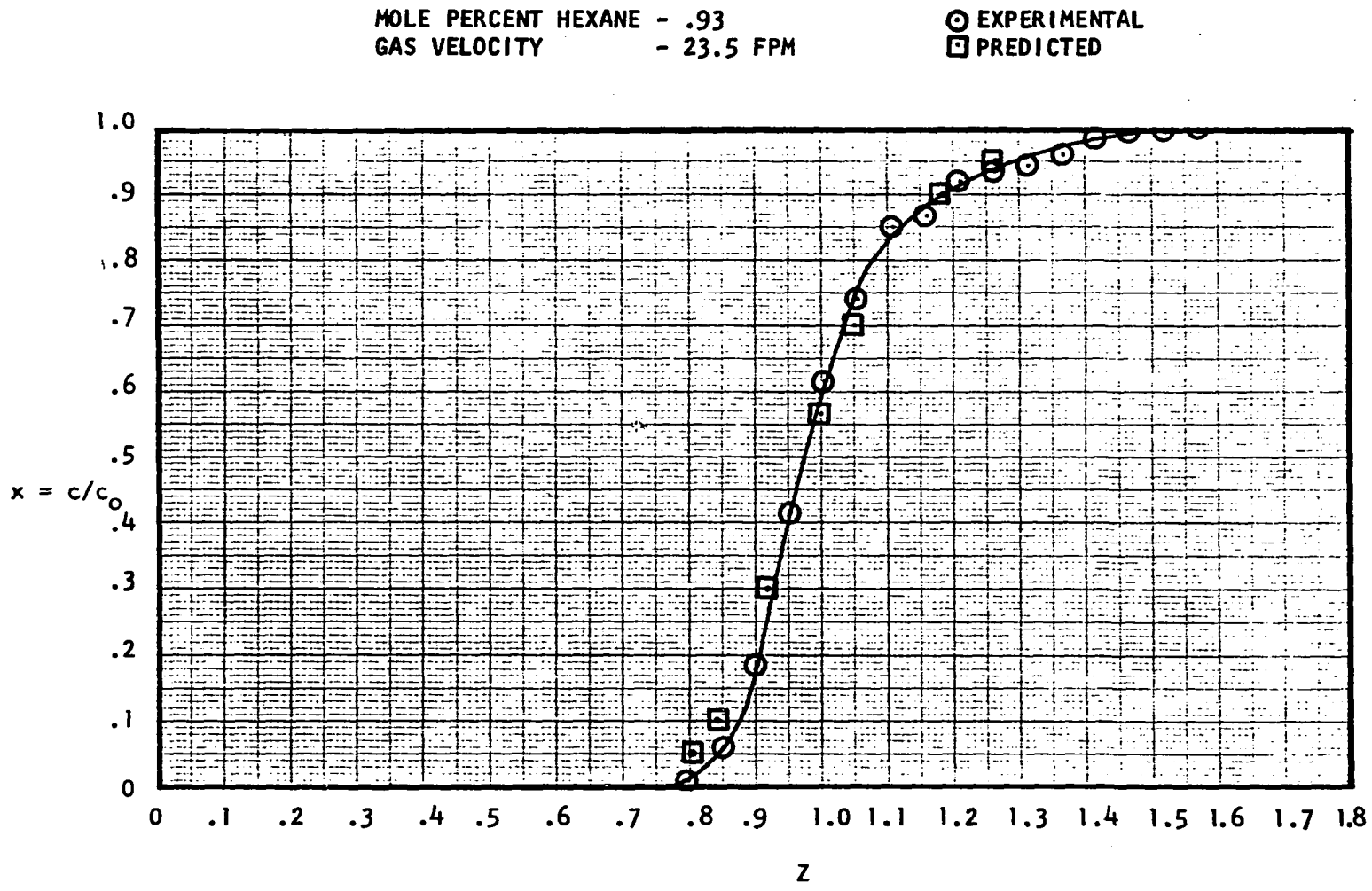


FIGURE 17 EFFLUENT CURVE PREDICTION - RUN NO. 70

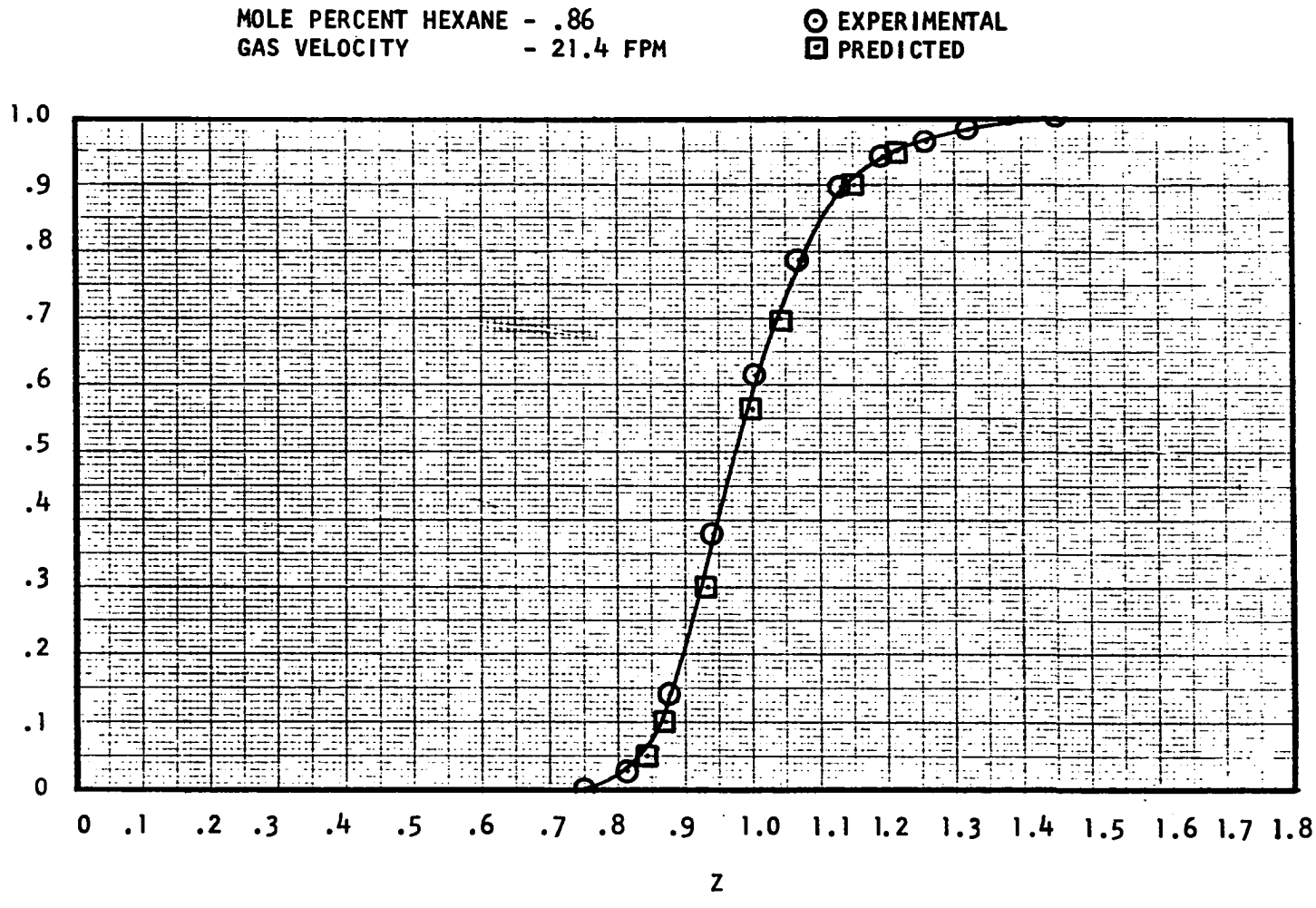


FIGURE 18 EFFLUENT CURVE PREDICTION - RUN NO. 208

the proper value of a_p.

Step No. 3 - Calculate the overall mass transfer coefficient, $k_{kin}C_o$, using Equation (4-29).

Step No. 4 - Calculate $\left(\frac{dx}{dZ}\right)_a$ from the differential form of Equation (4-17) at x = 0.5.

$$\left(\frac{dx}{dZ}\right)_a = N_R\,(1-r)(x)(1-x)\ . \qquad (7\text{-}1)$$

For pentane (x = 0.5, r = 0.667)

$$\left(\frac{dx}{dZ}\right)_a = \frac{k_{kin}C_o}{12}\,\frac{Dv\epsilon}{F}\ . \qquad (7\text{-}2)$$

For hexane (x = 0.5, r = 0.4)

$$\left(\frac{dx}{dZ}\right)_a = \frac{k_{kin}C_o}{6.67}\,\frac{Dv\epsilon}{F}\ . \qquad (7\text{-}3)$$

Step No. 4 - Correct $\left(\frac{dx}{dZ}\right)_a$ to $\left(\frac{dx}{dZ}\right)_t$ with Figure 10.

Step No. 5 - Calculate $k_{kin}C_o$ using $\left(\frac{dx}{dZ}\right)_t$ in Equations (7-2) and (7-3).

Step No. 6 - Assume $k_f a_p = \infty$ that is, that fluid phase diffusion offers no resistance to mass transfer. Calculate $k_p a_p$ from:

$$k_p a_p = \frac{k_{kin}C_o}{b} \qquad (7\text{-}4)$$

where b equals 1.2 for pentane and 1.43 for hexane.

Step No. 7 - Calculate the dimensionless effluent curve with Equation (4-16) for pentane (Z_2 = 1.0, X_2 = .53, r = 0.667) and hexane (Z_2 = 1.0, X_2 = .564, r = 0.4).

The results of this procedure for Runs Numbers 56, 63, 70, and 208 are shown in Figures 15, 16, 17, and 18. These curves show that the $k_p a_p$ correlation provides a very good estimate for these single component effluent curves as long as the adsorption capacity, X_T, is known.

The effect of X_T is shown in Figure 18 which is plotted on a time scale. A correlation value for X_T from Figure A-2, Appendix A, was used to calculate the curve. This result shows how much more important X_T is than $k_p a_p$ in predicting effluent curves.

Time values may be calculated from

$$t = \frac{Dv\epsilon}{F}\left(Z + \frac{1}{D}\right) . \qquad (7\text{-}5)$$

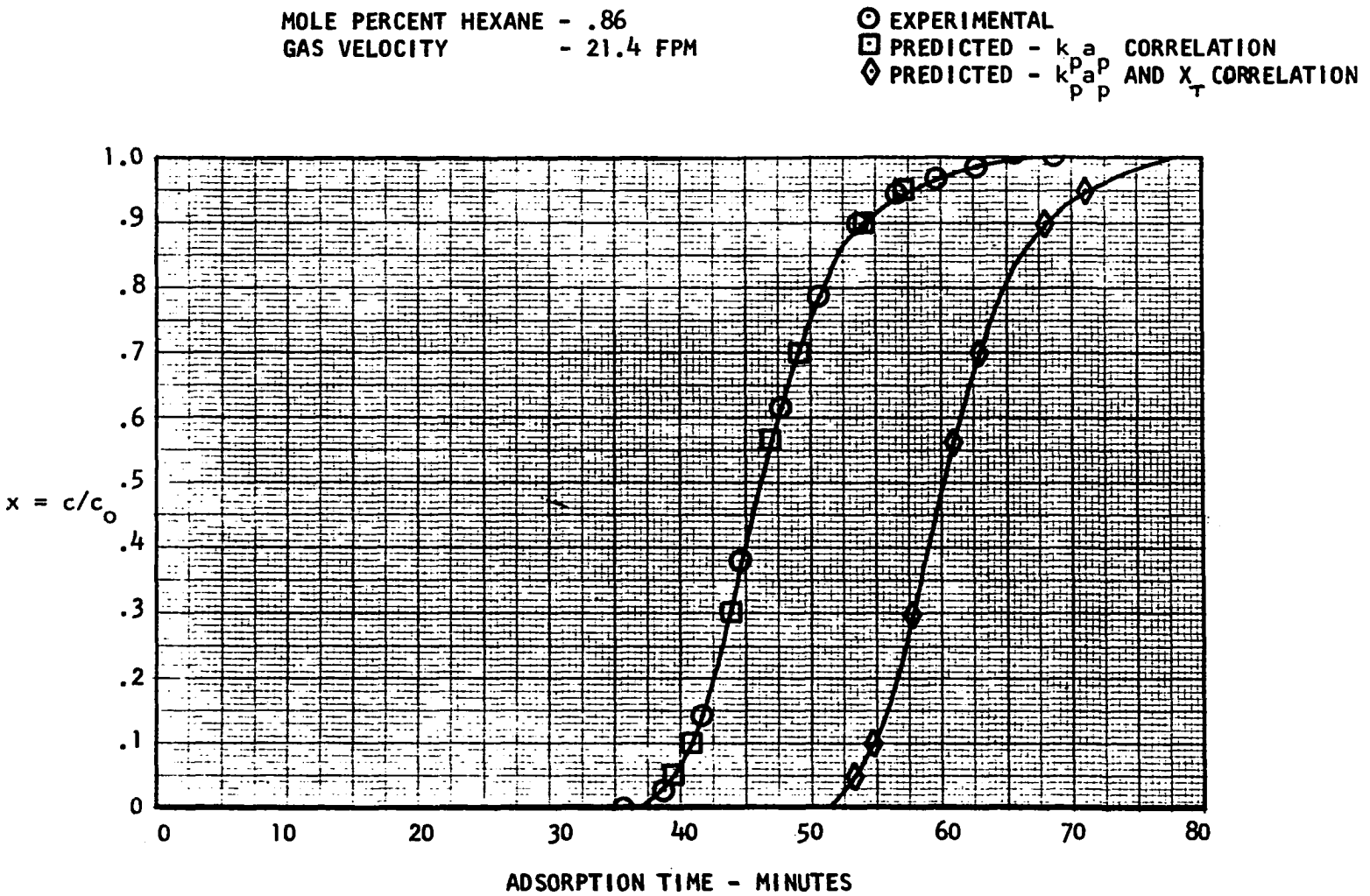


FIGURE 19 EFFLUENT CURVE PREDICTION - RUN NO. 208

CHAPTER VIII

SIGNIFICANCE OF RESULTS

The analysis of results and effluent curve predictions showed that the adsorption model which best fits the effluent curve behavior of pentane and hexane in a natural gas is the asymptote model. This model assumes that a stable transfer zone is established and that the transfer rate mechanism and the adsorption isotherm control the shape of the effluent curve (See Appendix I). The mechanism that controls the transfer rate is particle diffusion or diffusion of the adsorbate inside the particle, either through the pores as ordinary gas diffusion or along the solid surface as surface diffusion. Fluid phase diffusion, the ordinary diffusion of the adsorbate from the gas stream onto the outside particle surface, supplies a minor part of the series mass transfer resistance. The fluid phase diffusion may, however, be more important in a concept of transfer resistances in parallel. This chapter presents an explanation of these results and supporting basic theory.

Of primary concern in this discussion is the relative importance of the equilibrium adsorption isotherm curve shape,

the dependence of the mass transfer coefficient, $k_p a_p$, on adsorbate composition, and the importance of transfer zone stability on analysis.

A. Isotherm Shape

The results of this dynamic adsorption study show the importance of the shape of the isotherm curve on transfer zone stability and effluent curve shape. Previous studies (E2, G1, M2), and two runs (Figure 20) made on this project show that a stabilized transfer zone is achieved for the adsorption of components which have an equilibrium adsorption isotherm with a favorable curve shape.

This stabilization of the transfer zone agrees with theory of dynamic adsorption for curved isotherms. This stabilization is not allowed by a theory which assumes a linear isotherm. Although one literature source (D1) applies the concept of a stabilized transfer zone, they neglect the importance of the degree of curvature of the equilibrium isotherm. This degree of curvature which is represented by the equilibrium parameter, r, determines the rate of stabilization, or rather the length of a transfer column required to acheive a stabilized zone. The importance of the degree of curvature is shown by the results of the pentane and hexane adsorption behavior. This difference is discussed in Appendix I.

Where r is low, the controlling mechanism is easily

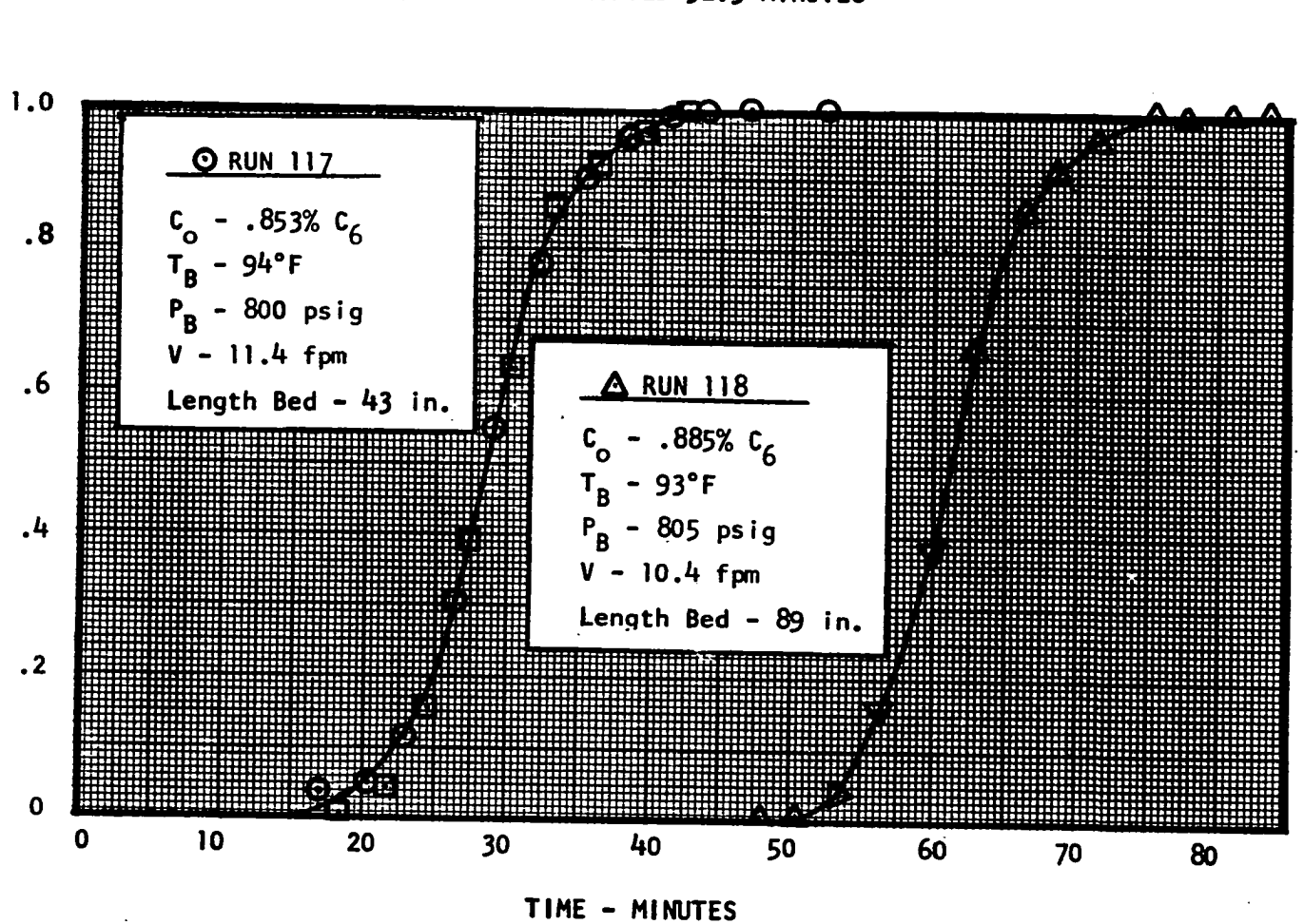


FIGURE 20 - STABILIZED ZONE RUN - HEXANE

recognized because the effluent concentration curve is less symmetrical about its midpoint. For particle diffusion controlling the first half of the curve is steeper and shorter than the second half. This curve shape, if rotated 180°, would represent fluid phase diffusion. Since the pentane ($r = 2/3$) isotherm is close to a linear ($r = 1$) isotherm, these two mechanisms are difficult to distinguish by effluent curve shape. However, in the case of hexane ($r = 0.4$), the two mechanisms are easily distinguished by effluent curve shape.

Heat is produced during adsorption of high concentrations of pentane or hexane as shown by the work of Needham et al. (N1). This heat may affect the transfer rate, more likely slowing it down; however, the constant shape wave front is not affected (G1, C11).

B. Adsorbate Concentration

The mass transfer coefficient is a function of the concentration of the adsorbing component. This supports the conclusion that mass transfer depends upon the transfer rate inside the particle. Figures 11 and 13 which are plots of mass transfer coefficient, $k_p a_p$, versus relative adsorbate concentration show a strong dependence of this coefficient on concentration. This conclusion is also supported by the studies of Carman, et al. (C4, C6), who in adsorbed phase diffusion studies through porous media, showed the increase of

mass transfer rate with concentration. They also showed that this behavior was divided into three modes. The first mode is for less than one monolayer adsorbed on the solid dessicant. In this range, the diffusivity increases from zero to monolayer concentration. From this point on the diffusivity is about constant throughout the multilayer adsorption range. The diffusivity increases rapidly at higher concentrations in the range of capillary condensation.

The diffusion of pentane and hexane in this study probably encompasses all three ranges. Those ranges can not be separated since only two surface layers fill the average pore size, and the second layer occupies just a fraction of the amount in the first layer. Since midpoint slopes from the effluent curves were used in the evaluation of $k_p a_p$, the diffusion is taking place in a partial monolayer.

Kiselev (K4) showed that pentane on silica gel began capillary condensation at $p/p_s = 0.3$ and reached adsorption capacity at $p/p_s = 0.6$ for a pore size of 25 Angstrom units (p represents partial pressure of the pentane and p_s represents saturated vapor pressure of the pentane). In other words capillary saturation can occur even before the vapor phase is saturated. Cohan (C13) stated this condensation would be reversible where the pore diameter is equal to or less than 4 molecular diameters.

That surface migration or transport rate is an increasing function of surface (adsorbate) concentration appears

to be well established and thus invalidates the simple concept of a diffusion process having a constant diffusion coefficient. Smith and Metzner (S7) showed that this transport rate was a function of both the slope of the adsorption isotherm and the adsorbate concentration squared (y^2). This increase with concentration below the full monolayer is attributed to surface heterogeneity (B4). As the more active or tenacious sites are filled, additional molecules move faster along the surface with lower activation energies (O6).

Diffusion coefficients for the adsorbed phase are of the order of $(10)^{-5} cm^2/sec$ (C4). This is within the range of coefficients calculated for hexane and pentane surface diffusion in this study.

Temperature increases the surface diffusion coefficient but decreases the adsorbed phase concentration more so that the net effect is to decrease the adsorption rate (S7).

Surface diffusion tends to dominate over pore diffusion for porosities less than 0.6 and particularly for larger and heavier molecules which are usually most easily condensed (C4). The calculated pore diffusion rate in this study was only as high as one-third of the surface diffusion rate. As the adsorbed phase increases, the path open to pore diffusion reduces even more. Furthermore this path is probably filled with counter diffusing methane molecules.

C. Transfer Zone Stability

The mass transfer coefficient calculated at the beginning of this study depended on velocity. If the transfer were controlled by fluid phase diffusion instead of particle diffusion, one would expect this (See Equation 3-7). However, the strong dependence upon adsorbate concentration shows that the transfer is controlled by internal particle diffusion which is unaffected by gas velocity. This discrepancy was not resolved until the velocity effect was substantially removed by a correction for the transient conditions of runs at high velocities. Some of the transfer zones had not stabilized within the length of dessicant bed. The equation of Thomas (Equation 4-27), was used to correct the slopes of the effluent curves. This procedure gave the stable slopes which would be obtained in a longer zone.

The transient change was noticeable in pentane adsorption, but not in hexane adsorption. Assuming stabilized zone transfer (Equation 4-16) made the calculated mass transfer coefficient a strong function of velocity. Equation 4-16 shows that as the parameter r approaches 1, the length of bed necessary to attain a stabilized zone transfer increases in length. A comparison of stabilized effluent curves (Equation 4-16) and transient curves (Equation 4-27) showed that the hexane curves were fairly well stabilized in the length of dessicant bed which we employed. However none of the runs on pentane were stabilized, and all had to be corrected. Since

this correction depends strongly upon the value of r, an incorrect value of r may result in inaccurate transfer coefficients.

The values of r used in this analysis are approximate because of the scatter in the equilibrium adsorption data. An r value which is based upon controlled experimental equilibrium isotherms would be more reliable because other distrubing influences would be removed. These will be discussed later. Fluid phase diffusion constituted about 15 percent of the transfer resistance. If particle diffusion is assumed to be the only resistance, the calculated coefficient will still vary slightly with velocity. This happened in the first analysis of hexane data.

The fluid-phase transfer coefficient was calculated from Equation (3-7) which requires the gas phase diffusivity. The diffusivities for both hexane and pentane in methane are not available in the literature. The correlations of Stiel and Thodos (S8), were used to obtain the diffusivities of hexane and pentane in a natural gas, and this is described in Appendix C. It was pointed out in this appendix that the calculated diffusivity and the experimental diffusivity for hexane of Carmichael, et al. (C7), did not agree. Other experimental data for hydrocarbon indicated an error in the data of Carmichael, and the correlation was used. A value of pentane diffusivity was not available from Carmichael's work. A lower diffusion coefficient would not affect the results

(See Appendix N).

One other effect of velocity may still exist in the $k_p a_p$ correlation which does not contradict particle transfer control. A parallel diffusion resistance exists in a bed of silica gel particles which may not exist in an ideal packing of spheres where flow of gases around all spheres is uniform. Surfaces of neighboring silica gel particles may touch with very narrow slits between the particles. At low flow rates the effective total transfer area of the particles is reduced because gas does not flow as rapidly by one part of a particle surface. At this low velocity laminar flow exists whereas the other flow paths are in turbulence. The fluid phase transfer at this point is much lower and reduces the total transfer rate to the particle. On one side of the particle the transfer rate is rapid; on the other side of the particle the transfer rate is slow. The transfer behavior is still controlled by the faster transfer rate, but the path for diffusion inside the particle is longer than if all sides of the particle were exposed to the turbulent gas flow.

Three different velocities were used in this study. Let us consider the effect of velocity change. As the velocity of the gas is increased, the fluid phase diffusivity around the whole particle increases. At a lower velocity, the fluid phase diffusion is already so rapid around one side of the surface that the internal particle diffusion controls. However, on the part of the surface where the gas velocity is

lower, the fluid phase resistance hinders transfer. As the gas flow rate is raised, the fluid phase diffusivity on this restricted side will also rise. As it rises, it allows a faster transfer rate to the particle surface so that this side of the particle will also contribute to the saturation of the individual particle. In effect this results in an increased particle surface area for transfer. Although the effluent curve does not reflect the mechanism of fluid phase diffusion, the apparent transfer rate may still increase a little with velocity because the effective particle transfer area increases with velocity.

One thing to consider in future studies is the importance of randomness of particle size which is present in the silica gel which we used. The mesh size of the gel used in this project ranged from 3 to 8. The quantity of adsorbate in the particle is a function of r^3 whereas the flow rate into the particle is a function of r^2. This may cause the first part of the effluent curve to be sharper and the end part to be longer.

D. Equilibrium Adsorption

There is a noticeable variation of equilibrium adsorbate concentration in the silica gel as plotted vs. the adsorbate in the gas. This variation may be due to several reasons.

At some of the high flow rates the calculated adsorbate

concentration may be too high. There is a small amount of lag time between the time at which the rich gases are turned through the beds and the time when the chromatograph samples the same gas. The gas must travel from the bed through a small line to the chromatograph. Even though this gas was being bled constantly during the runs, this lag time was longer at the first of the project. In some runs if the lag time were a minute or two, this would cause about a 10 percent increase in the calculated amount adsorbed.

Some of the runs show low values of equilibrium adsorbate concentration. This may result from three causes.

First, the silica gel adsorption capacity is lowered when residual heat remains after regeneration and insufficient cooling.

Second, accidental premature adsorption on the bed lowers the amount of hexane or pentane adsorbed. High concentrations of propane and butane in the gas stream may reduce pentane or hexane adsorption. Premature adsorption may also occur following a run. After the regeneration of the first run, the bed is cooled by recirculating dry gas through the bed. Although there are only small amounts of components which can be adsorbed from the limited volume of gas used for cooling, there may be more components heavier than methane in the gas at any one time. If any liquid remains in the system after the regeneration run, this may be re-adsorbed into the stream and affect the results of the next run. If the carbon

beds are not cooled enough after regeneration, components may pass through with the gas and take up some of the silica gel capicity.

Third, the capacity of the silica gel for hexane or pentane may be reduced by the entrapment of lighter hydrocarbons (methane, ethane, etc.) at fast transfer rates. Some of the light hydrocarbons will remain absorbed in the adsorbed phase of pentane or hexane.

The most variation in adsorbate capacity occurred when different batches of silica gel were used, and some of these runs were made by new personnel working on the project who were less familiar with experimental procedure. The above discussion concerns mechanisms which are present in any experimental project and particularly in field adsorption operations. Data for dynamic equilibrium are generally not as precise as for static equilibrium. The equilibrium data in this study are quite good for the purpose of transfer zone analysis.

E. Particle Transfer Mechanism

Surface diffusion is a function of the adsorbed phase concentration. In a natural gas components other than pentane or hexane or adsorbed at high pressures, even methane and ethane (L7). The effect these other components may have on the transfer rate of pentane and hexane is presented below.

Preadsorbed gas is displaced by a heavier component; for instance, hexane displaces methane. Since the high energy

sites are occupied, the hexane follows more mobile paths of surface diffusion. The transfer is higher at very low hexane concentrations with the lighter gas in place than if only hexane were present. The lighter gas counter diffuses out through the center of the pores since pore diffusion for hexane is so slow compared to surface diffusion. As adsorption continues, methane develops a positive gas pressure outward causing it to flow more rapidly out of the pore. This flow seeks the larger pore exits as more hexane adsorbs into the small pores where capillary condensation can take place. The methane adsorbs into the condensed liquid phase. Although the equilibrium adsorption data show hexane to be present in the silica gel as a monolayer or less, the presence of dissolved lighter gases may put the total gas adsorbed into the capillary condensation range. Multilayer adsorption and capillary condensation cause higher particle transfer rates.

One important part of this analysis is the use of a linear concentration gradient to approximate the mass transfer driving force. For diffusion into a sphere the spherical diffusion equation [Equation (3-5)] might be thought to be more representative of adsorption transfer. This equation assumes a constant surface diffusion coefficient which makes it at best an approximation. Since 90 percent of the volume of a sphere is located in the outer half of the diameter, this portion of the sphere's volume will control the effluent curve behavior. In the outer half of the sphere, a linear

gradient is a fair approximation. A gradient has the greatest change near the center of a sphere where the resistance to movement is higher because of the smaller flux area. In view of the complex mechanism involved, the linear driving force (Equation 3-6) is a reasonable assumption to make for analysis of hydrocarbon adsorption. Besides, there is a solution for a curved isotherm using the linear gradient equation, but there is not a solution using both the spherical diffusion equation and the curved isotherm relationship [Equation (4-1)].

The Thomas equation also assumes a constant transfer coefficient. Since this equation is used to evaluate transfer coefficients at one particular point on the effluent curve ($x = 0.5$), the procedure should be valid. Another error may occur because of the initial transfer at the top of the bed. The top of the bed sees high concentrations from the beginning. Since the mass transfer coefficient is higher at this concentration, the zone growth rate is slowed, and a longer bed is required for a constant zone length to form. The transient slope correction would be smaller, and the calculated transfer coefficient would be too high - particularly at higher velocities.

F. Restatement of Concepts

Although there are sources of error which cannot be removed from the analysis of experimental data at this time, the results justify the conclusion that particle diffusion

controls mass transfer. The influence of this mechanism on the shape of the effluent curve and the effect of the isotherm shape on forming a stabilized zone are important concepts. These concepts need to be used in the interpretation of dynamic hydrocarbon adsorption data and also in the design of field adsorption units.

It is important to multi-component adsorption design that an error in the particle transfer coefficient does not affect effluent curve prediction as much as an error in equilibrium adsorption. Equilibrium isotherm curves obtained with multi-component gases may be used with the coefficients of this study to predict effluent curves. These predictions will have to be modified when strong displacement of one gas by another occurs in multi-component adsorption.

The author also believes that the surface diffusion coefficients will not be changed much by a different gas pressure. Experiments should check this for it would be important in adsorption design.

CHAPTER IX

CONCLUSIONS

The following conclusions are based on the analysis of experimental data - as supported by basic adsorption and mass transfer theory - and on comparison of the mass transfer behavior of pentane and hexane in a fixed bed of silica gel:

1. The equilibrium adsorption isotherms of pentane and hexane in a dry natural gas at 90°F and 815 psia are curved and cannot be accurately described with a straight line equation. The hexane isotherm has more curvature than the pentane isotherm. The r values calculated according to Equation (4-1) are 0.4 and 0.667 for hexane and pentane respectively.

2. The shape of the isotherm affects the mass transfer behavior of pentane and hexane in two ways:

   a. The favorable isotherm ($r<1$) causes a mass transfer zone to attain a constant length. Hexane adsorption gave a constant transfer zone length for velocities of 10 and 24 ft/min; however, the pentane zones did not reach a constant zone length in a tower 14.65 feet long even at superficial velocities of 10 feet per minute.

b. When r is less than 0.5, the controlling mechanism is easily recognized as the effluent concentration-time curve is less symetrical about its midpoint. The first half of the curve is steeper and shorter than the second half for particle diffusion whereas the reverse is true for fluid phase diffusion. The difference in effluent curve shape caused by these two mechanisms vanishes as r approaches 1. The transfer mechanisms for pentane (r = 0.667) are difficult to distinguish by effluent curve shape, but the more asymmetric hexane (r = 0.4) effluent curves definitely show particle diffusion to control the mass transfer rate. Calculated fluid phase mass transfer coefficients [Wilke and Hougen (W5) correlation] were much higher than the total transfer coefficients calculated from the experimental data and confirmed particle diffusion as the controlling mechanism.

3. Particle diffusion was 85 percent of the total transfer resistance with fluid phase diffusion making up the remainder. Particle diffusion consists of two diffusion mechanisms, surface diffusion and pore diffusion. At low adsorbate concentrations, pore diffusion was responsible for 30 to 50 percent of the transfer rate. At high concentrations, pore diffusion contributed little to the total transfer rate.

4. A precise value of the fluid phase diffusion coefficient was not necessary in determing the particle transfer coefficients for pentane and hexane. A 30 percent error in the diffusion coefficient results in only a 5 percent error

in the particle transfer coefficient, $k_p a_p$, mainly because of the lesser importance of fluid phase diffusion in total transfer resistance. Stiel and Thodos (S8) in a recent article provide the best procedure for obtaining force constants from the critical properties of a gas. These force constants were used in the correlation of Hirschfelder, et al. (R1) to obtain the gas diffusion coefficients.

5. The Thomas Equation (Equation 4-27) is an aid in correcting transient effluent curve slopes to the stabilized zone values and vice versa, but this equation is difficult and tedious to use. A shortcut procedure was developed in this study for predicting transient mass transfer coefficients. These coefficients are in turn used to fit the effluent data.

6. The equation of Glueckauf and Coates [Equation (4-16)] fit the effluent data for pentane and hexane very well, even during transient zone lengths. This equation is based on particle diffusion as the controlling mechanism. Equation 4-14 for fluid phase diffusion controlling does not fit the data well. This equation was referred to by Dale et al. in their study of hydrocarbon adsorption.

7. Equilibrium adsorption capacity values are more important for predicting effluent curves than the mass transfer coefficients, particularly for low gas velocities where the effluent curve slopes are steeper.

8. The particle transfer coefficient, $k_p a_p$, is a function of hydrocarbon concentration in the particle and

increases with increasing concentration. A slight increase of $k_p a_p$ with velocity is attributed to an increase in the effective particle transfer area, a_p, at higher velocities. Parallel transfer resistances exist as well as series resistances because of the varied sizes and shapes of silica gel particles.

9. Effluent data may not be analyzed with constant zone length equations while the transfer zone is still growing. A longer bed is required for zone stabilization as gas velocity increases.

The particle mass transfer coefficient appears to be an increasing function of velocity when the constant zone length equation is used to analyze transient effluent curves. The transfer zone must have reached a constant length before those equations can be used. If an equation that is based upon a linear isotherm is used to analyze adsorption zones which stabilize, the transfer coefficient may be inversely proportional to a power of velocity. This result is clearly wrong.

10. Multicomponent adsorption will be more complicated when particle diffusion controls. Displacement of adsorbed hydrocarbons by heavier components changes the simple one-way diffusion to a slower counter diffusing process. The surface diffusion coefficient is also a function of the amount and composition of the adsorbed phase.

Fluid phase diffusion coefficients for trace components are not influenced as much by composition. If fluid

phase diffusion controlled, the transfer coefficient for each component would be constant.

The equilibrium and mass continuity relationships would be the same for both mechanisms, but the differential mass transfer rate equation for the particle diffusion model would be more complex. For present needs a hypothetical single component model should work best. A pseudo transfer coefficient would be based upon the equilibrium composition of the adsorbed phase.

The foregoing conclusions represent original analytical results for hydrocarbon adsorption and will be useful for analyzing future experimental data and for the design of hydrocarbon adsorption units.

BIBLIOGRAPHY

A1. Adamson, Arthur W., Physical Chemistry of Surfaces, Interscience Publishers, Inc., New York, 1960.

A2. Altshuller, Aubrey P., and Cohen, Israel R., "Application of Diffusion Cells to the Production of Known Concentrations of Gaseous Hydrocarbons," Analytical Chemistry, vol. 32, 1960, pp. 802-810.

A3. Amundson, Neal R., "A Note on the Mathematics of Adsorption in Beds," Journal of Physical Chemistry, pt. I. pp. 1153-1157, 1948, pt. II pp. 812-820, 1949.

A4. Ashford, Francisco E., A Thesis - "Dynamic Adsorption of n-Pentane and n-Hexane on Silica Gel," The University of Oklahoma, Norman, Oklahoma, 1962.

B1. Barrer, R. M., Diffusion In and Through Solids, Cambridge University Press, London, 1941.

B2. _____, "Two-Phase Flow of Adsorbed Vapors," Canadian Journal of Chemistry, vol. 41, no. 7, July, 1963, pp. 1768-1781.

B3. Barry, H. M., "Fixed-Bed Adsorption," Chemical Engineering, vol. 67, no. 3, Feb. 8, 1960, pp. 105-120.

B4. Basmadjian, D., "The Separation of H_2 and D_2 by Moving-Bed Adsorption: Corroboration of Adsorber Design Equations," The Canadian Journal of Chemical Engineering, December, 1963, pp. 269-272.

B5. Bieber, Herman; Steidler, F. E., and Selke, W. A., "Ion Exchange Rate Mechanism" Chemical Engineering Progress Symposium Series, no. 14, vol. 50, Ion Exchange, 1954, pp. 17-21.

B6. Bikerman, J. J., Surface Chemistry-Theory and Applications, Academic Press Inc., New York, 1958.

B7. Bohart, G. S., and Adams, E. Q., "Some Aspects of the Behavior of Charcoal with Respect to Chlorine," Journal of the American Chemical Society, vol. 42, 1920, pp. 523-544.

B8. Bowen, J. H., and Donald, M. B., "Fixed Bed Adsorption from a High Concentration Feed," Chemical Engineering Science, vol. 18, 1963, pp. 599-611.

B9. Brunauer, Stephen, The Adsorption of Gases and Vapours; Volume I-Physical Adsorption, Princeton University Press, Princeton, New Jersey, 1943.

B10. _____, "Solid Surfaces and the Solid-Gas Interface," Advances in Chemistry Series No. 33, American Chemical Society, Washington, D. C., 1961.

B11. Brunauer, Stephen; Emmett, P. H., and Teller, Edward; "Adsorption of Gases in Multimolecular Layers," Journal of the American Chemical Society, vol. 60, Feb., 1938, pp. 309-319.

B12. Brunauer, S.; Deeming, L. S.; Deeming, W. E., and Teller, E.; "On a Theory of Vander Waals Adsorption of Gases," Journal of the American Chemical Society, vol. 62, July, 1940, pp. 1723-1732.

C1. Calderbank, P. H., and Mackrakis, N. S., "Some Fundamentals of the Hypersorption Process," Transactions of the Institute of Chemical Engineers, vol. 34, 1956, pp. 320-338.

C2. Carman, P. C., Flow of Gases through Porous Media, Butterworths Scientific Publications, 1956 (London), Chapter V. "Flow of Sorbable Gases," pp. 104-136.

C3. Cohan, Leonard H., "Sorption Hysteresis and the Vapor Pressure of Concave Surfaces," Journal of the American Chemical Society, vol. 60, Feb., 1938, pp. 433-435.

C4. Carman, P. C., and Malherbe, P. L. R., "Diffusion and flow of gases and vapors through micropores II. Surface Flow," Proceedings of the Royal Society, vol. 203A, 1950, pp. 165-178.

C5. Carman, P. C., and Raal, F. A., "Physical Adsorption of Gases on Porous Solids - I. Comparison of Loose Powders and Porous Plugs," Proceedings of the Royal Society, vol. 209A, 1951, pp. 59-69.

C6. _____, "Diffusion and flow of gases and vapors through micropores III. Surface diffusion coefficients and activation energies," Proceedings of the Royal Society, vol. 209A, 1951, pp. 38-58.

C7. Carmichael, L. T.; Sage, B. H.; and Lacey, W. N., Supplementary Material for Article "Diffusion Coefficients on Hydrocarbon Systems," American Documentation Institute Number 4661.

C8. _____, "Diffusion Coefficients in Hydrocarbon Systems: n - Hexane in the Gas Phase of the Methane -, Ethane -, and Propane - n - Hexane Systems," American Institute of Chemical Engineers Journal, vol. 1, no. 3, pp. 385-390.

C9. Carter, J. W., "Adsorption Drying of Gases," British Chemical Engineering, Part I, July, 1960, pp. 472-476; Part II, August, 1960, pp. 552-555, Part III, Sept., 1960, pp. 625-631.

C10. _____, "Adsorption Processes," British Chemical Engineering, May, 1961, pp. 308-314.

C11. _____, "Advances in Adsorption Processes," British Chemical Engineering, vol. 9, no. 4, April, 1964, pp. 232-238.

C12. Chen, Ning Hsing, and Othmer, Donald F., "New Generalized Equation for Gas Diffusion Coefficient," Journal of Chemical and Engineering Data, vol. 7, no. 1, January, 1962, pp. 37-41.

C13. Cohan, Leonard H., "Sorption Hysteresis and the Vapor Pressure of Concave Surfaces," Journal of the American Chemical Society, vol. 60, Feb., 1938, pp. 433-435.

C14. Cummings, G. A. M., McLaughlin, El, and Ubbelohde, A. R., "Collision Parameters of C_6-C_9Hydrocarbons in the Vapour Phase: The Hydrogen Effect," Journal of the Chemical Society, 1955, pp. 1141-1144.

D1. Dale, G. H., Haskell, D. M., Keeling, H. E., and Worael, L. A., "Dynamic Adsorption of Isobutane and IsoPentane on Silica Gel," Chemical Engineering Progress Symposium Series, vol. 57, no. 34, 1961, pp. 42-49.

D2. de Boer, J. H., "The Shapes of Capillaries," The Structure and Properties of Porous Materials (Ed. Everett, D. H., and Stone, F. S.), Butterworths Scientific Publications, London, 1958, pp. 68-94.

D3. Deitz, Victor R., Bibliography of Solid Adsorbents - 1943 to 1953, National Bureau of Standards Circular 566, 1956.

D4. DeVault, Don, "The Theory of Chromatography," Journal of the American Chemical Society, vol. 65, April, 1943, pp. 532-540.

D5. Dodge, F. W., and Hougen, D. A., Drying of Gases, Edwards, Ann Arbor, Michigan, 1947.

D6. du Domaine, John, Swain, R. L., Hougen, O. A., "Cation-Exchange Water Softening Rates," Industrial and Engineering Chemistry, vol. 35, no. 5, May, 1943, pp. 546-553.

E1. Ebach, Earl A., and White, Robert R., "Mixing of Fluids Flowing through Beds of Packed Solids," American Institute of Chemical Engineers Journal, vol. 4, no. 2, June, 1958, pp. 161-169.

E2. Eagleton, L. C., and Bliss, Harding, "Drying of Air in Fixed Beds," Chemical Engineering Progress, 1953, vol. 49, no. 10, pp. 543-548.

E3. Eberly, P. E., Jr., and Vohsberg, D. B., "Diffusion of Benzene and Inert Gases through Porous Media at Elevated Temperatures and Pressures," a paper presented before the Division of Petroleum Chemistry, American Chemical Society, Chicago, Illinois, Sept. 4, 1964.

F1. Flood, E. A., and Heyding, R. D., "Stresses and Strains in Adsorbent-Adsorbate Systems," Canadian Journal of Chemistry, 1954, vol. 32, pp. 660-682.

F2. Flood, E. A., and Lakhanpal, M. L., "Stresses and Strains in Adsorbent-Adsorbate Systems, III," Second International Congress of Surface Activity, vol. II, Academic Press, New York, 1957, pp. 131-144.

F3. Flood, E. A., Tomlinson, R. H., Leger, A. E., "The Flow of Fluids through Activated Carbon Rods," pp. 348-372, "The Pore Structure of Activated Carbon," pp. 372-387, "The Flow of Adsorbed Fluids," pp. 389-410, Canadian Journal of Chemistry, vol. 30, 1952.

F4. Foster, A. Graham, "The Sorption of Condensible Vapours by Porous Solids. Part I. The Applicability of the Capillary Theory," Transactions of the Faraday Society, vol. 28, 1932, pp. 645-657.

G1. Geser, J. J., and Canjar, L. N., "Adsorption of Methane and Hydrogen on Packed Beds of Activated Carbon," American Institute of Chemical Engineers Journal, vol. 8, no. 4, September, 1962, pp. 494-497.

G2. Getty, R. J., and Armstrong, W. P., "Drying Air with Activated Alumina under Adiabatic Conditions," I and EC Process Design and Development, vol. 3, no. 1, January, 1964, pp. 60-65.

G3. Gupta, A. S., and Thodos, G., "Transitional Behavior for the Simultaneous Mass and Heat Transfer of Gases Flowing through Packed and Distended Beds of Spheres," I and EC Fundamentals, vol. 3, no. 3, August, 1964, pp. 218-220.

G4. Gilliland, E. R., and Baddour, R. F., "The Rate of Ion Exchange," Industrial and Engineering Chemistry, vol. 45, no. 2, Feb., 1953, pp. 330-337.

G5. Gilliland, E. R., Baddour, R. F., and Russell, J. L., "Rates of Flow through Microporous Solids," American Institute of Chemical Engineers Journal, vol. 4, 1958, pp. 90-96.

G6. Glueckauf, E., and Coates, J. I., "Theory of Chromatography. Part IV, The Influence of Incomplete Equilibrium on the First Boundary of Chromatograms and on the Effectiveness of Separation," Journal of the Chemical Society, vol. 150, no. 231, 1947, pp. 1315-1321.

G7. Goldstein, S., "On the Mathematics of Exchange Processes in Fixed Columns," Proceedings of the Royal Society, 219A, 1953, pp. 151-185.

G8. Grafton, E. W., "Prediction of Mass Transfer from Spheres and Cylinders in Forced Convection," Chemical Engineering Science, vol. 18, 1963, pp. 457-466.

G9. Grant, R. J., "Basic Concepts of Adsorption on Activated Carbon" Technical Information Report of Pittsburg Chemical Co., Pittsburg, Pennsylvania.

G10. Grant, R. J., Manes, M., and Smith, S. G., "Adsorption of Normal Paraffins and Sulfur Compounds on Activated Carbon," American Institute of Chemical Engineers Journal, vol. 8, no. 3, pp. 403-406.

G11. Granville, W. H., "Some Aspects of Gas Separation," Industrial and Engineering Chemistry, vol. 56, no. 5, May, 1964, pp. 32-37.

G12. Gregg, S. J., The Adsorption of Gases by Solids, Chemical Publishing Co., Inc., New York, 1934.

H1. Harman, J. F., and Kammermeyer, Karl, "Adsorption Rates on a Vapor-Solid System," Journal of Chemical Engineering Data, vol. 8, no. 4, October, 1963, pp. 519-524.

H2. Hiester, N. K., Radding, S. B., Nelson, R. L., Jr., and Vermuelen, Theodore, "Interpretation and Correlation of Ion Exchange Column Performance under Nonlinear Equilibria," American Institute of Chemical Engineers Journal, vol. 2, no. 3, September, 1956, pp. 404-411.

H3. Hiester, Nevin K., and Vermuelen, Theodore, "Saturation Performance of Ion-Exchange and Adsorption Columns," Chemical Engineering Progress, vol. 48, no. 10, 1952, pp. 505-516.

H4. Hougen, O. A., and Marshall, W. R., "Adsorption from a Fluid Stream Flowing through a Stationary Granular Bed," Chemical Engineering Progress, vol. 43, no. 4, 1947, p. 197.

H5. Huber, M. E., Flood, E. A., Heyding, R. D., "The Micropore Flow of H_2O and D_2O through Activated Carbon Rods," Canadian Journal of Chemistry, vol. 34, 1956, pp. 1288-1301.

J1. Jury, S. H., and Licht, W., Jr., "Drying of Gases-Adsorption Wave in Dessicant Beds," Chemical Engineering Progress, vol. 48, no. 2, February, 1952, pp. 102-109.

K1. Kaplan, Wilfred, Advanced Calculus, Addison-Wesley Publishing Co., Inc., Reading, Massachusetts, 1957, p. 219.

K2. Kaston, P. R., Lapidus, L., and Amundson, N. R., "Mathematics of Adsorption in Beds. V. Effect of Intraparticle Diffusion in Flow Systems in Fixed Beds," Journal of Physical Chemistry, vol. 56, 1952, pp. 683-688.

K3. Kiselev, A. V., "The Structure of Certain Corpuscular Adsorbents and Its Influence on their Adsorptive Properties," The Structure and Properties of Porous Materials, Butterworths Scientific Publications, London, 1958, pp. 195-226.

K4. Kiselev, A. V., and Eltekov, Y. A., "Effect of Nature of Adsorbent and Pore Size on Shape of BET Vapour Adsorption Isotherm," Proceedings Second International Congress of Surface Activity, vol. II, Solid-Gas Interface, Academic Press, New York, 1957, pp. 228-229.

K5. Klinkenberg, Adriaan, "Numerical Evaluation of Equations Describing Transient Heat and Mass Transfer in Packed Solids," Industrial and Engineering Chemistry, vol. 40, no. 10, October, 1948, pp. 1992-1994.

K6. Klotz, I. M., "The Adsorption Wave," Chemical Reviews, vol. 39, 1946, pp. 241-268.

L1. Lamb, L. L., "Which to Use-Adsorption or Refrigeration," The Oil and Gas Journal, April 8, 1963, pp. 81-83.

L2. Langmuir, I., "The Adsorption of Gases on Plane Surfaces of Glass, Mica, and Platinum," Journal of the American Chemical Society, vol. 40, 1918, pp. 1361-1403.

L3. Lapidus, L., and Rosen, J. B., "Experimental Investigation of Ion Exchange Mechanisms in Fixed Beds by Means of an Asymptotic Solution," Ion Exchange, Chemical Engineering Progress, Symposium Series no. 14, vol. 50, 1954, pp. 97-102.

L4. Leavitt, F. W., "Non-isothermal Adsorption in Large Fixed Beds," Chemical Engineering Progress, vol. 58, no. 8, August, 1962, pp. 54-59.

L5. Ledoux, Edward, "Redistribution of Adsorbate by Diffusion," Journal of Physical and Colloid Chemistry, vol. 53, 1949, pp. 960-966.

L6. Leland, Thomas W., Jr., and Holmes, Richard E., "The Design of Hydrocarbon Recovery Units Using Solid Adsorbents," Petroleum Transactions AIME, 1962, pp. 179-186.

L7. Lewis, W. K., Gilliland, E. R., Chertow, R., and Cadogan, W. P., "Adsorption Equilibria" Pt. 1 "Hydrocarbon Gas Mixtures," pp. 1319-1325, Pt. 2 "Pure Gas Isotherms," pp. 1326-1332, Industrial and Engineering Chemistry, vol. 42, no. 7, July, 1950.

M1. Mantel, C. L., Adsorption, McGraw-Hill Book Company, Inc., 1951.

M2. Marks, E. E., Robinson, R. J., Arnold, C. W., and Hoffmann, A. E., "Dynamic Behavior of Fixed-Bed Adsorbers," Petroleum Transactions AIME, 1963, pp. 443-449.

M3. Matheson Natural Gas Handbook, The Matheson Company, Inc., East Rutherford, New Jersey, 1961, pp. 275-281.

M4. McHenry, K. W., Jr., and Wilhelm, R. H., "Axial Mixing of Binary Gas Mixtures Flowing in a Random Bed of Spheres," American Institute of Chemical Engineering Journal, vol. 3, no. 1, March, 1957, pp. 83-91.

M5. Michaels, Alan S., "Simplified Method of Interpreting Kinetic Data in Fixed-Bed Ion Exchange," Industrial and Engineering Chemistry, vol. 44, no. 8, 1922-1930 (1952).

M6. Mickley, H. S., Sherwood, T. K., and Reid, C. E., Applied Mathematics in Chemical Engineering, McGraw-Hill Book Co., New York, 1957.

N1. Needham, R. B., Campbell, J. M., and McLeod, H. O., "A Critical Evaluation of the Mathematical Models Used for Dynamic Adsorption of Hydrocarbons," Presented at A.I. Ch.E. Adsorption Symposium, Memphis, Tennessee, 1964.

N2. NGSMA Engineering Data Book, Natural Gasoline Supply Men's Association, Tulsa, Oklahoma, 7th Edition, 1957.

O1. Opler, A., and Heister, N. K. "Tables for Predicting the Performance of Fixed-Bed Ion Exchange and Similar Mass Transfer Processes," Stanford Research Institute, Stanford, California, 1954.

O2. Osipow, Lloyd I., Surface Chemistry - Theory and Industrial Applications, Reinhold Publishing Corporation, New York, 1962.

P1. Parks, A. S., and Dow, W. M., "Development of Dry-desicant Wellhead Adsorption Units, API Drilling and Production Practices, 1956, pp. 399-413.

P2. Perry, R., Editor, Chemical Engineering Handbook, McGraw Hill Book Co., New York, Chapter 14, pp. 19-23.

P3. Pfeiffer, P. W., "A Graphical Method for Calculating Ion Exchange Columns," Chemical Engineering Science, vol. 2, no. 2, April, 1953, pp. 45-52.

R1. Reid, R. C., and Sherwood, T. K., The Properties of Gases and Liquids, Chapter 8, Diffusion Coefficients, McGraw Hill, New York, 1958.

R2. Rosen, J. B., "General Numerical Solution for Solid Diffusion in Fixed Beds," Industrial and Engineering Chemistry, vol. 46, no. 8, August, 1924, pp. 1590-1594.

R3. Ross, Sydney, and Olivier, James P., On Physical Adsorption, Interscience Publishers, New York, 1964.

R4. Rounsley, R. R., "Multimolecular Adsorption Equation," American Institute of Chemical Engineering Journal, vol. 7, no. 2, June, 1961, pp. 308-311.

S1. Saffman, P. G., "On the Effect of the Molecular Diffusivity in Turbulent Diffusion," Journal of Fluid Mechanics, vol. 8, 1960, pp. 273-283.

S2. Schwartz, C. E., and Smith, J. M., "Flow Distributions in Packed Beds," Industrial and Engineering Chemistry, vol. 45, no. 6, pp. 1209-1218.

S3. Sherwood, T. K., and Pigford, R. L., Adsorption and Extraction, McGraw Hill Book Co., New York, 1952.

S4. Sillen, L. G., "On Filtration through a Sorbent Layer - I. An Attempt at a Simple Mathematical Treatment," ArKiv Kemi Mineral Geologia, A 22, no. 15, 1946, pp. 1-22.

S5. Sillen, L. G., and Ekedahl, E., "On Filtration through a Sorbent Layer-II. Experiments with an Ion Exchanger; Theory, Apparatus, and Preliminary Results," ArKiv Kemi Mineral Geologia, 22 A, no. 16, 1946, pp. 1-12.

S6. Slattery, John C., and Bird, R. Byron, "Calculation of the Diffusion Coefficient of Dilute Gases and of the Self-diffusion Coefficient of Dense Gases, American Institute of Chemical Engineering Journal, June, 1958, vol. 4, no. 2, pp. 137-142.

S7. Smith, R. K., and Metzner, A. B., "Rates of Surface Migration of Physically Adsorbed Gases," Journal of Physical Chemistry, vol. 68, no. 10, October, 1964, pp. 2741-2747.

S8. Stiel, Leonard I., and Thodos, George, "Lennard-Jones Force Constants Predicted from Critical Properties," Journal of Chemical and Engineering Data, vol. 7, no. 2, April, 1962, pp. 234-236.

T1. Thomas, H. C., "Heterogeneous Ion Exchange in a Flowing System," Journal of the American Chemical Society, vol. 66, 1944, pp. 1664-1666.

V1. Vermuelen, Theodore, "Theory for Irreversible and Constant-Pattern Solid Diffusion," Industrial and Engineering Chemistry, vol. 45, no. 8, 1953, pp. 1664-1670.

V2. Vermuelen, Theodore, "Separation by Adsorption Methods," Advances in Chemical Engineering, vol. 2, Academic Press, Inc., New York, 1958, pp. 147-208.

V3. Villet, Ruxton H., and Wilhelm, Richard H., "Knudsen-Flow-Diffusion in Porous Pellets," Industrial and Engineering Chemistry, vol. 53, no. 10, October, 1961, pp. 837-840.

W1. Wade, William H., "The Surface Area of Water Preadsorbed on Powdered Substrates," Journal of Physical Chemistry, vol. 68, no. 5, May, 1964, pp. 1029-1034.

W2. Walter, John E., "Multiple Adsorption from Solutions," Journal of Chemical Physics, vol. 13, 1945, pp. 229-234; "Rate Dependent Chromatographic Adsorption," Journal of Chemical Physics, vol. 13, 1945, pp. 332-336.

W3. Wheeler, A., Advances in Catalysis, vol. 3, 1951, pp. 250-327; Catalysis, vol. 2 (P. H. Emmett, editor) Reinhold, New York, 1955, pp. 105-165.

W4. White, C. G. C., and Helf, S., "Surface Phenomena in Solids - A Literature Review," U. S. Department of Commerce, Office of Technical Services, May, 1959.

W5. Wilke, C. R., and Hougen, D. A., Transactions from American Institute of Chemical Engineers, vol. 41, 1945, p. 445.

W6. Wilke, C. R., and Lee, C. Y., "Estimation of Diffusion Coefficients for Gases and Vapors, Industrial and Engineering Chemistry, vol. 47, no. 6, June, 1955, pp. 1253-1257.

W7. Wilson, J. N., "A Theory of Chromatography," Journal of the American Chemical Society, vol. 62, 1940, pp. 1583-1591.

W8. Wynne-Jones, W. F. K., "The Surface Characteristics of Carbons," The Structure and Properties of Porous Materials, Butterworths Scientific Publications, London, 1958, pp. 25-46.

Y1. Young, D. M., and Crowell, A. D., Physical Adsorption of Gases, Butterworth, Inc., Washington, 1962.

Z1. Zweitering, P., Discussion, Proceedings of 10th Symposium of the Colston Research Society, Butterworths, London, 1958, pp. 286-289.

APPENDICES

APPENDIX A

EXPERIMENTAL DATA

As explained in Chapter V we recorded the effluent concentration of the particular hydrocarbon component as analyzed by the gas chromatograph. These effluent concentrations of the component relative to the inlet concentration (C/C_o) were plotted versus the throughput time. These effluent data are listed in Tables A-1 and A-2. The physical conditions for each run are listed in Tables A-3 and A-6, the effluent curve parameters are listed in Tables A-4 and A-7, and the calculated adsorption values are shown in Tables A-5 and A-8. These data are analyzed in Chapter VI to determine the relationship of the important variables.

Some variations occurred in the effluent concentrations. These variations in effluent concentration may result from slight variations in liquid injection rate into the gas stream. At times small fines coming from inside the tank restricted flow from the metering valve on the constant head injection tank. Fluctuation in the pressure of the tank can also cause slight changes in liquid output. At times the recorder or chromatograph was unstable and caused slight shifting in the peak heights on the recorder charts. This variation may result from line current changes or misbehavior in some of the electrical components.

In 45 runs, including 21 runs for hexane and 24 for

pentane, pressure and temperature were constant. Only the gas velocity and hydrocarbon component composition were varied.

The gas composition was calculated on the basis of the total flow rate and the quantity of liquid hydrocarbon added to the gas system. The amount of hydrocarbon either pentane or hexane, which was absorbed during each run was calculated from the effluent curves. A ratio of the effluent curve area which lies above the curve to the total area gives the proportion of the gas throughput adsorbed. Since the ordinate of the area is one, then the total area is equal to the time at the end of the effluent curve. The adsorption equilibrium value for each run and composition were calculated by dividing the bed weight into the weight of hydrocarbon adsorbed. The equilibrium adsorption contents of the dessicant, X_T, were plotted versus mole percent of pentane or hexane to give adsorption equilibrium curves. These curves which are shown on log-log paper in Figures A-1 and A-2 do not give a straight line relationship on coordinate plots, a relationship which has been assumed in several previous analyses of fixed-bed adsorption data. The variation in these adsorption values is discussed in Chapter IX.

The two lower points in Figure A-1 and the points within the dashed curve in Figure A-2 are from a later set of data than the others.

TABLE A-I

PENTANE EFFLUENT DATA

Run No. 56		Run No. 57-A		Run No. 57-B	
Time Min.	C/C_o	Time Min.	C/C_o	Time Min.	C/C_o
15.3	.005	20.7	.0104	15.0	0
17.9	.027	23.3	.0416	17.7	.005
20.6	.070	26.0	.104	20.3	.023
23.3	.132	28.7	.187	23.0	-
25.9	.232	31.3	.282	25.7	.115
28.6	.336	34.0	.399	28.3	.208
31.3	.462	36.7	.520	31.0	.305
33.9	.570	39.3	.613	33.7	.380
36.6	.685	42.0	.716	36.3	.480
39.3	.756	44.7	.800	39.0	.584
41.9	.826	47.3	.862	41.7	.660
44.6	.866	50.0	.903	44.3	.734
47.3	.916	52.7	.955	47.0	-
49.9	.935	55.3	.976	49.7	.863
52.6	.962	58.0	1.000	52.3	.880
55.3	.991			55.0	.912
57.9	.995			57.7	.938
60.6	1.000			60.3	.970
				63.0	1.000

TABLE A-I--Continued

Run No. 58		Run No. 59		Run No. 60	
Time Min.	C/C_o	Time Min.	C/C_o	Time Min.	C/C_o
36.1	0	34.0	0	45.0	0
38.8	.009	36.7	.017	47.7	.011
41.4	.036	39.3	.021	50.3	.023
44.1	.055	42.0	.053	53.0	.061
46.8	.132	44.7	.088	55.7	.086
49.4	.215	47.3	.158	58.3	.148
52.1	.314	50.0	.235	61.0	.208
54.8	.419	52.7	.333	63.7	.282
57.4	.529	55.3	.446	66.3	.360
60.1	.623	58.0	.555	69.0	.442
62.8	.710	60.7	.640	71.7	.536
65.4	.790	63.3	.726	74.3	.611
68.1	.850	66.0	.794	77.0	.674
70.8	.932	68.7	.876	79.7	.750
73.4	.935	71.3	.917	82.3	.804
76.1	.960	74.0	.939	85.0	.853
78.8	1.000	76.7	.961	87.7	.895
		79.3	.982	90.3	.916
		82.0	.984	93.0	.946
		84.7	1.000	95.7	.970
				98.3	.988
				101.0	.990
				103.7	.990
				106.3	1.000

TABLE A-I--Continued

Run No. 61		Run No. 62		Run No. 63	
Time Min.	C/C_o	Time Min.	C/C_o	Time Min.	C/C_o
36.1	0	39.1	0	39.0	0
38.8	.017	41.8	.010	41.7	.005
41.4	.051	44.4	.022	44.3	.014
44.1	.113	47.1	.049	47.0	.032
46.8	.215	49.8	.065	49.7	.062
49.4	.339	52.4	.143	52.3	.097
52.1	.480	55.1	.222	55.0	.141
54.8	.611	57.8	.309	57.7	.208
57.4	.716	60.4	.400	60.3	.268
60.1	.819	63.1	.495	63.0	.342
62.8	.893	65.8	.573	65.7	.416
65.4	.921	68.4	.674	68.3	.490
68.1	.950	71.1	.748	71.0	.574
70.8	.973	73.8	.800	73.7	.640
73.4	.984	76.4	.839	76.3	.707
76.1	.996	79.1	.887	79.0	.773
78.8	1.000	81.8	.924	81.7	.831
		84.4	.936	84.3	.864
		87.1	.954	87.0	.900
		89.8	.978	89.7	.926
		92.4	1.000	92.3	.947
				95.0	.973
				97.7	1.000

TABLE A-I--Continued

Run No. 64		Run No. 65		Run No. 66	
Time Min.	C/C_o	Time Min.	C/C_o	Time Min.	C/C_o
15.2	.026	12.5	0	11.7	0
17.8	.085	15.2	.008	14.3	.012
20.5	.190	17.8	.039	17.0	.065
23.2	.335	20.5	.103	19.7	.163
25.8	.492	23.2	.199	22.3	.275
28.5	.644	25.8	.315	25.0	.415
31.2	.755	28.5	.449	27.7	.572
33.8	.830	31.2	.574	30.3	.705
36.5	.885	33.8	.682	33.0	.810
39.2	.935	36.5	.770	35.7	.880
41.8	.935	39.2	.829	38.3	.930
44.5	.955	41.8	.892	41.0	.950
47.2	.966	44.5	.920	43.7	.965
49.8	.968	47.2	.944	46.3	.975
		49.8	.956	49.0	.985
		52.5	.967		
		55.2	.970		
		57.8	.980		
		60.5	.978		
		63.2	.985		
		65.8	.989		
		68.5	1.000		

TABLE A-I--Continued

Run No. 68		Run No. 84		Run No. 86	
Time Min.	C/C_o	Time Min.	C/C_o	Time Min.	C/C_o
17.7	0	7.0	0	10.0	0
20.3	.016	9.7	.044	12.7	.052
23.0	.045	12.3	.135	15.3	.148
25.7	.091	15.0	.301	18.0	.300
28.3	.157	17.7	.494	20.7	.456
31.0	.261	20.3	.683	23.3	.606
33.7	.361	23.0	.769	26.0	.738
36.3	.461	25.7	.859	28.7	.834
39.0	.567	28.3	.914	31.3	.906
41.7	.660	31.0	.934	34.0	.963
44.3	.750	33.7	.949	36.7	1.000
47.0	.817	36.3	1.000		
49.7	.878				
52.3	.942				
55.0	.996				
57.7	.978				
60.3	1.000				

TABLE A-I--Continued

Run No. 87		Run No. 88		Run No. 89	
Time Min.	C/C_o	Time Min.	C/C_o	Time Min.	C/C_o
7.3	0	7.0	0	9.5	.005
10.0	.086	9.7	.015	12.2	.056
12.7	.245	12.3	.091	14.8	.185
15.3	.418	15.0	.197	17.5	.374
18.0	.626	17.7	.303	20.2	.565
20.7	.755	20.3	.476	22.8	.706
23.3	.830	23.0	.606	25.5	.802
26.0	.876	25.7	.724	28.2	.875
28.7	.922	28.3	.819	30.8	.915
31.3	1.000	31.0	.879	33.5	.943
		33.7	.957	36.2	.965
		36.3	.967	38.8	.984
		39.0	.988	41.5	.995
		41.7	1.000		

TABLE A-I--Continued

Run No. 90		Run No. 193		Run No. 194	
Time Min.	C/C_o	Time Min.	C/C_o	Time Min.	C/C_o
7.2	.001	3.7	0.07	1.5	.065
9.8	.044	6.7	.132	4.5	.145
12.5	.176	9.7	.328	7.5	.482
15.2	.396	12.7	.536	10.5	.747
17.8	.601	15.7	.686	13.5	.884
20.5	.739	18.7	.781	16.5	.945
23.2	.824	21.7	.867	19.5	.971
25.8	.896	24.7	.902	22.5	.992
28.5	.932	27.7	.918	25.5	.980
31.2	.971	30.7	.929	28.5	.988
33.8	.996	33.7	.937	31.5	.994
36.5	1.000	36.7	.948	34.5	1.000
		39.7	.964		
		42.7	.953		
		45.7	.980		
		48.7	1.001		

TABLE A-I--Continued

Run No. 205		Run No. 209		Run No. 210	
Time Min.	C/C_o	Time Min.	C/C_o	Time Min.	C/C_o
29	0	14.25	0	5.5	0
32	trace	17.25	.054	8.5	.135
35	.043	20.25	.126	11.5	.326
38	.153	23.25	.266	14.5	.527
41	.290	26.25	.445	17.5	.764
44	.463	29.25	.641	20.5	.838
47	.614	32.25	.746	23.5	.905
50	.724	35.25	.835	26.5	.943
53	.820	38.25	.897	29.5	.943
56	.884	41.25	.921	32.5	1.000
59	.920	44.25	.947		
62	.957	47.25	.940		
65	.970	50.25	1.000		
68	.990				
71	.997				
74	1.000				

TABLE A-II

HEXANE EFFLUENT DATA

Run No. 69		Run No. 70		Run No. 71			
Time Min.	C/C_o	Time Min.	C/C_o	Time Min.	C/C_o	Time Min.	C/C_o
50.2	.005	41.7	.01	123.8	0	177.1	.952
52.8	.016	44.3	.06	126.4	.004	179.8	.960
55.5	.045	47.0	.185	129.1	.017	182.4	.984
58.2	.130	49.7	.415	131.8	.039	185.1	1.000
60.8	.225	52.3	.615	134.4	.074		
63.5	.373	55.0	.74	137.1	.104		
66.2	.505	57.7	.855	139.8	.135		
68.8	.602	60.3	.868	142.4	.209		
71.5	.720	63.0	.92	145.1	.278		
74.2	.780	65.7	.935	147.8	.361		
76.8	.860	68.3	.943	150.4	.469		
79.5	.890	71.0	.96	153.1	.556		
82.2	.906	73.7	.985	155.8	.626		
84.8	.963	76.3	.995	158.4	.684		
87.5	.966	79.0	.995	161.1	.774		
90.2	1.000	81.7	1.000	163.8	.795		
				166.4	.853		
				169.1	.878		
				171.8	.914		
				174.4	.921		

TABLE A-II--Continued

Run No. 72		Run No. 73			
Time Min.	C/C_o	Time Min.	C/C_o	Time Min.	C/C_o
79.0	0	122.7	0	176.0	.857
81.7	.004	125.3	.006	178.7	.890
84.3	.023	128.0	.019	181.3	.931
87.0	.043	130.7	.031	184.0	.940
89.7	.134	133.3	.062	186.7	.946
92.3	.266	136.0	.069	189.3	1.000
95.0	.423	138.7	.093		
97.7	.610	141.3	.154		
100.3	.759	144.0	.222		
103.0	.846	146.7	.278		
105.7	.940	149.3	.346		
108.3	.951	152.0	.420		
111.0	1.000	154.7	.462		
		157.3	.525		
		160.0	.586		
		162.7	.646		
		165.3	.666		
		168.0	.740		
		170.7	.778		
		173.3	.820		

TABLE A-II--Continued

Run No. 74		Run No. 76		Run No. 77	
Time Min.	C/C_o	Time Min.	C/C_o	Time Min.	C/C_o
92.3	0	28.8	0	47.0	.025
95.0	.018	31.5	.011	49.7	.072
97.7	.029	34.2	.044	52.3	.190
100.3	.036	36.8	.178	55.0	.345
103.0	.100	39.5	.400	57.7	.515
105.7	.136	42.2	.613	60.3	.655
108.3	.214	44.8	.746	63.0	.760
111.0	.314	47.5	.789	65.7	.845
113.7	.378	50.2	.854	68.3	.900
116.3	.504	52.8	.884	71.0	.935
119.0	.650	55.5	.900	73.7	.950
121.7	.754	58.2	.925	76.3	.983
124.3	.804	60.8	.966	79.0	.996
127.0	.893	63.5	.978		
129.7	.930	66.2	1.000		
132.3	.965				
135.0	.982				
137.9	1.000				

TABLE A-II--Continued

Run No. 78		Run No. 79		Run No. 80	
Time Min.	C/C_o	Time Min.	C/C_o	Time Min.	C/C_o
52.5	.007	23.0	.008	25.3	.032
55.2	.025	25.7	.055	28.0	.103
57.8	.036	28.3	.122	30.7	.200
60.5	.065	31.0	.255	33.3	.297
63.2	.106	33.7	.388	36.0	.400
65.8	.175	36.3	.555	38.7	.496
68.5	.255	39.0	.666	41.3	.600
71.2	.405	41.7	.795	44.0	.660
73.8	.425	44.3	.870	46.7	.746
76.5	.515	47.0	.906	49.3	.794
79.2	.605	49.7	.945	52.0	.844
81.8	.725	52.3	.980	54.7	.886
84.5	.750	55.0	1.000	57.3	.904
87.2	.784			60.0	.930
89.8	.807			62.2	.940
92.5	.878			65.3	.979
95.2	.895			68.0	1.000
97.8	.955				

TABLE A-II--Continued

Run No. 81		Run No. 82		Run No. 83	
Time Min.	C/C_o	Time Min.	C/C_o	Time Min.	C/C_o
17.2	.005	13.0	.005	17.8	.026
19.8	.025	15.6	.140	20.5	.350
22.5	.086	18.3	.560	23.2	.692
25.2	.220	21.0	.745	25.8	.822
27.8	.375	23.6	.875	28.5	.918
30.5	.505	26.3	.920	31.2	.952
33.2	.632	29.0	.980	33.8	.983
35.8	.762	31.6	1.000	36.5	1.000
38.5	.820				
41.2	.860				
43.8	.885				
46.5	.915				
49.2	.944				

TABLE A-II--Continued

Run No. 190		Run No. 191		Run No. 192	
Time Min.	C/C_o	Time Min.	C/C_o	Time Min.	C/C_o
16.5	0	8	.068	23	0
19.5	.106	11	.097	26	.017
22.5	.235	14	.443	29	.085
25.5	.384	17	.790	32	.369
28.5	.587	20	.925	35	.711
31.5	.721	23	.957	38	.878
34.5	.716	26	.971	41	.930
37.5	.850	29	.966	44	.968
40.5	.824	32	.962	47	.983
43.5	.871	35	1.032	50	.890
46.5	.921	38	.957	53	.965
49.5	.903	41	.977	56	.990
52.5	.962	44	1.000	59	1.000
55.5	.962	47	1.000		
58.5	.968				
61.5	1.000				

TABLE A-II--Continued

Run No. 204		Run No. 206	
Time Min.	C/C_o	Time Min.	C/C_o
8	0	17.5	0
11	.035	20.5	trace
14	.314	23.5	.055
17	.686	26.5	.082
20	.840	29.5	.274
23	.931	32.5	.432
26	1.000	35.5	.580
29	1.000	38.5	-
		41.5	-
		44.5	.844
		47.5	.930
		50.5	.941
		53.5	.950
		56.6	.993
		59.5	1.000

TABLE A-II--Continued

Run No. 207		Run No. 208	
Time Min.	C/C_o	Time Min.	C/C_o
14.75	0	35.75	0
17.75	.018	38.75	.028
20.75	.086	41.75	.143
23.75	.294	44.75	.380
26.75	.557	47.75	.615
29.75	.726	50.75	.787
32.75	.836	53.75	.898
35.75	.904	56.75	.943
38.75	.950	59.75	.965
41.75	.974	62.75	.985
44.75	1.000	65.75	1.006
		68.75	1.000

TABLE A III

EXPERIMENTAL CONDITIONS

PENTANE RUNS

Run Number	Pressure psia	Temperature °F	Flow Rate SCF/hr	Injection Rate gms/min	Bed Weight lbs
56	815	91	3230	47.4	34.09
57-A	828	90	3185	23.4	34.09
57-B	819	91	3220	27.8	34.09
58	829	92	1583	33.2	34.09
59	815	92	1609	39.2	34.09
60	845	91	1581	15.0	34.09
61	825	97	1562	45.8	34.09
62	825	91	1566	33.5	34.09
63	815	89	1600	12.9	34.09
64	815	96	3280	71.6	34.09
65	815	92	3390	55.7	34.09
66	824	92	3340	74.4	34.09
68	820	91	3390	26.2	34.09
84	820	89	6640	117.0	35.48
86	823	90	6550	35.6	35.48
87	818	91	6430	149.9	35.48
88	840	89	6688	44.8	35.48
89	830	91	6460	91.9	35.48
90	825	90	6640	153.0	35.48
193	815	92.8	6790	41.8	35.65
194	815	91	6795	189.2	35.65
205	820	90	1425	44.1	35.65
209	805	89.6	3045	76.7	35.65
210	820	90.3	6730	129.0	35.65

TABLE A IV

EFFLUENT CURVE PARAMETERS

PENTANE RUNS

Run Number	θ_β-min	θ_E min	θ_Z-min	$\frac{1}{\theta_Z}\int_{\theta_\beta}^{\theta_E}(1-x)dt$	Q_T-lb moles
56	19.5	50.0	30.5	.444	.04794
57-A	24.0	52.5	28.5	.464	.02665
57-B	21.4	57.0	35.6	.463	.03223
58	42.5	73.8	31.3	.491	.05885
59	41.5	75.0	33.5	.482	.06918
60	52.5	93.5	41.0	.461	.03278
61	41.8	68.0	26.3	.427	.07434
62	47.0	84.5	37.5	.461	.06596
63	48.5	91.0	42.5	.493	.02744
64	16.7	42.5	25.8	.394	.05890
65	18.5	48.0	29.5	.424	.05287
66	16.0	40.7	24.7	.447	.06160
68	23.5	54.0	30.5	.471	.03037
84	9.8	31.3	21.5	.401	.0660
86	12.5	33.3	20.8	.447	.02377
87	8.8	28.8	20.0	.419	.07885
88	11.25	33.75	22.5	.460	.02964
89	11.75	34.0	22.25	.347	.05478
90	9.75	29.50	19.75	.399	.08260
193	0	-	-	-	.01832
194	0	-	-	-	.0486
205	35.3	61.0	25.7	.41	.0619
209	17	43	26	.43	.0661
210	7	27	20	.38	.0577

TABLE A V

CALCULATED ADSORPTION VALUES

PENTANE RUNS

Run Number	C_o mole percent	X_T lb C_5/lb gel	D $q_o \rho_b / C_o \epsilon$	F cu ft/min	$Dv\epsilon/F$ min
56	1.022	.1012	126.4	1.029	33.0
57-A	.511	.0563	138.0	.996	37.3
57-B	.601	.0680	143.8	1.021	37.9
58	1.461	.1243	106.9	.497	57.9
59	1.694	.1461	110.2	.513	57.8
60	.660	.0693	129.1	.486	71.4
61	2.040	.1570	98.0	.497	53.0
62	1.489	.1393	118.0	.493	64.3
63	.561	.0580	131.5	.508	69.6
64	1.519	.1243	105.4	1.054	26.9
65	1.144	.1117	124.7	1.081	31.0
66	1.551	.1301	106.1	1.054	27.1
68	.538	.0642	151.3	1.074	37.9
84	1.227	.1339	144.3	2.096	18.53
86	.378	.0482	167.6	2.061	21.86
87	1.623	.1600	130.5	2.042	17.19
88	.467	.0601	165.4	2.061	21.58
89	.990	.1112	146.5	2.021	19.50
90	1.604	.1676	136.9	2.087	17.65
193	.429	.0370	114.8	2.176	14.24
194	1.94	.0982	67.2	2.17	8.36
205	2.155	.1250	76.4	.452	45.6
209	1.752	.1335	102.4	.983	28.1
210	1.333	.1165	115	2.135	14.55

TABLE A VI

EXPERIMENTAL CONDITIONS

HEXANE RUNS

Run Number	Pressure psia	Temperature ^{o}F	Flow Rate SCF/hr	Injection Rate gms/min	Bed Weight lbs
69	815	92	3541	30.2	34.09
70	822	89	3420	54.3	34.09
71	823	91	1525	16.0	34.09
72	820	90	1550	31.9	34.09
73	817	91	1605	12.9	34.09
74	800	92	1592	27.2	34.09
76	830	93	3090	72.4	34.09
77	835	88	2940	47.4	34.09
78	815	99	3019	24.8	34.09
79	815	91	6150	44.8	34.09
80	823	90	6430	40.5	34.09
81	815	88	5650	73.2	34.09
82	820	90	6500	135.5	35.48
83	817	91	6600	148.1	35.48
190	815	93.7	6830	47	35.65
191	815	93	6790	142	35.65
192	812	92.4	2920	68.5	35.65
204	820	93.5	6300	104.8	35.65
206	800	88.5	6670	39.2	35.65
207	815	91	6800	72.7	35.65
208	815	89	3085	45.7	35.65

TABLE A VII

EFFLUENT CURVE PARAMETERS

HEXANE RUNS

Run Number	θ_β-min	θ_E-min	θ_Z-min	$\frac{1}{\theta_Z}\int_{\theta_\beta}^{\theta_E}(1-x)dt$	Q_T-lb moles
69	55.0	83.5	28.5	.454	.0526
70	43.7	66.0	22.3	.363	.0721
71	132.5	176.0	43.5	.474	.0628
72	87.0	107.0	20.0	.414	.0779
73	134.0	185.0	51.0	.456	.0521
74	100.0	132.0	32.0	.500	.0809
76	35.0	59.0	24.0	.330	.0797
77	49.0	72.5	22.5	.400	.0705
78	59.0	97.5	38.5	.456	.0487
79	25.7	49.0	23.3	.434	.0411
80	26.4	62.0	35.6	.392	.0419
81	21.0	50.0	29.0	.377	.0599
82	14.4	26.8	12.4	.357	.0654
83	18.3	31.5	13.2	.352	.0871
190	18.0	52.5	34.5	.342	.0500
191	8.0	22.5	14.5	.460	.0743
192	28.0	43.0	15.0	.341	.0809
204	11.2	23.7	12.5	.364	.0589
206	23.0	51.0	28.0	.430	.0490
207	19.5	38.5	19.0	.380	.0693
208	39.5	58.0	18.5	.420	.0771

TABLE A VIII

CALCULATED ADSORPTION VALUES

HEXANE RUNS

Run Number	C_o mole percent	X_T lbs C_6/lb gel	D $q_o\rho_b/C_o\epsilon$	F cu ft/min	$Dv\epsilon/F$ min
69	.497	.1327	285.4	1.130	67.9
70	.926	.1819	207.3	1.076	51.8
71	.611	.1584	274.3	.481	153.5
72	1.199	.1966	173.8	.490	95.4
73	.469	.1313	298.2	.510	157.3
74	.996	.2040	223.3	.518	116.0
76	1.366	.2010	154.8	.970	42.9
77	.940	.1778	195.9	.909	58.0
78	.479	.1228	273.8	.962	76.6
79	.425	.1037	260.8	1.959	35.8
80	.367	.1057	304.2	2.024	40.4
81	.755	.1511	212.5	1.789	32.0
82	1.216	.1586	143.8	2.055	18.8
83	1.308	.2110	178.8	2.096	22.9
190	.400	.0866	242.0	2.195	29.8
191	1.220	.1289	118.0	2.176	14.6
192	1.372	.1402	114.5	.936	33.0
204	.970	.1020	116.6	2.010	15.7
206	.342	.0850	280.5	2.160	35.1
207	.635	.1200	210.0	2.170	26.1
208	.862	.1336	172.0	.982	47.2

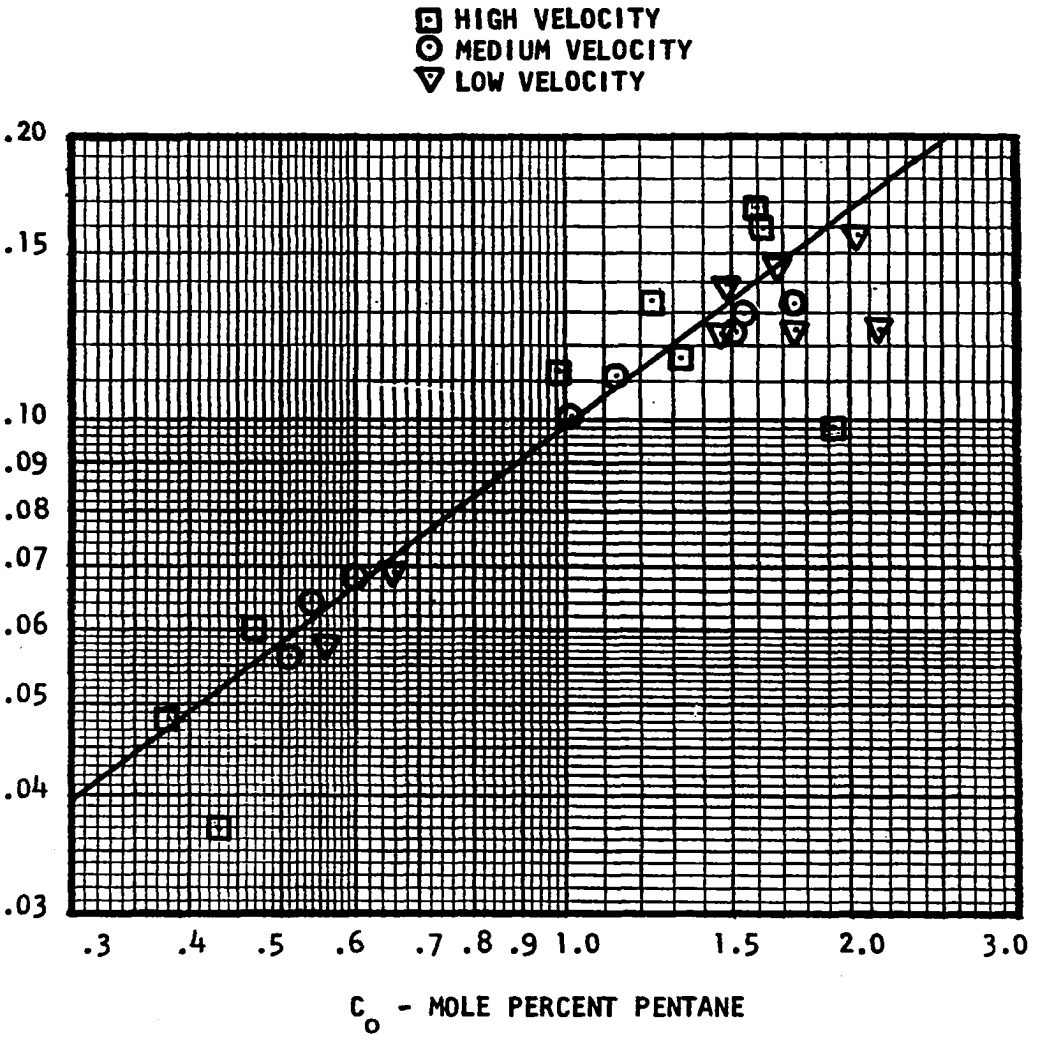


FIGURE A-1 EQUILIBRIUM ADSORPTION VALUES - PENTANE

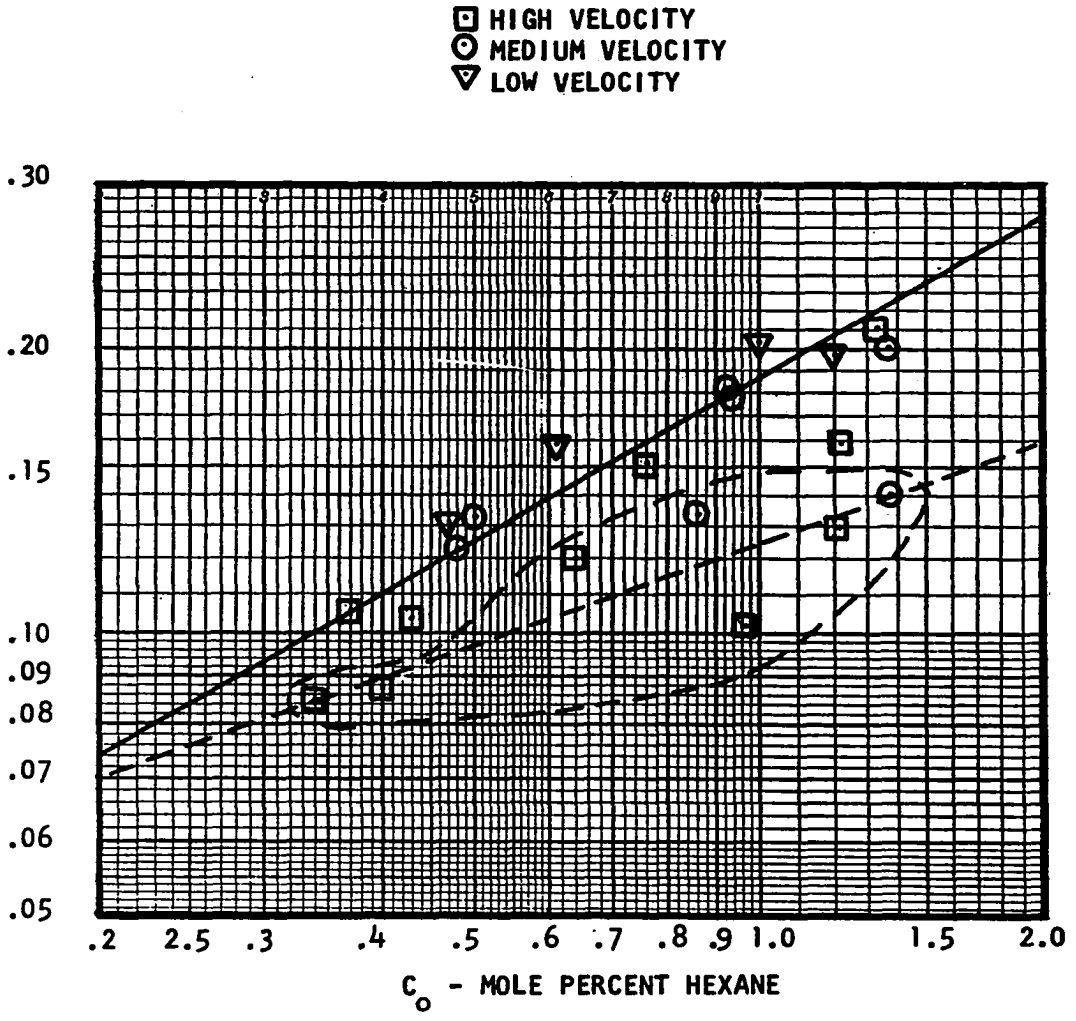


FIGURE A-2 EQUILIBRIUM ADSORPTION VALUES - HEXANE

APPENDIX B

Example Calculations - Run No. 210

1. Bed Calculation

Bed Length	=	448 cm	= 14.65 ft
Bed Diameter	=		2.90 in
Cross Section Area	=		.0459 ft^2
Volume	=		0.675 ft^3
Weight of Dessicant	=	16, 176 gms	= 35.65 lbs
Bed Density	=	$\frac{35.65}{.675}$	= 52.8 lbs/ft^3
ϵ = porosity	=		0.40

2. Gas Flow Calculations - General

Orifice Equation

$$Q = C'\sqrt{h_w P_f}$$

h_w - differential pressure - inches water

Q - flow rate at base pressure - CFH

P_f - static pressure - psia

$C' = F_b \times F_{pb} \times F_{tb} \times F_g \times F_{tf}$

F_b - basic orifice factor

F_{pb} - pressure base factor

= 1.0 (Pressure base = 14.7 psia)

F_{tb} - temperature base factor

= 1.0 (Temperature base = $60^\circ F$)

F_g - Specific gravity factor

= 1.25 (Sp. Gr. = 0.65)

F_{tf} - Flowing temperature factor

(F_{tf} = 1.00 @ $60^\circ F$)

Orifice Size	F_b
0.690	98
0.375	28.4
0.420	36.4

3. Flow Calculations - Specific

Flange Tap Orifice Meter

Orifice = 0.690 x 2.067, F_b =98.0

Gas Gravity = 0.64 , F_g = 1.250

Gas Orifice Temperature = 61°F, F_{tf} = 0.999

P_D = 14.4 inches fluid at Sp.Gr. = 1.75

P_f = 120 psia

Avg Bed Inlet Temperature = 90.3°F

Avg Bed Inlet Pressure = 820 psia

Liguid Pentane Injection Rate

$$= \frac{15.67 \text{ lbs}}{55 \text{ mins}} = .285 \text{ lbs/min.}$$

$$= 129.0 \text{ gms/min.}$$

$$C' = F_b F_g F_{tf} = (98)(1.25)(.999) = 122.4$$

$$Q = C' \sqrt{P_f h_w} = 122.4 \left[(14.4)(1.75)(120)\right]^{1/2} = 6730 \text{ SCFH}$$

$$V = .0103 \frac{QT}{P} = \frac{(.0103)(6730)(550.3)}{820} = 46.5 \text{ ft/min.}$$

$$\% \quad C_5 = \frac{(\text{Injection Rate - gms/min})(50.1)(100)}{(72)\ Q}$$

$$= \frac{(129)(50.1)(100)}{(72)(6730)} = 1.333 \%$$

4. Adsorption Calculations

$$\rho = \frac{RT}{P} = \frac{(10.72)(550)}{(820)} = 7.19 \frac{\text{lb moles}}{\text{ft}^3}$$

$$C_o = \frac{.01333}{7.19} = .001855 \text{ lb moles } C_5/ft^3 \text{ gas}$$

$$Q_a = qi \left[\theta_B + \int_{\theta_B}^{\theta_E} (1-x)dt\right]$$

Q_a = grams of hydrocarbon component adsorbed

q_i = Injection rate of liquid hydrocarbon into gas stream-gms/min

θ_B = Breakthrough time - min at x = 0.05

θ_E = End of adsorption time - min at x = 0.95

$$Q_a = 129\ [7 + 7.6] = 1863 \text{ gms}$$

$$W_a = \frac{\text{Wt. Adsorbate}}{\text{Wt. Dessicant}} = \frac{1863}{16176} = .1165 \frac{\text{gms}}{\text{gm}}$$

$$q_o = \frac{.1165}{72} = .001618 \frac{\text{lb moles pentane}}{\text{lb of silica gel}}$$

$$C_o = (.001855)(.40) = .000742$$

$$D = \frac{q_o \rho_B}{C_o \epsilon} = \frac{.0854}{.000742} = 115$$

$$Dv\epsilon = (115)(.270) = 31.05$$

$$F = VA = (46.5)(.0459) = 2.135 \frac{\text{cubic feet}}{\text{minute}}$$

5. Particle Transfer Coefficient

$k_{kin}\ C_o = 0.585$ (Table III - Evaluated from effluent curve)

$$k_f = 1.916\ U^{0.49} \text{ ft/hr}$$

$$k_f a_p = 67.3\ U^{0.49} \text{ min}^{-1} = 67.3(116.2)^{.49} = 691 \text{ min}^{-1}$$

$= 116.2$ ft/min, D = 115

$$\frac{k_f a_p}{D} = 6.01 \text{ min}^{-1}$$

$$\frac{1}{k_p a_p} = \frac{b}{k_{kin} C_o} - \frac{D}{k_f a_p} = \frac{1.2}{.585} - .166 = 1.886$$

$$k_p a_p = \frac{1}{1.886} = 0.530 \text{ min}^{-1}$$

APPENDIX C

HYDROCARBON DIFFUSION COEFFICIENTS

In order to use the Wilke and Hougen correlation for a gas phase mass transfer coefficient, the diffusion coefficients of pentane and hexane in natural gas are required. In the literature I found only one diffusion coefficient (hexane in either methane, ethane or propane). Since a coefficient for pentane was needed, the Gilliland correlation for diffusion coefficients was used; however, the value obtained this way did not agree at all with the experimental diffusion coefficient as published by Carmichael, Sage, and Lacey (C7). More reading in the literature showed that the Gilliland correlation method (R1) was the least accurate of several diffusion coefficient correlations; that is, wider discrepancies existed between published experimental data and diffusivities calculated according to the Gilliland equation. Other equations or correlations were employed to give a diffusion coefficient for hexane in methane. These different correlations are discussed in Appendix F. In order to use these published correlations, some basic physical property data were required. These data, which were secured from several sources, are listed in Table C-I and identified as to literature source. The calculated coefficients of hexane in methane are shown in Table C-II. These answers are still quite different from the data of Carmichael, Sage and Lacey (C7).

In order to resolve these discrepancies in calculated and experimental data for the diffusivity of hexane, the literature was searched for other experimental diffusivities of hydrocarbons in other gases. Much of this data was at a different temperature, and it was necessary to correct the data to the same temperature base. The functional dependency of the diffusion coefficient upon temperature was different in several correlation equations. The correlations show D_{12} to vary with T^n where n ranges from 1.5 to 1.82. The data of Altshuller and Cohen (A2) were used to select a functional power. This diffusivity data for normal hexane in air at various temperatures is plotted in Figure C-1. The slope calculated from this plot is 1.5 and this power is used to correct other diffusivity coefficients to the same temperature base. The published data which are corrected to a temperature base of 21°C (70°F) are shown in Table C-III with the data publication source. These data are also plotted in Figure C-2 for a quick comparison. The diffusivity data which were calculated according to the various correlations are also plotted on this figure.

This graph shows that most of the data agree except for the data of Carmichael, et al. The calculated values from the various correlations lie above the published data, but the deviation is not as much as that of the data of Carmichael, et al.

In order to be consistent, I decided to use a

correlation which was close to the general experimental data. The diffusivities for both hexane and pentane are therefore obtained by the same method. The correlation of Hirschfelder, Bird, and Spotz (R1) was used, but the Stiel and Thodos (S8) method was used to predict the Lennard-Jones force constants from critical properties of the pentane, hexane, and dry supply gas. This way of calculating the diffusion coefficients allows one to compute the diffusion coefficient of hexane and pentane in a dry gas mixture. This calculation is based upon the dry gas gravity and calculated psuedo-critical properties of the dry gas. The psuedo-critical pressure and temperature of the dry gas were obtained from the NGSMA natural gas handbook (N2). The critical volume for the gas mixture was estimated using the gas gravity and a plot of critical volumes for the different hydrocarbons. Figure C-3 shows this method of estimating the dry gas critical volume. The critical compressibility factor, Z_c, was calculated from the other psuedo-critical properties of this dry gas.

In order to calculate the diffusion coefficients for hexane and pentane at the high pressures involved in the adsorption system, the method of Slattery and Bird (S6) was used to compensate for the dense gas effect on self-diffusion coefficients. The final diffusivity values which were obtained were .00528 and .00443 ft^2/hr for pentane and hexane, respectively, at 90^oF and 815 psia.

A viscosity of .0152 contipoises for the natural gas

was obtained from the NGSMA Handbook (N2). An ideal gas density of 2.89 pounds per cubic foot was also used in the Wilke and Hougen equation. Assuming ideal gas behavior simplified the mass flow rate calculations in the analysis of data. This ideal assumption is self-compensating in the Reynolds number which is part of the correlation. Since there is a gas gravity in the Schmidt number, which also contains the diffusivity, this assumption of ideal gas behavior for the density and velocity calculations would involve only a small error. The calculations for the gas phase mass transfer coefficient are available in Appendix M. The results for this coefficient as a function of velocity are shown below:

$$k_f = 1.916\ U^{0.49}\ \text{ft/hr} \qquad \text{(pentane)}$$

$$k_f = 1.70\ U^{0.49}\ \text{ft/hr} \qquad \text{(hexane)}$$

Although these numbers which are obtained in this manner may be inexact, they are the most consistent available under the circumstances. The diffusivities as obtained this way have an effect upon the final interpretation of the mass transfer behavior of hydrocarbons in a fixed bed of silica gel. This possible effect is discussed in the chapter on significance of results.

TABLE C-I

PHYSICAL PROPERTIES OF HYDROCARBONS

PROPERTY	METHANE	PENTANE	HEXANE	SUPPLY GAS (SG = .64)
Molecular Weight	16.04 (1)	72.15(1)	86.17 (1)	18.52 (5)
Critical				
Pressure, P_c - psia	673.1 (1)	489.5 (1)	439.7 (1)	670 (1)
Temperature, T_c - ^oF	-116.5 (1)	385.9 (1)	454.5 (1)	370 (1)
Volume, V_c - cc/gm mole	99.01 (2)	311.0 (2)	368 (5)	106.2 (5)
Compressibility, Z_c	.289(2)	.269 (2)	.264(5)	.2875 (5)
Boiling Point				
Temperature, T_b - ^oF	-258.7 (1)	96.93(1)	155.7 (1)	
Liquid Molar Volume cc/gm-mole	37.8 (3)	120.4 (5)	146 (5)	
Force Constants (4)				
ϵ/k - ^oK	136.5	345	413	
σ - Angstrom Units	3.822	5.769	5.909	

References:
(1) NGSMA Handbook
(2) Stiel and Thodos
(3) Matheson Gas Handbook
(4) Reid and Sherwood
(5) Calculated from NGSMA Data

TABLE C-II

CALCULATED DIFFUSIVITY OF HEXANE IN METHANE

Correlation	Diffusivity at 21° C cm^2/sec
Arnold	.0801
Chen and Othmer	.0834
Gilliland	.0805
Hirshfelder et al.	.0808
Slattery and Bird	0.1003
Stiel and Thodos	.0779
Wilke and Lee	.0811

TABLE C-III

EXPERIMENTAL DIFFUSIVITIES

Component	D_T cm^2/sec	T ^oK	D_{294^oK} cm^2/sec	Literature Source
$n\text{-}C_4 - N_2$	.0960	298	.0941	Reid and Sherwood
$iC_4 - N_2$	.0908	298	.0891	Reid and Sherwood
$n\text{-}C_6$ - Air	.0797	298	.0782	Altshuller and Cohen
$n\text{-}C_6$ - Air	.0811	303	.0776	Altshuller and Cohen
$n\text{-}C_6$ - Air	.0889	321.5	.0777	Altshuller and Cohen
$n\text{-}C_6$ - Air	.0903	322.5	.0786	Altshuller and Cohen
$n\text{-}C_6$ - Air	.0903	323.75	.0781	Altshuller and Cohen
$n\text{-}C_6$ - A	.0663	288	.0684	Perry
$n\text{-}C_6 - O_2$	.0753	305	.0713	Perry
$n\text{-}C_6 - N_2$	.0757	301	.0730	Perry
$n\text{-}C_6 - CH_4$	.0476	294	.0476	Carmichael, et al.
$n\text{-}C_7 - N_2$	.0743	303	.0711	Cummings
$n\text{-}C_7 - CH_4$	.066	311	.0606	Perry
$n\text{-}C_8$ - Air	.0505	273	.0564	Perry
$n\text{-}C_8$ - A	.0642	303	.0614	Perry
$n\text{-}C_8 - O_2$	.0705	303	.0674	Perry
$n\text{-}C_8 - N_2$	.0710	303	.0679	Perry
$n\text{-}C_8$ - Air	.0602	298	.0591	Chen and Othmer
$n\text{-}C_9 - N_2$	.0737	340	.0593	Cummings

$$D_{294} = D_T\left(\frac{294}{T}\right)^{1.5}$$

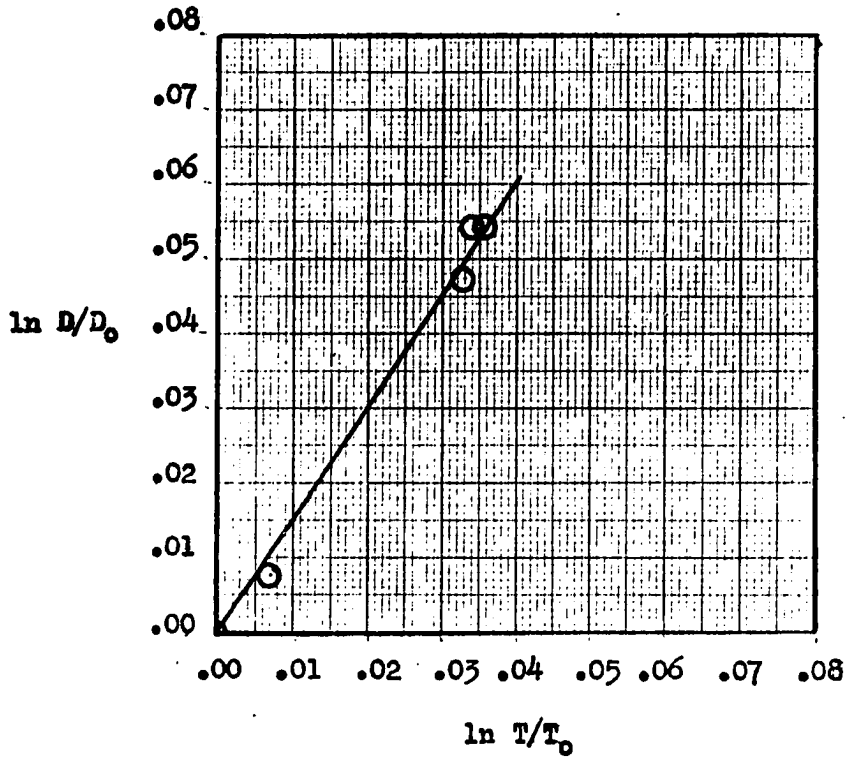


FIGURE C-1. TEMPERATURE DEPENDENCE OF DIFFUSIVITY

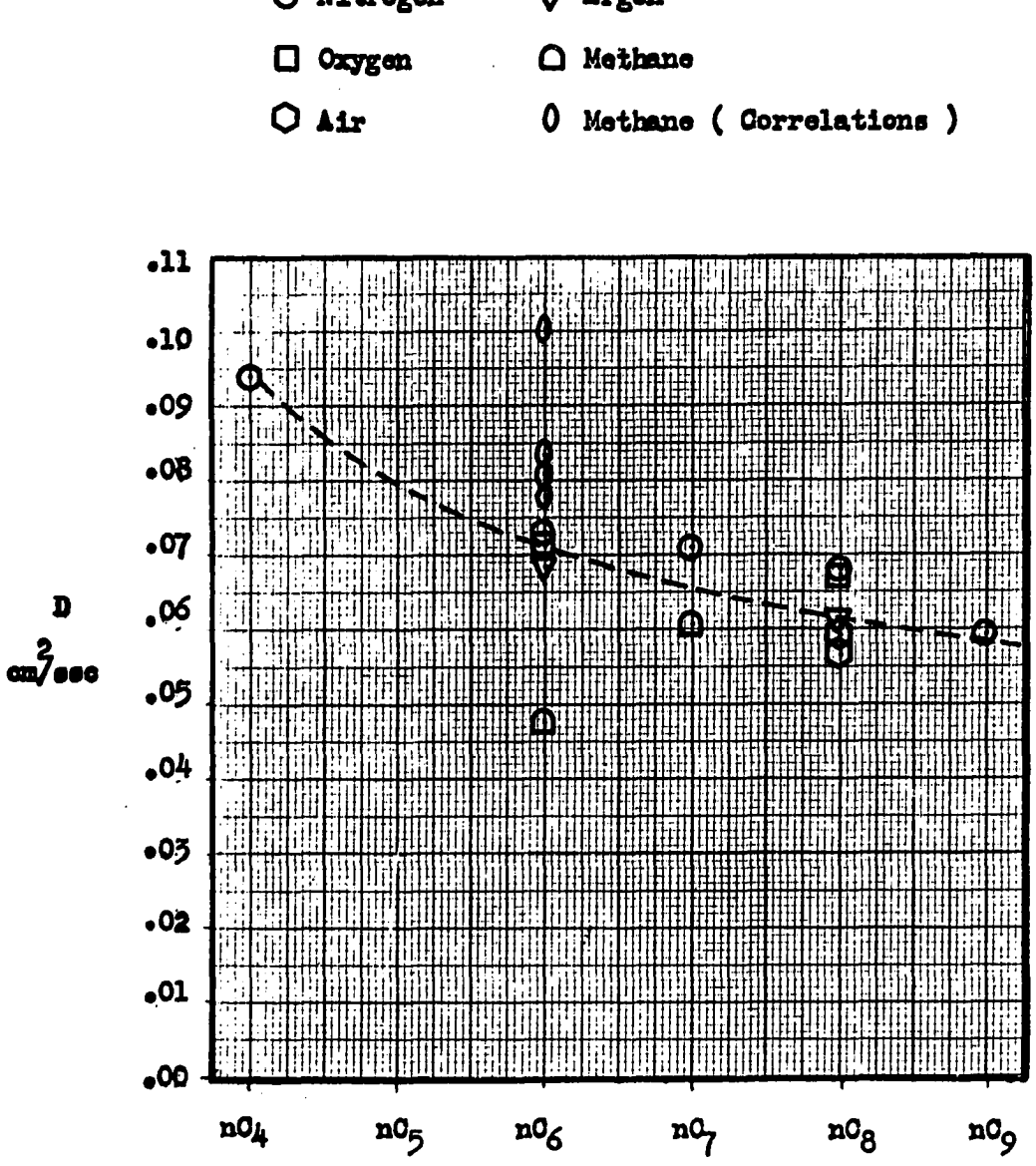


FIGURE C-2. HYDROCARBON DIFFUSION COEFFICIENTS AT 21°C

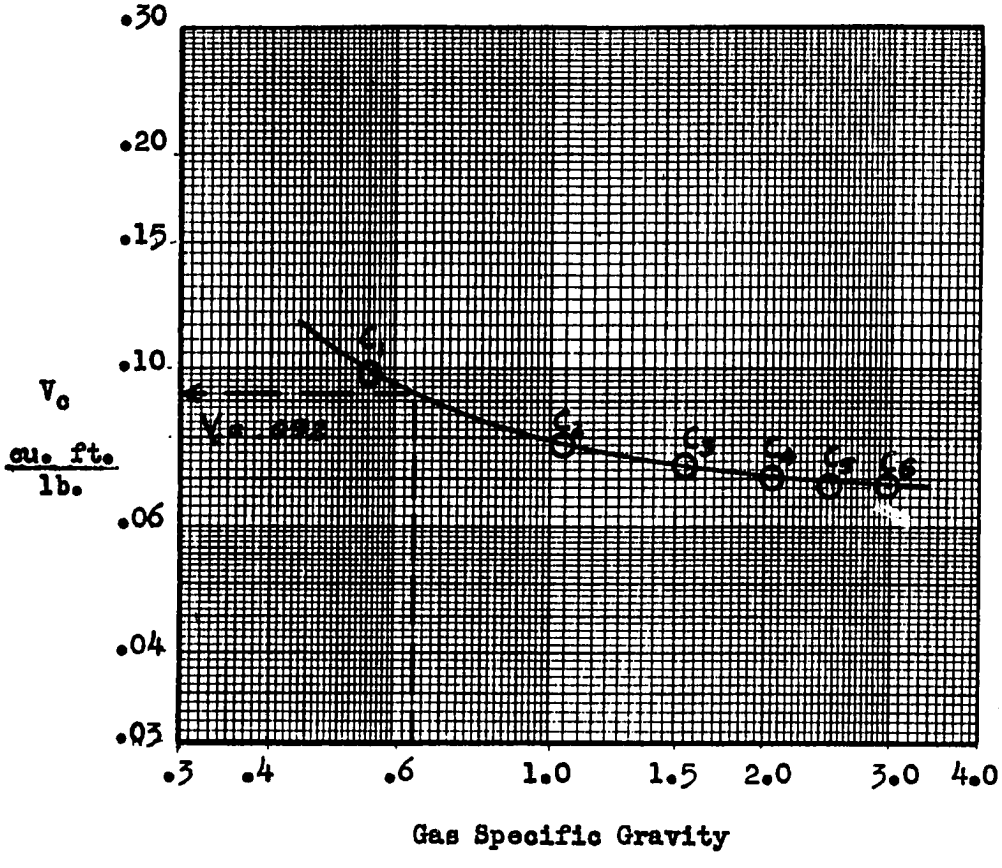


FIGURE C-3. ESTIMATION OF CRITICAL VOLUME OF DRY GAS (S.G.=.64)

APPENDIX D

METHOD OF OBTAINING EFFLUENT CURVE CONCENTRATION-TIME SLOPE FROM PLOT ON PROBABILITY-COORDINATE PAPER

The ordinate of probability paper is laid off in units of ρ. The numbers that are printed on the side are related to the even units of ρ by the following equation:

$$N = \tfrac{1}{2} + \tfrac{1}{2} \operatorname{erf} \rho \ . \qquad \text{(D-1)}$$

If these printed numbers are used to represent x or $\frac{C}{C_o}$, the resulting plot of x versus time will give a straighter line than one obtained on plain coordinate paper. To obtain a slope $\frac{dx}{dt}$ at the midpoint, $x = 0.5$, we must relate $\frac{dx}{dt}$ to the slope taken from probability paper. We do this by differentiating equation D-1:

$$\frac{dx}{dt} = \tfrac{1}{2} \frac{d}{dt} (\operatorname{erf} \rho) \ . \qquad \text{(D-2)}$$

In order to differentiate the error function, we must apply the Leinbnitz rule (K1, p. 220).

$$\frac{d}{dt} \int_{a(t)}^{b(t)} f(x,t)dx = f\left[b(t),t\right] b'(t) - f\left[a(t),t\right] a'(t) + \int_{a(t)}^{b(t)} \frac{\partial f}{\partial t}(x,t)dx \qquad \text{(D-3)}$$

$$\frac{d}{dt}\,\text{erf}\,\rho = \frac{d}{dt}\left\{\frac{2}{\sqrt{\pi}}\int_0^{\rho} e^{-\alpha^2}d\alpha\right\} = \frac{2}{\sqrt{\pi}}\left\{e^{-\rho^2}\frac{d\rho}{dt} - e^{-0}(0) + \int_0^{\rho}(0)d\rho\right\}$$

$$= \frac{2}{\sqrt{\pi}}\, e^{-\rho^2}\,\frac{d\rho}{dt} \quad . \qquad \text{(D-4)}$$

If we now let

$$\frac{d\rho}{dt} = A \qquad \text{(D-5)}$$

at $\frac{C}{C_o} = x$

$$\frac{d\ C/C_o}{dt} = \frac{dx}{dt} = \tfrac{1}{2}\,\frac{d}{dt}\,\text{erf}\,\rho = \tfrac{1}{2}\,\frac{2}{\sqrt{\pi}}\, e^{-\rho^2}\frac{d\rho}{dt} = \frac{e^{-\rho^2}}{\sqrt{\pi}}\, A \qquad \text{(D-6)}$$

at $x = 0.5$, $\rho = 0$. Therefore, $\frac{d\ C/C_o}{dt} = \frac{A}{\sqrt{\pi}}$ @ $x = 0.5$. (D-7)

To obtain the slope, A, on probability paper, we draw a tangent to the curve at $x = 0.5$. To compute the slope, $\frac{\Delta\rho}{\Delta t}$, we set $\Delta\rho$ equal to 1.

$$\Delta\rho = 1 \qquad \rho = 1 \text{ @ } x = C/C_o = 0.9214$$

$$\rho = 0 \text{ @ } x = C/C_o = 0.50 \qquad \text{(D-8)}$$

Since $\Delta\rho$ is set, then we pick the t_2 and t_1 accordingly:

$$t_2 \text{ @ } x = 0.9214$$

$$t_1 \text{ @ } x = 0.50 \qquad \text{(D-9)}$$

Therefore,

$$\frac{\Delta\rho}{\Delta t} = \frac{1}{t_{x=.9214} - t_{x=.5}} \quad . \qquad \text{(D-10)}$$

Once we have the slope, A, from the probability paper, we apply the correction from equation (D-7) to the slope to obtain the derivative $\frac{dx}{dt}$.

APPENDIX E

CORRECTION OF TRANSIENT MIDPOINT SLOPES TO LIMITING VALUES

In order to use the experimental data breakout curves to evaluate the relative effects of internal and external gas diffusion, the transient effects had to be either removed or corrected. It was decided to take the midpoint slopes of the data plots, that is, the slope of a plot of x, dimensionless composition, versus Z, a throughput parameter. Solutions which took into consideration the adsorption equilibrium parameter, r, for transient and limiting conditions are the solutions of Thomas (T1) and Sillén (S4) respectively. The Thomas equation reduces to this same limiting solution at long times.

The midpoint slopes for the transient solution were found by plotting the calculated x and Z values on probability paper. The slopes in the limiting case were calculated directly. In order to calculate x values from the Thomas transient solution, values for the J function were required. Values of this function were recently made available by Marks, et al. Once the x and Z values were calculated from both solutions (shown in Tables E-I and E-II), these were plotted on probability paper. The slopes at $x = 0.5$ were measured and then calculated to give the coordinate paper midpoint slope by the method of Appendix D. The slope found graphically

for the limiting case was compared to the calculated value for a check. With this information (Table E-III), a graph was plotted showing the asymptotic slope $\left(\frac{dx}{dZ}\right)_a$, versus the transient slope $\left(\frac{dx}{dZ}\right)_t$ for both pentane and hexane. Since the experimental data in most cases was in the transient range, the midpoint slopes from the experimental runs were corrected with these figures. Once the limiting slopes were found from these graphs, the number of transfer units, N_R, were calculated for each run. This value, together with other run data, was used to calculate the kinetic mass transfer coefficient, $k_{kin}C_o$. This coefficient was later separated into two transfer coefficients, the fluid or gas phase transfer coefficient and the internal or particle transfer coefficient. Since the fluid phase transfer coefficient was evaluated according to the correlation of Wilke and Hougen, the only unknown left was the internal or particle transfer coefficient which could then be solved. The separation of this empirical kinetic transfer coefficient into the fluid phase and solid phase coefficients is discussed in Appendix G.

TABLE E-I

CALCULATED VALUES OF x AND Z - PENTANE

Z	x			
	N_R = 10		N_R = 15	
	S	T	S	T
.2	.065	.005	.0186	.00057
.4	.119	.030	.0474	.00902
.5				
.6	.209	.120	.119	.0581
.7			.1824	.1214
.8	.339	.287	.269	.205
.9			.392	.358
1.0	.500	.520	.500	.516
1.1			.622	.667
1.2	.662	.736	.731	.790
1.3			.817	.877
1.4	.791	.875	.880	.931
1.5				
1.6	.881	.948	.952	.980
1.8	.935	.980	.983	.995
2.0	.966	.993		

TABLE E-I--Continued

Z	x			
	$N_R = 20$		$N_R = 30$	
	S	T	S	T
.2	.005	0		
.4	.018	.003		
.5			.0067	.0015
.6	.065	.03	.0180	.0075
.7	.119		.0473	.0297
.8	.208	.167	.119	.0951
.9	.339	.317	.269	.251
1.0	.500	.511	.500	.507
1.1	.661	.698	.726	.751
1.2	.792	.836	.880	.905
1.3	.881		.953	.967
1.4	.935	.963	.982	.990
1.5			.993	.997
1.6	.982	.993		
1.8	.995	.999		
2.0	.999	1.000		

TABLE E-II

CALCULATED VALUES OF x AND Z - HEXANE

Z	x			
	$N_R = 4$		$N_R = 7$	
	S	T	S	T
.1	.0945	.0390		
.2				
.3		.0992	.0502	.0246
.4				
.5	.231	.190	.109	.079
.6			.157	.129
.7			.221	.199
.8	.383	.395	.298	.289
.9			.397	.398
1.0	.50	.535	.500	.514
1.1			.603	.628
1.2	.618	.673	.698	.728
1.3			.779	.809
1.4			.843	.871
1.5	.768	.83	.890	.915
1.6				
1.7			.950	.965
1.8	.872	.918		
2.0	.917	.951		

TABLE E-II--Continued

Z	x			
	$N_R = 10$		$N_R = 15$	
	S	T	S	T
.1				
.2			.0007	.0001
.3			.	.
.4			.0077	.00426
.5	.048	.034		
.6	.083	.068	.0266	.022
.7	.142	.127	.0631	.0568
.8	.232	.221	.142	.135
.9	.355	.353	.269	.266
1.0	.500	.507	.500	.503
1.1	.643	.661	.731	.738
1.2	.768	.785	.857	.865
1.3	.858	.874	.937	.941
1.4	.916	.930	.973	.976
1.5	.952	.961		
1.6			.9955	.996
1.7				
1.8			.9993	.9994
2.0				

TABLE E-III

MID-POINT SLOPE COMPUTATION

$\frac{dx}{dZ}$ at $x = 0.5$

N_R	Hexane		Pentane	
	Stable	Transient	Stable	Transient
4	0.60	0.736	-	-
7	1.05	1.17	-	-
10	1.50	1.59	.833	1.21
15	2.25	2.30	1.250	1.550
20	-	-	1.667	1.944
30	-	-	2.50	2.645

APPENDIX F

DIFFUSIVITY CORRELATIONS

Diffusion is defined by Reid and Sherwood (R1) as the transfer of a substance through a homogenous solution (single gas, liquid, or solid phase) resulting from a difference in concentrations (or, more generally, chemical potential) at two regions in the mixture. Molecular diffusion is defined as the transfer resulting from the random motion of the molecules and is to be distinguished from mixing due to convection or bulk motion of the system. Although molecular speeds in liquids and gases are not greatly different, diffusion is very much more rapid in gases because of the smaller interference of the other molecules. The diffusion coefficient or diffusivity, is the proportionality constant between the rate of diffusion, or diffusion flux, and the gradient of the potential causing diffusion. The diffusion potential is ordinarily taken to be the concentration or partial pressure of the diffusing substance.

The various diffusivity correlations are based upon the rigid-sphere picture of gas molecules undergoing elastic collisions. This concept has produced various theoretical equations of the form

$$D_{12} = \frac{bT^{3/2}\left[(M_1+M_2)/M_1M_2\right]^{\frac{1}{2}}}{Pd^2} \qquad \text{(F-1)}$$

Various theoretical values of the constant b have been obtained by several persons. See Reid and Sherwood (R1), page 267. The nomenclature is listed in order at the end of this appendix.

Arnold

Arnold, who adopted the Sutherland temperature function, evaluated b empirically from data on diffusivities and obtained

$$D_{12} = \frac{0.00837\ T^{5/2}\left[(M_1+M_2)/M_1M_2\right]^{\frac{1}{2}}}{P(V_b^{1/3}+V_b^{1/3})^2(T+S_{12})} \quad . \qquad (F\text{-}2)$$

The quantity d has been replaced by the sum of the cube roots of the molal volumes of the pure substances at their normal boiling temperatures. The Sutherland constant, S_{12} is defined by the following equation:

$$S_{12} = 1.47\ F(T_{b_1}T_{b_2})^{\frac{1}{2}} \qquad (F\text{-}3)$$

where

$$F = \frac{2\left(V_{b_1}^{1/3}\ V_{b_2}^{1/3}\right)^{\frac{1}{2}}}{V_{b_1}^{1/3} + V_{b_2}^{1/3}} \quad . \qquad (F\text{-}4)$$

Gilliland

Gilliland evaluated b from several hundred experimental values of diffusivity, D_{12}, and evaluated d from atomic volumes as did Arnold (see Reid and Sherwood R1). His result

is

$$D_{12}P = \frac{0.0043\ T^{3/2} \left(\frac{1}{M_1} + \frac{1}{M_2}\right)^{\frac{1}{2}}}{\left(V_{b_1}^{1/3} + V_{b_2}^{1/3}\right)^2} \quad . \tag{F-5}$$

Hirschfelder, Bird, and Spotz

These authors applied the Lennard-Jones potential to give an equation for D_{12} similar to equation F-1.

$$D_{12}P = \frac{.001858\ T^{3/2} \left(\frac{1}{M_1} + \frac{1}{M_2}\right)^{\frac{1}{2}}}{\sigma_{12}^{\ 2}\ \Omega(1,1)^*} \tag{F-6}$$

with the replacement of d by the force constant σ_{12} and a "collision integral" $\Omega(1,1)^*$. This integral is a function of $\frac{kT}{\epsilon_{12}}$.

Force constants ϵ and σ may be estimated by the simple empirical relations relating these constants to critical values

$$\epsilon = 0.77\ T_c \tag{F-7}$$

$$\sigma = 0.833\ V_c^{\ 1/3} \quad . \tag{F-8}$$

For a binary system σ_{12} is equal to the arithmetic mean of σ_1 and σ_2. ϵ_{12} is taken as the geometric mean of ϵ_1 and ϵ_2.

$$\sigma_{12} = \frac{\sigma_1 + \sigma_2}{2} \tag{F-9}$$

$$(\epsilon/k)_{12} = \left[(\epsilon/k)_1 (\epsilon/k)_2\right]^{\frac{1}{2}} \qquad \text{(F-10)}$$

Both Wilke and Lee (W6) and Stiel and Thodos (S8) have used the collision integral equation of Hirschfelder et al.

Wilke and Lee

Wilke and Lee modified the equation of Hirschfelder by making the b constant a variable depending upon the molecular weights of the binary gas system as given below.

$$D_{12}P = \frac{B\, T^{3/2} \left[\frac{1}{M_1} + \frac{1}{M_2}\right]^{\frac{1}{2}}}{r_{12}^2\, I_D} \qquad \text{(F-11)}$$

$$r_{12} \equiv \sigma_{12}$$

$$I_D \equiv \frac{\Omega_{(1,1)}^*}{2}$$

$$B = \left[1.0 - 2.46\left(\frac{1}{M_1} + \frac{1}{M_2}\right)^{\frac{1}{2}}\right] (10)^{-4} . \qquad \text{(F-12)}$$

Stiel and Thodos

By fitting calculated Lennard-Jones forced constants as functions of the critical properties of many gases, Stiel and Thodos obtained the relations:

$$\sigma = 0.1866\, V_c^{1/3}\, Z_c^{-6/5} \qquad \text{(F-13)}$$

$$\epsilon/k = 65.3\, T_c\, Z_c^{18/5} . \qquad \text{(F-14)}$$

Chen and Othmer

Chen and Othmer (C12) evaluated the forced constants as functions of a gas's critical properties. The collision integral is a function of the force constant and the temperature, $\frac{kT}{\epsilon}$. By curve fitting these various relationships, Chen and Othmer arrived at the following equation for diffusivity based upon the critical constants and molecular weight of a binary gas mixture.

$$D_{12}P = \frac{0.43\left(\frac{T}{100}\right)^{1.81}\left(\frac{1}{M_1}+\frac{1}{M_2}\right)^{0.5}}{\left(\frac{T_{c_1}T_{c_2}}{10{,}000}\right)^{0.1405}\left[\left(\frac{V_{c_1}}{100}\right)^{0.4}-\left(\frac{V_{c_2}}{100}\right)^{0.4}\right]^2} . \quad \text{(F-15)}$$

Slattery and Bird

An empirical equation was developed by Slattery and Bird (S6) which was based upon the critical pressure and temperature of the two gases in a binary mixture. This equation is represented below along with the definition of the constants:

$$D_{12}P = aT_r^{\,b}(P_{c_1}P_{c_2})^{1/3}(T_{c_1}T_{c_2})^{5/12}\left(\frac{1}{M_1}+\frac{1}{M_2}\right)^{\frac{1}{2}} . \quad \text{(F-16)}$$

$$a = 2.74(10)^{-4}$$

$$b = 1.823$$

$$T_r = \frac{T}{\left(T_{c_1}T_{c_2}\right)^{\frac{1}{2}}} . \quad \text{(F-17)}$$

Various correlating methods have been compared by both Sherwood and Reid and by Perry (P2). The equation which is based on the collision integral developed from the Lennard-Jones potential generally gives the least deviation when compared to actual data.

Effect of Total Pressure on Diffusion Coefficients

The best present basis for the prediction of diffusivity at high pressures is that of Slattery and Bird. This dependence of diffusivity on pressure is plotted in curves as a function of the independent variables: reduced temperature and reduced pressure. This chart resembles the compressibility factor chart for real gases.

NOMENCLATURE FOR DIFFUSIVITY CORRELATIONS

D_{12}	gas diffusivity, cm^2/sec
M	molecular weight, grams/gram mole
P	absolute pressure, atm
T	absolute temperature, ^oK
V	specific volume, cc/gm-mole
Z	compressibility factor
$\sigma_{12} = r_{12}$	collision diameter, Angstroms
ϵ_{12}	energy of molecular interaction, ergs
k	Boltzmann constant = $1.38\ (10)^{-6}$ erg/^oK
$\Omega\ (1,1)^* = 2I_D$	collision integral (function of $\frac{kT}{\epsilon_{12}}$)

APPENDIX G

COMBINED TRANSFER COEFFICIENT

Heister et al. (H2) developed a method for combining the series resistances of mass transfer in the fluid phase and in the particle for adsorption where the equilibrium isotherm was not linear. The following development is a summary of this work.

The driving force equation for the mass transfer through the fluid phase film next to the particle is:

$$\frac{dq}{dt} = k_f a_p \frac{\epsilon}{\rho_b} (C-C_i) \quad . \tag{G-1}$$

The driving force equation for the particle mass transfer is:

$$\frac{dq}{dt} = k_p a_p (q_i-q) \quad . \tag{G-2}$$

Since transfer is in series, these two equations may be set equal and the gradients combined to give

$$\frac{dq}{dt} = \frac{(C-C_i)\frac{q_o}{C_o} + (q_i-q)}{\frac{q_o \rho_b}{\epsilon C_o k_f a_p} + \frac{1}{k_p a_p}} \quad . \tag{G-3}$$

The kinetic expression for mass transfer as developed by Heister and Vermuelen to fit the solution by Thomas is, for one component,

$$\frac{dq}{dt} = \frac{C(q_o-q) - \frac{q}{K}(C_o-C)}{\frac{q_o \rho_b}{\chi_{kin}\epsilon}} \quad . \tag{G-4}$$

The equation then for the transfer with combined fluid phase and particle resistance may be set equal to the equation for mass transfer rate following the reaction-kinetic expression to give

$$\frac{D}{k_f a_p} + \frac{1}{k_p a_p} = \frac{D}{\chi_{kin}} \left\{ \frac{q_o(C-C_i) + C_o(q_i-q)}{C(q_o-q) - \frac{q(C_o-C)}{K}} \right\} \quad . \tag{G-5}$$

If the expression in brackets is replaced by a parameter, b, the following expression for combined resistances or combined coefficients results

$$\frac{1}{k_f a_p} + \frac{1}{Dk_p a_p} = \frac{b}{\chi_{kin}} = \frac{b}{k_{kin} q_o \rho_b} = \frac{b}{Dk_{kin} C_o} \quad . \tag{G-6}$$

where

$$\chi_{kin} = \frac{k_{kin}\, q_o \rho_b}{\epsilon} \tag{G-7}$$

and

$$\frac{D}{k_f a_p} + \frac{1}{k_p a_p} = \frac{b}{k_{kin} C_o} \tag{G-8}$$

This is the method which is used in this thesis to separate the two resistances by using this combined mass transfer coefficient. It remains to be shown how the parameter, b, is evaluated. In order to determine b the above

authors (H2) chose a coefficient, $\mathcal{J}$, which is a ratio of concentration gradients in the two phases (gas and solid).

$$\mathcal{J} = \frac{q_o\ (C-C_i)}{C_o\ (q_i-q)} = \frac{x - x_i}{y_i - y} \qquad \text{(G-9)}$$

b also depends upon the equilibrium parameter, r,

$$y_i = \frac{x_i}{r + (1-r)x_i} \quad . \qquad \text{(G-10)}$$

For the computation of b, it is assumed that the stable zone has been obtained for the absorption behavior under a favorable equilibrium isotherm. In this case,

$$x = y \quad . \qquad \text{(G-11)}$$

To evaluate b, a value of $\mathcal{J}$ is assumed and b is calculated. Heister et al. plotted the results of this procedure for values of r from zero to 10. In the range of r in which we are interested, the parameter b is almost independent of the mechanism parameter, $\mathcal{J}$. The maximum value of b is at a $\mathcal{J}$ of 1 and the minimum value is at a $\mathcal{J}$ of either zero or infinity. The limits for the pentane and hexane data were solved at $\mathcal{J}$ equals zero and infinity and at $\mathcal{J}$ equals 1. The values of b at $\mathcal{J}$ equals zero and infinity are the same. For pentane, b equals 1.20 at both points. For hexane at $\mathcal{J}$ equals 1, b equals 1.48. At $\mathcal{J}$ equals zero, b equals 1.43. Since the curve showed more influence by one resistance, the particle resistance, the value of b equals 1.43 was used for the evaluation of hexane. It is restated here that these values

are solved at the midpoint of the effluent curve where x equals 0.5. So this evaluation would only be valid for evaluating the midpoint slope. If another point would be used, the b values would have to be recalculated.

APPENDIX H

SOLUTION FOR x WHEN Z = 1

For the asymptotic solution where the internal particle diffusion controls the adsorption behavior, the following equation applies:

$$Np\ (Z_2-Z_1) = \frac{r}{1-r} \ln \frac{x_2(1-x_1)}{x_1(1-x_2)} + \ln \frac{1-x_1}{1-x_2} . \qquad (H-1)$$

If we replace $\frac{r}{1-r}$ with a variable constant, a, the following development will apply for all values of r.

At a given x_1 and variable $x_2 = x$ and by differentiating each side of the equation, we obtain

$$N_p dZ = \left[\frac{a}{x(1-x)} + \frac{1}{1-x}\right] dx = \frac{(a+x)dx}{x(1-x)}$$

$$dZ = \frac{1}{N_p} \frac{(a+x)}{x(1-x)} dx. \qquad (H-2)$$

First of all, we note that

$$\int_{Z=0}^{x=1} (1-x)dZ = 1.0 \qquad (H-2)$$

Furthermore all of a component emitted up to Z = 1.0 must equal amount of component picked up past Z = 1.0. Hence

$$\int_0^{x_{Z=1}} xdZ = \int_{x_{Z=1}}^{1.0} (1-x)dZ \quad . \qquad (H-4)$$

From H-2:

$$\frac{1}{N_p} \int_0^{x_{Z=1}} \left(\frac{a+x}{1-x}\right) dx = \frac{1}{N_p} \int_{x_{Z=1}}^{1.0} \left(\frac{a+x}{x}\right) dx$$

$$[a \ln(1-x) - x - \ln(1-x)]_0^x = [a \ln x + x]_x^{1.0} .$$

Remember that we are solving for $x = \frac{C}{C_0}$ at $Z = 1.0$. After integrating, the result then becomes

$$\ln\left[\frac{x^a}{(1-x)^{a+1}}\right] = 1 . \qquad \text{(H-5)}$$

This relationship is true as long as $\frac{C}{C_0} = x = 0$ at $Z = 0$. If there is an initial effluent concentration, this relationship will not be true. This same procedure of solving for x at $Z = 1.0$ can be applied to the equation where fluid-phase diffusion controls the adsorption behavior. This equation is:

$$N_f(Z_2-Z_1) = \frac{1}{1-r} \ln \frac{x_2(1-x_1)}{x_1(1-x_2)} + \ln \frac{1-x_2}{1-x_1} . \qquad \text{(H-6)}$$

By differentiating and integrating around the midpoint of the effluent curve, we can reach a relationship similar to that in Equation H-5. This relationship for fluid phase diffusion controlling is:

$$\ln\left[\frac{(1-x)^{b-1}}{x^b}\right] = 1$$

where: $b = \frac{1}{1-r}$

which also holds true as long as the initial effluent concentration equals 0. By substituting the values of 0.4 and 0.667 for the r parameter of hexane and pentane, respectively, the midpoint ($Z = 1.0$) concentrations of the curves are as follows:

	N_p	N_f
Pentane	.53	.470
Hexane	.564	.436

Once these values are known, they can then be used to calculate typical effluent curves under limiting conditions (a stabilized zone).

APPENDIX I

INFLUENCE OF r ON EFFLUENT CURVE SHAPE

Curve shapes are affected by both r and the controlling diffusion mechanism. First, to illustrate the effect of r on curve shape, a curve for hexane (r = 0.4) and the curve for pentane (r = 2/3) were calculated for a N_p of 10. This result is shown on Figure I-1 where x is plotted versus Z. These curves show that adsorption behavior stabilizes faster as the parameter r decreases. As r approaches 1, the stabilizing of a zone takes longer. A much longer bed length is needed for this limiting behavior to apply.

The second characteristic to examine is the influence of the controlling mechanism. Two curves are calculated, one each for pentane and hexane, respectively. The curves for each component are plotted for 10 transfer units. Figures I-2 and I-3 show the effect of two different controlling mechanisms on pentane and hexane, respectively. This illustrates how the curve shape can be influenced according to whether the adsorption behavior is controlled by either internal particle diffusion or fluid-phase external diffusion. As r approaches 1, the adsorption effluent curve behavior shows less and less dependence upon the type of mechanism controlling the behavior. At r = 1, the effluent curves would be the same regardless of which mechanism controls. Therefore with components having an r much less than 1, the controlling mechanisms can more easily be distinguished.

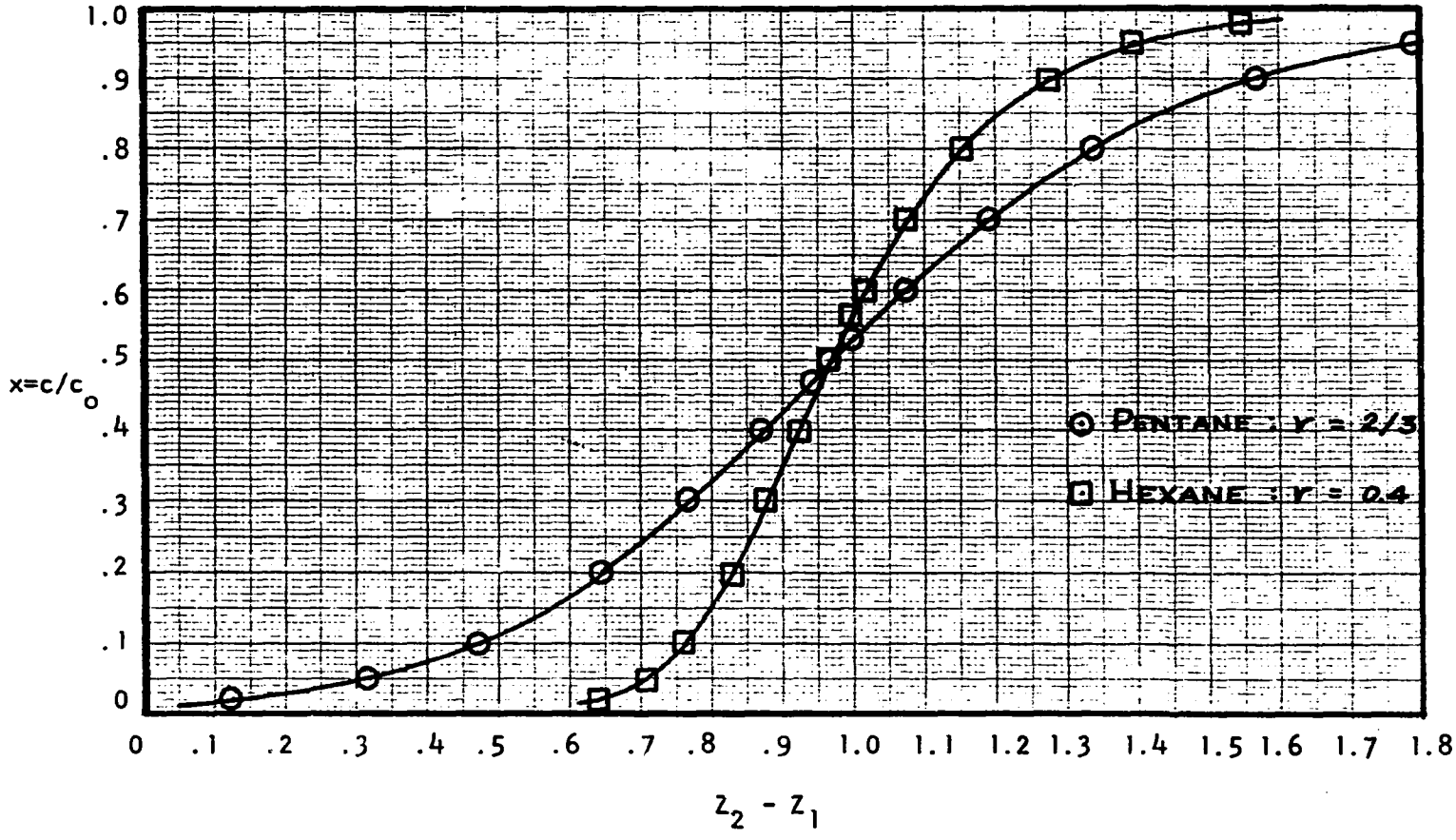


FIGURE I-1. EFFECT OF r PARAMETER ON EFFLUENT CURVE SHAPE - PARTICLE DIFFUSION

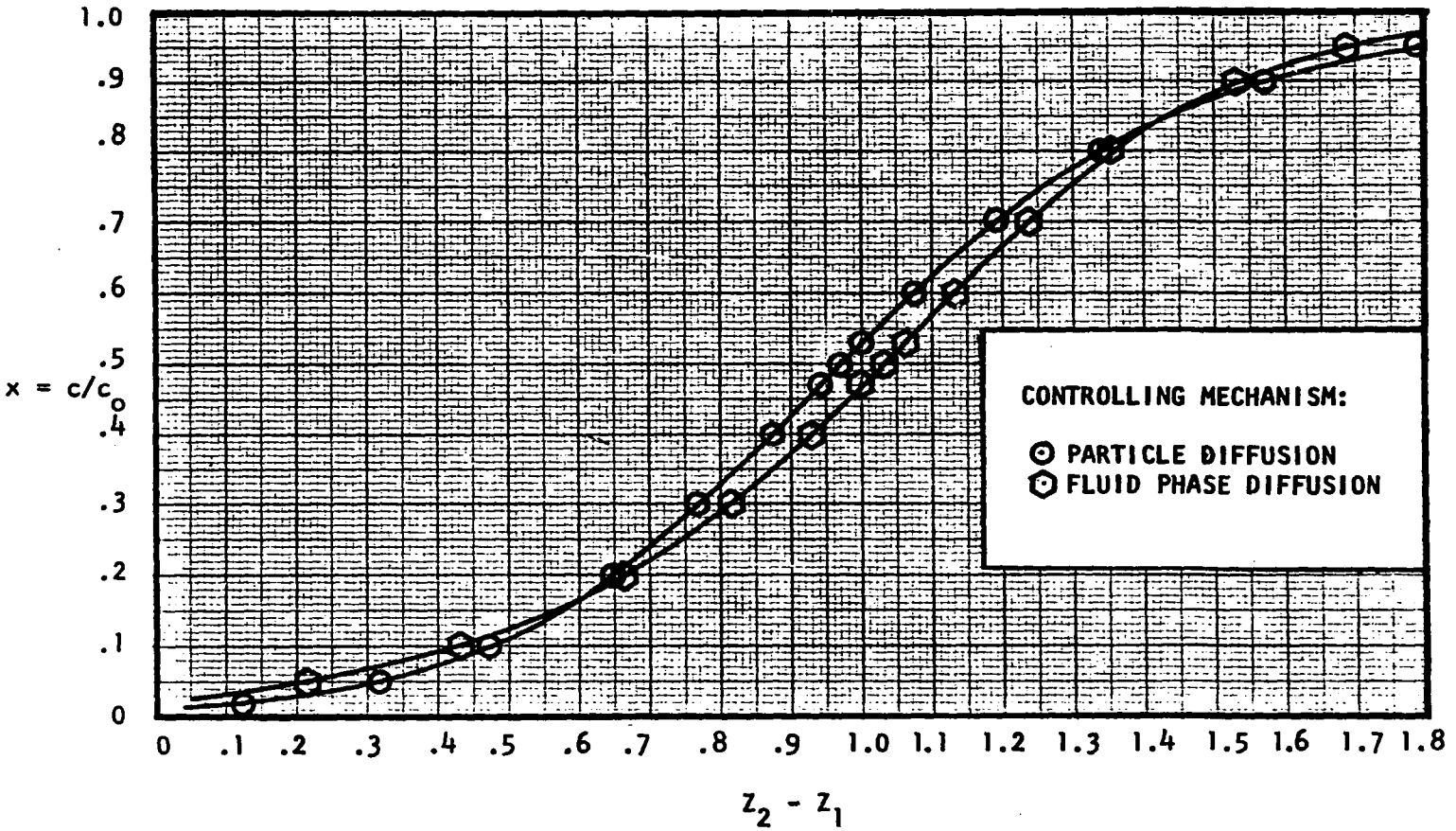


FIGURE I-2 EFFECT OF DIFFUSION MECHANISMS ON EFFLUENT CURVE SHAPE - PENTANE

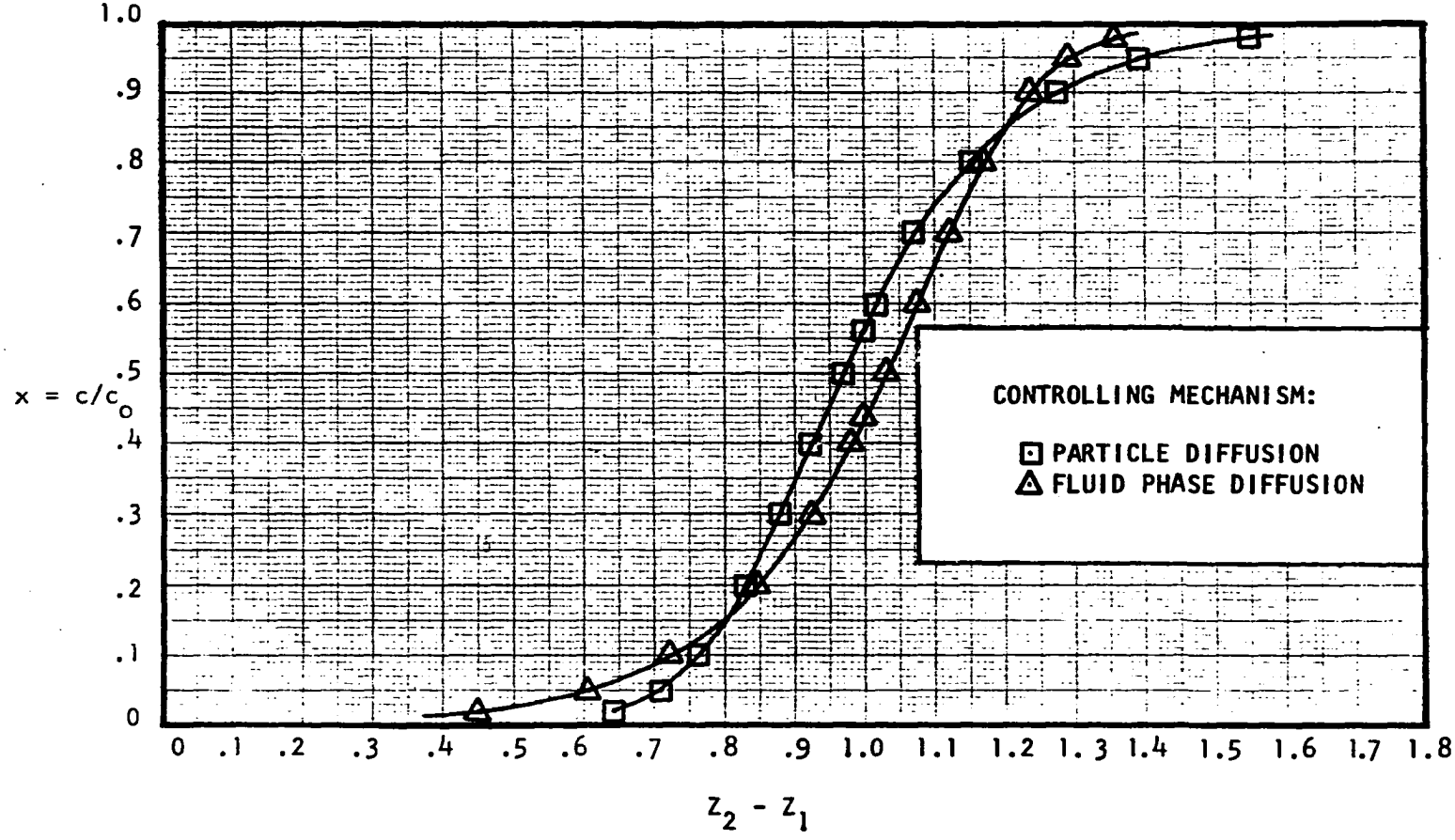


FIGURE I-3 EFFECT OF DIFFUSION MECHANISMS ON EFFLUENT CURVE SHAPE - HEXANE

APPENDIX J

MASTER CURVES FOR THE LIMITING CASE

The following equations are used when one mechanism dominates the behavior of the effluent gas stream concentrations. The first equation is that of Michaels (M5) for fluid phase diffusion as the controlling mechanism.

$$N_f(Z_2-Z_1) = \frac{1}{1-r} \ln \frac{x_2(1-x_1)}{x_1(1-x_2)} + \ln \frac{1-x_2}{1-x_1} . \qquad (J-1)$$

The second equation is that of Glueckauf and Coates (G3), which is for the case of particle diffusion as the controlling mechanism.

$$N_p(Z_2-Z_1) = \frac{r}{1-r} \ln \frac{x_2(1-x_1)}{x_1(1-x_2)} + \ln \frac{1-x_1}{1-x_2} . \qquad (J-2)$$

Master curves which were used in data analysis were calculated on the basis of these two equations. Each equation was calculated for the adsorption of both pentane and hexane. The difference in the behavior of these two components lies in the equilibrium parameter, r. The value of r for pentane is 0.667 (r = 2/3), and r for hexane is 0.4.

From these equations are plotted curves giving x versus $Z_2 - Z_1$ for various numbers of transfer units, N. Figures J-1 and J-2 are for pentane with fluid diffusion and particle diffusion as the respective mechanisms. The same type curves for hexane are shown in Figures J-3 and J-4.

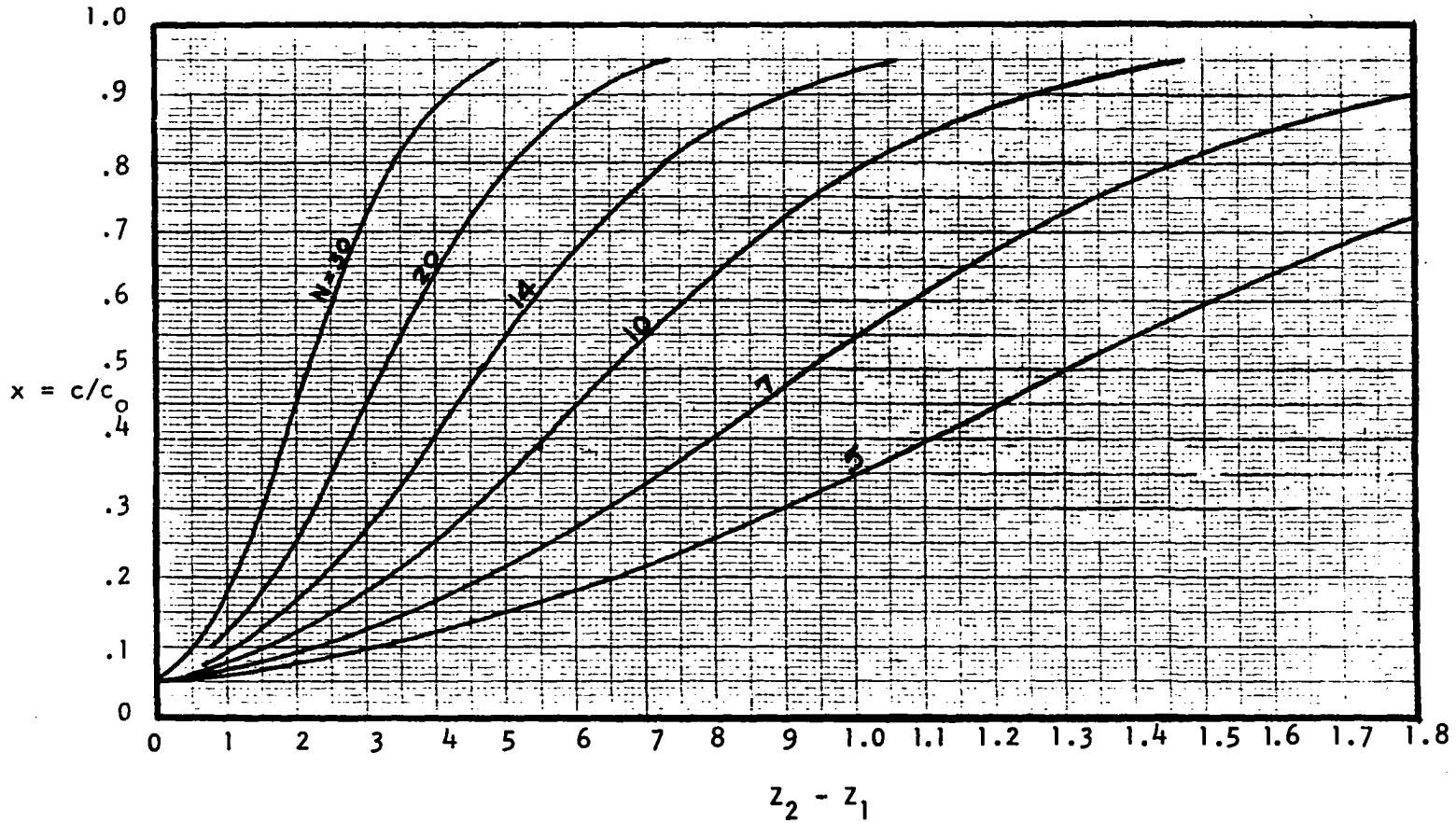


FIGURE J-1 - ASYMPTOTIC EFFLUENT CURVES - PENTANE - PARTICLE DIFFUSION

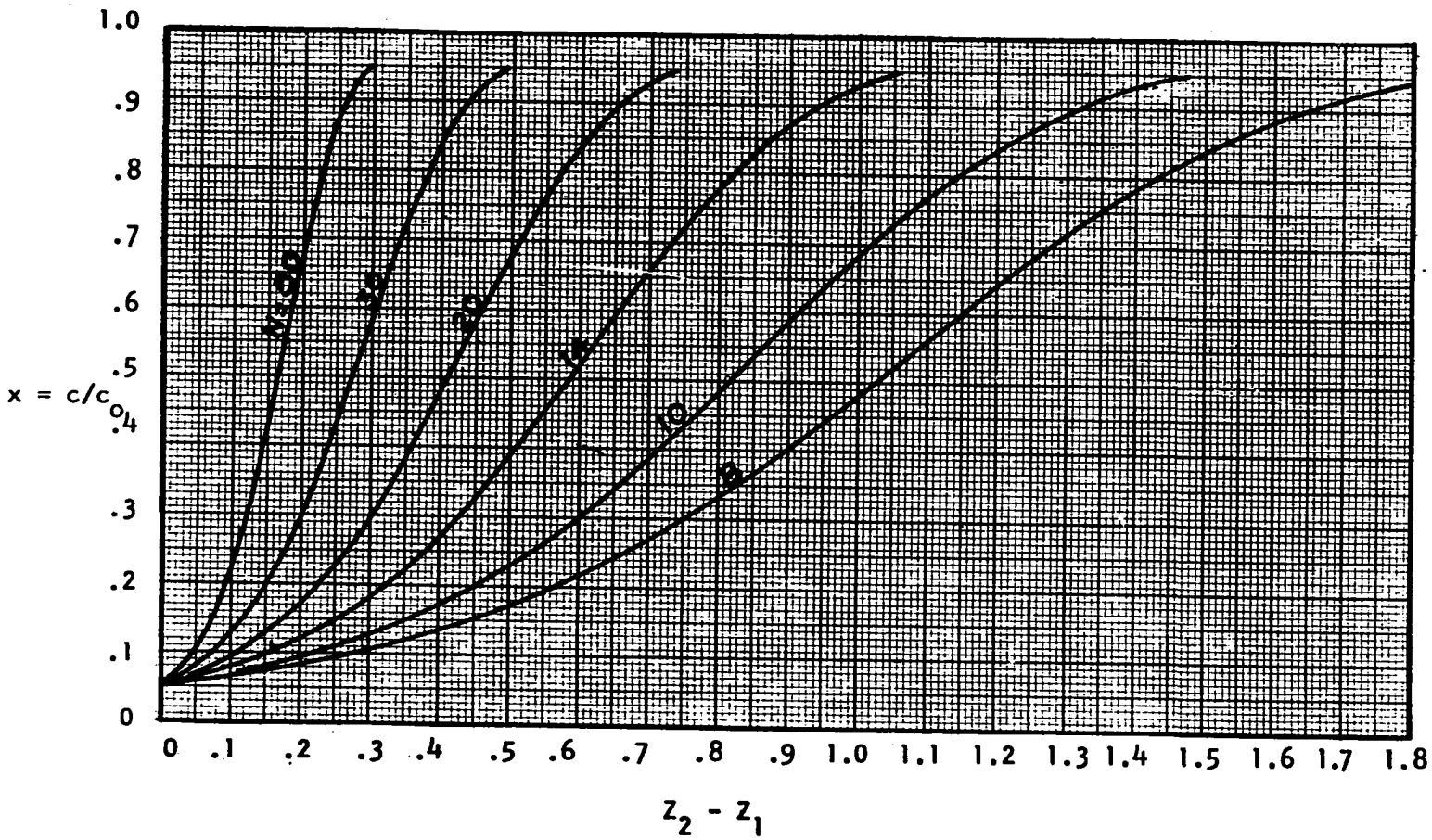


FIGURE J-2 - ASYMPTOTIC EFFLUENT CURVES - PENTANE - FLUID PHASE DIFFUSION

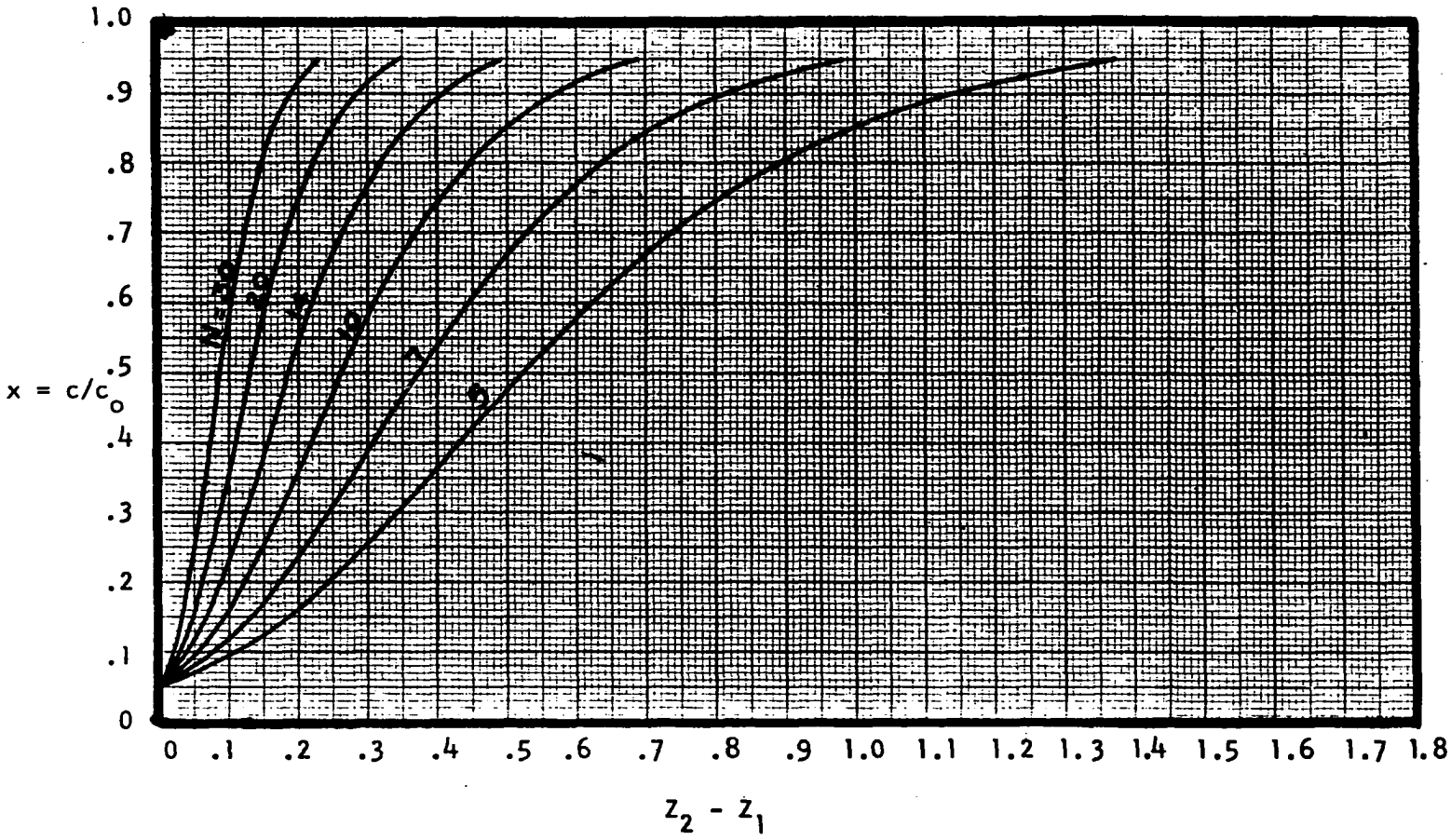


FIGURE J-3 - ASYMPTOTIC EFFLUENT CURVES - HEXANE - PARTICLE DIFFUSION

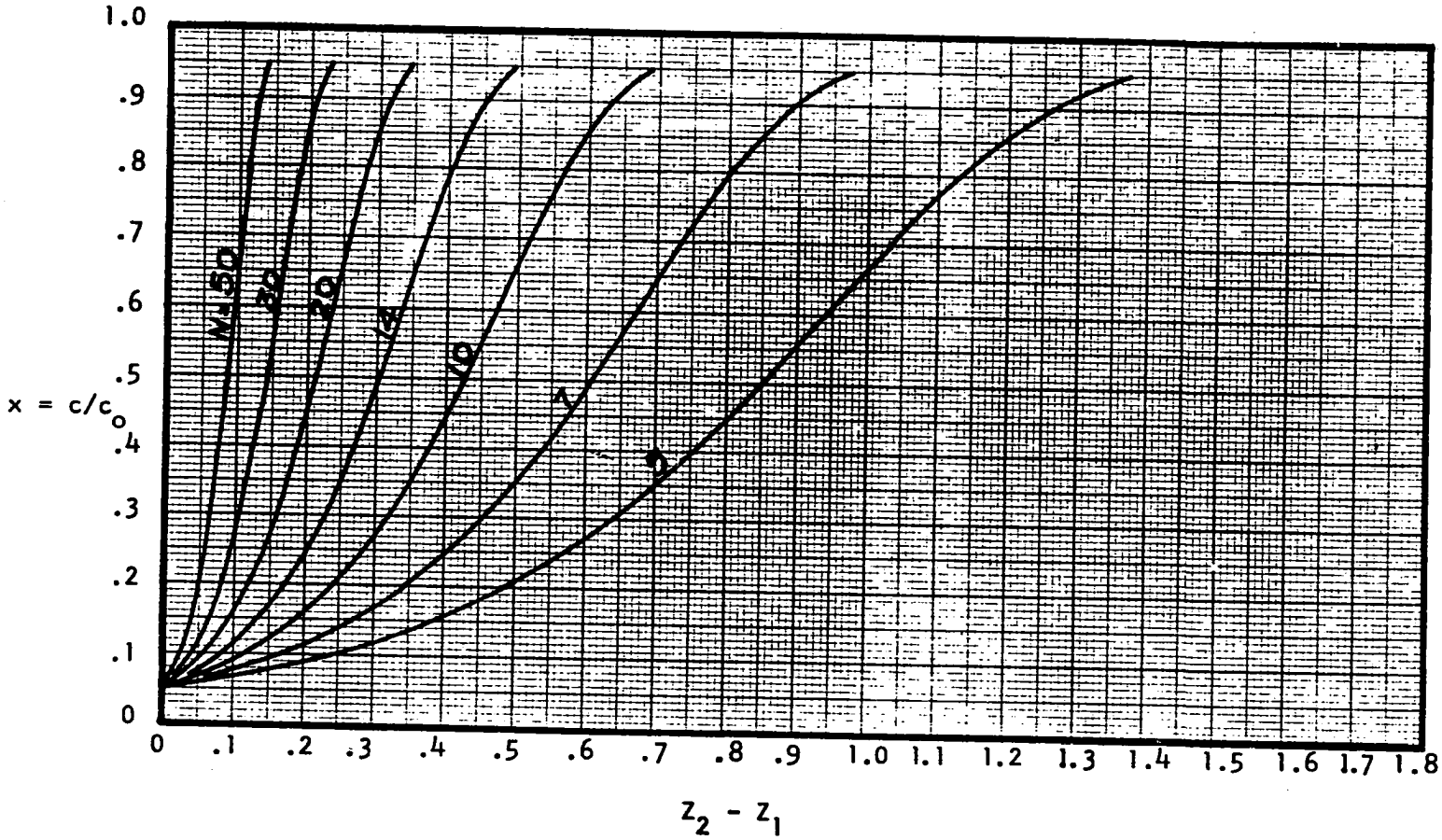


FIGURE J-4 - ASYMPTOTIC EFFLUENT CURVES - HEXANE - FLUID PHASE DIFFUSION

APPENDIX K

CORRELATION OF PARTICLE MASS TRANSFER COEFFICIENTS BASED ON THE ASYMPTOTIC SOLUTION

The master curves described in Appendix J were used to obtain the number of transfer units, N_p, for each experimental run. For this correlation, it was assumed that the effluent curves could be represented by these limiting solutions as given by Equations J-1 and J-2. Each experimental run was plotted as x, dimensionless concentration of hydrocarbon, versus the throughput parameter, Z. The plots of master curves were taped to a glass plate with a light underneath. The plotted effluent curves were then lain on top of the master curves. The curve which best matched the effluent behavior of the experimental run was recorded. By this method the author obtained the number of transfer units, N_p, for each run. The mass transfer coefficients based on particle diffusion, $k_p a_p$, were calculated from the N_p values and the factor $\frac{Dv\epsilon}{F}$. These results are shown in Tables K-I and K-II.

At first transfer coefficients were plotted versus composition only. There was some scatter which I attributed to different adsorption equilibrium values. In order to correct for this difference, the coefficients were replotted against the ratio, C_o/X_T. The transfer coefficient for both pentane and hexane showed a dependence upon hydrocarbon concentration of the component studied. Although the transfer

coefficient for hexane showed little dependence upon velocity, the coefficient for pentane varied considerably from one velocity to the other. This dependence of the transfer coefficient on velocity contradicted the dependence upon concentration. If particle diffusion controls, concentration affects the total diffusion rate, but the velocity outside the particle can not affect this internal diffusivity.

In working with the master curves, it was apparent that the fluid phase coefficient, $\frac{k_f a_p}{D}$, was not the controlling factor. For small values of r, the equilibrium parameter, the curve shapes were quite different where either fluid phase diffusion or particle diffusion controlled the transfer behavior. Fluid phase diffusion as the controlling mechanism gave no correlation because the experimental effluent curve would not match one of the master curves for fluid diffusion. This difference is illustrated in the appendix discussing the effect of the controlling mechanism on the effluent curve shape. Although some dependence upon velocity could be explained by an uneven velocity distribution around the particle, the dependence upon velocity shown by the pentane behavior assuming asymptotic behavior was too large to be explained this way. Therefore it was decided that any transient behavior of the effluent curves must be removed for a clear-cut conclusion. These transient effects were removed by making a correction based on the Thomas solution. This

was described in Appendix E. The results are covered throughly in the chapters on analysis of data and significance of results.

TABLE K-I

ASYMPTOTIC PARTICLE TRANSFER

COEFFICIENTS - PENTANE

Run Number	C_o	X_T	C_o/X_T	$k_p a_p$	N_p
58	1.461	.1243	11.77	.432	25
59	1.694	.1461	11.5	.433	25
60	.660	.0693	9.62	.350	25
61	2.040	.1570	13.0	.528	28
62	1.489	.1393	10.65	.357	23
63	.561	.0580	9.62	.316	22
205	2.16	.1250	13.9	.526	23
56	1.022	.1012	10.11	.424	14
57-A	.511	.0563	9.1	.429	16
57-B	.601	.0680	8.86	.369	14
64	1.519	.1243	12.2	.595	16
65	1.144	.1117	10.21	.516	16
66	1.551	.1301	11.9	.591	16
68	.538	.0642	8.4	.422	16
209	1.75	.1335	13.16	.68	19
84	1.942	.1339	9.18	.76	14
86	.378	.0482	7.88	.594	13
87	1.623	.1600	10.11	.698	12
88	0.467	.0601	7.82	.602	13
89	.990	.1112	8.93	.615	12
90	1.604	.1676	9.53	.680	12
193	.429	.0370	11.63	.63	9
194	1.94	.0982	19.62	.96	8
210	1.33	.1165	11.37	.96	14

TABLE K-II

ASYMPTOTIC PARTICLE TRANSFER

COEFFICIENT - HEXANE

Run Number	C_o	X_T	C_o/X_T	$k_p a_p$	N_p
71	.611	.1584	3.85	.163	25
72	1.199	.1966	6.1	.314	30
73	.469	.1313	3.58	.120	19
74	.996	.2040	4.91	.194	22.5
69	.497	.1327	3.78	.235	16
70	.926	.1819	5.13	.347	18
76	1.366	.2010	6.80	.419	18
77	.940	.1778	5.29	.293	17
78	.479	.1228	3.91	.170	13
192	1.372	.1402	10.21	.55	18
208	.86	.1336	6.46	.40	18
79	.425	.1037	4.15	.279	10
80	.367	.1057	3.50	.173	7
81	.755	.1511	5.03	.266	8.5
82	1.216	.1586	7.70	.43-.74	8-14
83	1.308	.2110	6.21	.48-.65	12-16
190	.40	.0866	4.61	.24	7
191	1.22	.1289	9.44	.65	9.5
204	.970	.1020	9.53	.57	9
206	.34	.0850	4.00	.23	8
207	.64	.1200	5.35	.40	11.5

APPENDIX L

PORE DIFFUSION

A pore diffusion coefficient was evaluated based upon the gas phase diffusivity of both hydrocarbon components in a natural gas and upon an estimated pore size of the dessicant particle. Gas diffusion through pores may take place either by Knudsen flow or by ordinary molecular diffusion. Knudsen flow only occurs where the pore diameter is small compared to the mean free path of a molecule. For a pore size of approximately 22 Angstrom units in the dessicant and for an average molecular diameter of hexane of about 10 Angstroms, ordinary gas diffusion applies. The pore diffusivity for liquids or high pressure gases is described by the following equation (W3):

$$D_{pore} = \frac{D_f \chi}{2} . \qquad \text{(L-1)}$$

A particle transfer coefficient was evaluated for each of the two hydrocarbon components based upon the pore diffusivity of both hexane and pentane according to the following equation:

$$k_p a_p = \frac{60\ D_{pore}}{d_p^2\ D} \qquad \text{(L-2)}$$

Using the diffusivities evaluated at high pressures for the two components, an average particle diameter of .00909 feet, and values of D for pentane and hexane as 150 and 250 respectively, the particle mass transfer coefficients for these components respectively were .0853 and .043 per minute. The lower particle mass transfer coefficients in Figures 11 and 13 are close to this range.

APPENDIX M

EXAMPLE CALCULATIONS FOR FLUID PHASE MASS TRANSFER COEFFICIENTS

Using the data from Table C-I and the prediction method of Hirschfelder, et al. (R1)

$$D_{12}P = \frac{.001858\ T^{3/2}\left(\frac{1}{M_1} + \frac{1}{M_2}\right)^{\frac{1}{2}}}{\sigma_{12}^{2}\ \Omega(1,1)^{*}}$$

with the force constants determined according to Stiel and Thodos (58)

$$\sigma = 0.1866\ v_c^{1/3}\ Z_c^{-6/5}$$

$$\epsilon/k = 65.3\ T_c\ Z_c^{18/5}$$

Dry Gas Constants

$$\sigma_1 = 0.1866\ v_c^{1/3}\ Z_c^{-6/5}$$

$$= 0.1866\ (106.2)^{1/3}(.2875)^{-6/5}$$

$$= 3.94$$

$$(\epsilon/k)_1 = 65.3\ T_c\ Z_c^{18/5}$$

$$= (65.3)(205.5)(.2875)^{3.6}$$

$$= 151$$

Pentane Force Constants

$$\sigma_2 = 0.1866(311)^{1/3}(.269)^{-6/5} = 6.12$$

$$(\epsilon/k)_2 = (65.3)(470)(.269)^{3.6} = 271.5$$

Pentane Diffusivity

$$\sigma_{12} = \frac{\sigma_1 + \sigma_2}{2} = \frac{3.94 + 6.12}{2} = 5.03$$

$$(\epsilon/k)_{12} = \left[(\epsilon/k)_1(\epsilon/k)_2\right] = \left[(151)(271.5)\right]^{\frac{1}{2}} = 202.4$$

$$\left(\frac{kT}{\epsilon}\right)_{12} = \frac{294}{202.4} = 1.453$$

$$\Omega_{(1,1)^*} = 1.214$$

$$D_{12}P_o = \frac{(.001858)(294)^{3/2}\left(\frac{1}{18.52} + \frac{1}{72.15}\right)^{\frac{1}{2}}}{(1.214)(5.03)^2}$$

$$= .0841 \text{ atm cm}^2/\text{sec at } 70^\circ \text{ F}$$

$$D_{12}P_o = (.0841)\left(\frac{305}{294}\right)^{1.5} = .0889 \text{ atm cm}^2/\text{sec at } 90^\circ \text{ F}$$

From Reid and Sherwood (R1), page 279

$$P_r = \frac{815}{670} = 1.22$$

$$T_r = \frac{550}{370} = 1.49$$

$$\frac{D_{12}P}{D_{12}P_o} = 0.85$$

$$D_{12}P = (0.85)(.0889) = .0755 \text{ atm cm}^2/\text{sec}$$

$$D_{12} = .0755/P = \frac{.0755}{55.5 \text{ atm}} = .00136 \text{ cm}^2/\text{sec}$$

$$= 0.00528 \text{ ft}^2/\text{hr}$$

(D_{12} at 90° F and 815 psia)
C_5

Hexane Force Constants

$$\sigma_2 = (.1866)(368)^{1/3}(.264)^{-1.2} = 6.6$$

$$(\epsilon/k)_2 = (65.3)(508)(.264)^{3.6} = 275$$

Binary Force Constants

$$\sigma_{12} = \frac{3.94 + 6.6}{2} = 5.27$$

$$(\epsilon/k)_{12} = \left[(275)(151)\right]^{\frac{1}{2}} = 204$$

$$\frac{kT}{\epsilon_{12}} = \frac{294}{204} = 1.44$$

$$\Omega_{(1,1)^*} = 1.219$$

Hexane Diffusivity

$$D_{12}P_o = \frac{(.001858)(294)^{3/2}\left(\frac{1}{18.52} + \frac{1}{86.17}\right)^{\frac{1}{2}}}{(1.219)(5.27)^2}$$

$$= .0707 \text{ atm cm}^2/\text{sec at } 70^\circ \text{ F}$$

$$D_{12}P_o = 0.0707 \left(\frac{305}{294}\right)^{1.5} = 0.0747 \text{ atm cm}^2/\text{sec at } 90^\circ \text{ F}$$

$$P_r = 1.22 \quad , \quad T_r = 1.49$$

$$\frac{D_{12}P}{D_{12}P_o} = 0.85$$

$$D_{12}P = (0.85)(.0747) = .0635 \text{ atm cm}^2/\text{sec}$$

At 815 psia = 55.5 atm,

$$D_{12} = \frac{.0635}{55.5 \text{ atm}} = 0.001144 \text{ cm}^2/\text{sec}$$

$$= .00443 \text{ ft}^2/\text{hr}$$

$$(D_{12_{C_6}} \text{ at } 90^\circ \text{ F and } 815 \text{ psia})$$

The diffusivity in a dry natural gas (Sp.Gr. = 0.64) at 90° F and 815 psia equals .00528 ft^2/hr for pentane and .00443 ft^2/hr for hexane.

Fluid Phase Mass Transfer Coefficient

According to Wilke and Hougen - see Vermuelen (V2)

$$k_f = 1.82\ U \left(\frac{dU\epsilon\rho}{\mu}\right)^{-0.51} \left(\frac{\mu}{\rho D_f}\right)^{-0.67}$$

μ = 0.0152 cp = 0.0367 lb/ft hr (N2, p. 145)

ρ = 2.89 lb/cu ft (0.65 Sp.Gr. - ideal gas)

D_f = .00528 ft^2/hr - pentane

= .0043 ft^2/hr - hexane

$$\left(\frac{\mu}{\rho D_f}\right) = 0.556 \text{ - pentane}$$

$$= 0.494 \text{ - hexane}$$

$$\left(\frac{dU\epsilon\rho}{\mu}\right)^{-0.51} = \left[\frac{(.00909)(0.4)(2.89)\ U}{0.0367}\right]^{-0.51}$$

$$= 1.894\ U^{-0.51}$$

Therefore:

$$k_f = (1.82)(1.894)(.556)\ U^{0.49}$$

$$= 1.916\ U^{0.49} \text{ ft/hr}$$

(Pentane)

$$k_f = (1.82)(1.894)(.494)\ U^{0.49}$$

$$= 1.70\ U^{0.49} \text{ ft/hr}$$

(Hexane)

APPENDIX N

EFFECT OF USING DIFFERENT GAS DIFFUSIVITY ON $k_p a_p$ CORRELATION

The following calculations are presented to show what effect the use of the experimental diffusivity of Carmichael, et al. (C7) would have on the $k_p a_p$ correlation.

D'_{12_o} = Experimental Diffusivity of Carmichael, et al.

D'_{12_o} = .0476 cm^2/sec at 70°F and 1 atm.

$$D'_{12}P = (.0476)\left(\frac{305}{296}\right)^{1.5}(0.85) = .0428 \text{ atm } cm^2/sec$$

$$D'_{12} = \frac{.0428}{55.5} = .000772 \text{ } cm^2/sec \text{ at } 90^\circ F \text{ and } 815 \text{ psia}$$

$$= .00299 \text{ } ft^2/hr$$

$$\frac{D'_{12}}{D_{12}} = \frac{.00299}{.00443} = .675$$

D'_{12} is 67.5% of D_{12}, the diffusivity used in obtaining the $k_p a_p$ correlation.

$$\frac{k'_f}{k_f} = (.675)^{0.67} = .769 \quad .$$

The maximum resistance offered by fluid phase diffusion in the correlation was 15%. If k'_f were used, this would change to 19.5%. This would in turn alter the particle resistance to 80.5% of the total transfer resistance instead of 85 which represents a change in the evaluated $k_p a_p$ of 5.6% which is minor. Therefore in the analysis of the hydrocarbon

adsorption data, an error of 32.5% in the gas phase diffusion coefficient would cause an error of only 5.6% in the calculated particle transfer coefficient, $k_p a_p$.